

# Density Model for White-Beaked Dolphin (*Lagenorhynchus albirostris*) for the U.S. East Coast: Supplementary Report

Model Version 3.1

Duke University Marine Geospatial Ecology Laboratory\*

2023-05-27


## Citation

When citing our methodology or results generally, please cite Roberts et al. (2016, 2023). The complete references appear at the end of this document. We are preparing a new article for a peer-reviewed journal that will eventually replace those. Until that is published, those are the best general citations.

When citing this model specifically, please use this reference:

Roberts JJ, Yack TM, Cañadas A, Fujioka E, Halpin PN, Barco SG, Boisseau O, Chavez-Rosales S, Cole TVN, Cotter MP, Cummings EW, Davis GE, DiGiovanni Jr. RA, Garrison LP, Gowan TA, Jackson KA, Kenney RD, Khan CB, Lockhart GG, Lomac-MacNair KS, McAlarney RJ, McLellan WA, Mullin KD, Nowacek DP, O'Brien O, Pabst DA, Palka DL, Quintana-Rizzo E, Redfern JV, Rickard ME, White M, Whitt AD, Zoidis AM (2022) Density Model for White-Beaked Dolphin (*Lagenorhynchus albirostris*) for the U.S. East Coast, Version 3.1, 2023-05-27, and Supplementary Report. Marine Geospatial Ecology Laboratory, Duke University, Durham, North Carolina.

## Copyright and License

 This document and the accompanying results are © 2023 by the Duke University Marine Geospatial Ecology Laboratory and are licensed under a [Creative Commons Attribution 4.0 International License](https://creativecommons.org/licenses/by/4.0/).

## Model Version History

Version	Date	Description
1	2014-11-20	Initial version.
2	2015-03-06	Fixed bug that applied the wrong detection function to segments NE_narwss_1999_widgeon_hapo dataset. Refitted model. Updated documentation.
2.1	2015-05-14	Updated calculation of CVs. Switched density rasters to logarithmic breaks. No changes to the model.
2.2	2015-10-06	Updated the documentation. No changes to the model. Model files released as supplementary information to Roberts et al. (2016).

\*For questions or to offer feedback please contact Jason Roberts ([jason.roberts@duke.edu](mailto:jason.roberts@duke.edu)) and Tina Yack ([tina.yack@duke.edu](mailto:tina.yack@duke.edu))

*(continued)*

---

Version	Date	Description
3	2022-06-20	This model is a major update over the prior version, with substantial additional data, improved statistical methods, and an increased spatial resolution. It was released as part of the final delivery of the U.S. Navy Marine Species Density Database (NMSDD) for the Atlantic Fleet Testing and Training (AFTT) Phase IV Environmental Impact Statement. Several new collaborators joined and contributed survey data: New York State Department of Environmental Conservation, TetraTech, HDR, and Marine Conservation Research. We incorporated additional surveys from all continuing and new collaborators through the end of 2020. (Because some environmental covariates were only available through 2019, certain models only extend through 2019.) We increased the spatial resolution to 5 km and, at NOAA's request, we extended the model further inshore from New York through Maine. We reformulated and refitted all detection functions and spatial models. We updated all environmental covariates to newer products, when available, and added several covariates to the set of candidates. For models that incorporated dynamic covariates, we estimated model uncertainty using a new method that accounts for both model parameter error and temporal variability.
3.1	2023-05-27	Completed the supplementary report documenting the details of this model. Corrected the 5 and 95 percent rasters so that they contain the value 0 where the taxon was assumed absent, rather than NoData. Nothing else was changed.

---

# 1 Survey Data

We built this model from data collected between 1998-2020 (Table 1, Figure 1). We excluded surveys that did not target small cetaceans or were otherwise problematic for modeling them. To maintain consistency with the other models developed during the 2022 modeling cycle, most of which excluded data prior to 1998 in order to utilize biological covariates derived from satellite ocean color observations, we also excluded data prior to 1998 from this model. We restricted the model to aerial survey transects with sea states of Beaufort 4 or less (for a few surveys we used Beaufort 3 or less) and shipboard transects with Beaufort 5 or less (for a few we used Beaufort 4 or less). We also excluded transects with poor weather or visibility for surveys that reported those conditions.

Table 1: Survey effort and observations considered for this model. Effort is tallied as the cumulative length of on-effort transects. Observations are the number of groups and individuals encountered while on effort. Off effort observations and those lacking an estimate of group size or distance to the group were excluded.

Institution	Program	Period	Effort	Observations		
			1000s km	Groups	Individuals	Mean Group Size
<b>Aerial Surveys</b>						
HDR	Navy Norfolk Canyon	2018-2019	10	0	0	
NEFSC	AMAPPS	2010-2019	83	3	29	9.7
NEFSC	NARWSS	2003-2016	380	6	43	7.2
NEFSC	Pre-AMAPPS	1999-2008	45	4	11	2.8
SEFSC	AMAPPS	2010-2020	112	0	0	
SEFSC	MATS	2002-2005	27	0	0	
UNCW	MidA Bottlenose	2002-2002	15	0	0	
UNCW	Navy Cape Hatteras	2011-2017	34	0	0	
UNCW	Navy Jacksonville	2009-2017	92	0	0	
UNCW	Navy Norfolk Canyon	2015-2017	14	0	0	
UNCW	Navy Onslow Bay	2007-2011	49	0	0	
UNCW	SEUS NARW EWS	2005-2008	106	0	0	
VAMSC	MD DNR WEA	2013-2015	15	0	0	
VAMSC	Navy VACAPES	2016-2017	18	0	0	
VAMSC	VA CZM WEA	2012-2015	19	0	0	
		<b>Total</b>	<b>1,020</b>	<b>13</b>	<b>83</b>	<b>6.4</b>
<b>Shipboard Surveys</b>						
MCR	SOTW Visual	2012-2019	9	5	30	6.0
NEFSC	AMAPPS	2011-2016	15	0	0	
NEFSC	Pre-AMAPPS	1995-2007	17	1	7	7.0
NJDEP	NJEBS	2008-2009	14	0	0	
SEFSC	AMAPPS	2011-2016	16	0	0	
SEFSC	Pre-AMAPPS	1998-2006	30	0	0	
		<b>Total</b>	<b>100</b>	<b>6</b>	<b>37</b>	<b>6.2</b>
		<b>Grand Total</b>	<b>1,120</b>	<b>19</b>	<b>120</b>	<b>6.3</b>

Table 2: Institutions that contributed surveys used in this model.

Institution	Full Name
HDR	HDR, Inc.
MCR	Marine Conservation Research
NEFSC	NOAA Northeast Fisheries Science Center
NJDEP	New Jersey Department of Environmental Protection
SEFSC	NOAA Southeast Fisheries Science Center
UNCW	University of North Carolina Wilmington
VAMSC	Virginia Aquarium & Marine Science Center

Table 3: Descriptions and references for survey programs used in this model.

Program	Description	References
AMAPPS	Atlantic Marine Assessment Program for Protected Species	Palka et al. (2017), Palka et al. (2021)
MATS	Mid-Atlantic Tursiops Surveys	
MD DNR WEA	Aerial Surveys of the Maryland Wind Energy Area	Barco et al. (2015)
MidA Bottlenose	Mid-Atlantic Onshore/Offshore Bottlenose Dolphin Surveys	Torres et al. (2005)
NARWSS	North Atlantic Right Whale Sighting Surveys	Cole et al. (2007)
Navy Cape Hatteras	Aerial Surveys of the Navy’s Cape Hatteras Study Area	McLellan et al. (2018)
Navy Jacksonville	Aerial Surveys of the Navy’s Jacksonville Study Area	Foley et al. (2019)
Navy Norfolk Canyon	Aerial Surveys of the Navy’s Norfolk Canyon Study Area	Cotter (2019), McAlarney et al. (2018)
Navy Onslow Bay	Aerial Surveys of the Navy’s Onslow Bay Study Area	Read et al. (2014)
Navy VACAPES	Aerial Survey Baseline Monitoring in the Continental Shelf Region of the VACAPES OPAREA	Malette et al. (2017)
NJEBS	New Jersey Ecological Baseline Study	Geo-Marine, Inc. (2010), Whitt et al. (2015)
Pre-AMAPPS	Pre-AMAPPS Marine Mammal Abundance Surveys	Mullin and Fulling (2003), Garrison et al. (2010), Palka (2006)
SEUS NARW EWS	Southeast U.S. Right Whale Early Warning System Surveys	
SOTW Visual	R/V Song of the Whale Visual Surveys	Ryan et al. (2013)
VA CZM WEA	Virginia CZM Wind Energy Area Surveys	Malette et al. (2014), Malette et al. (2015)



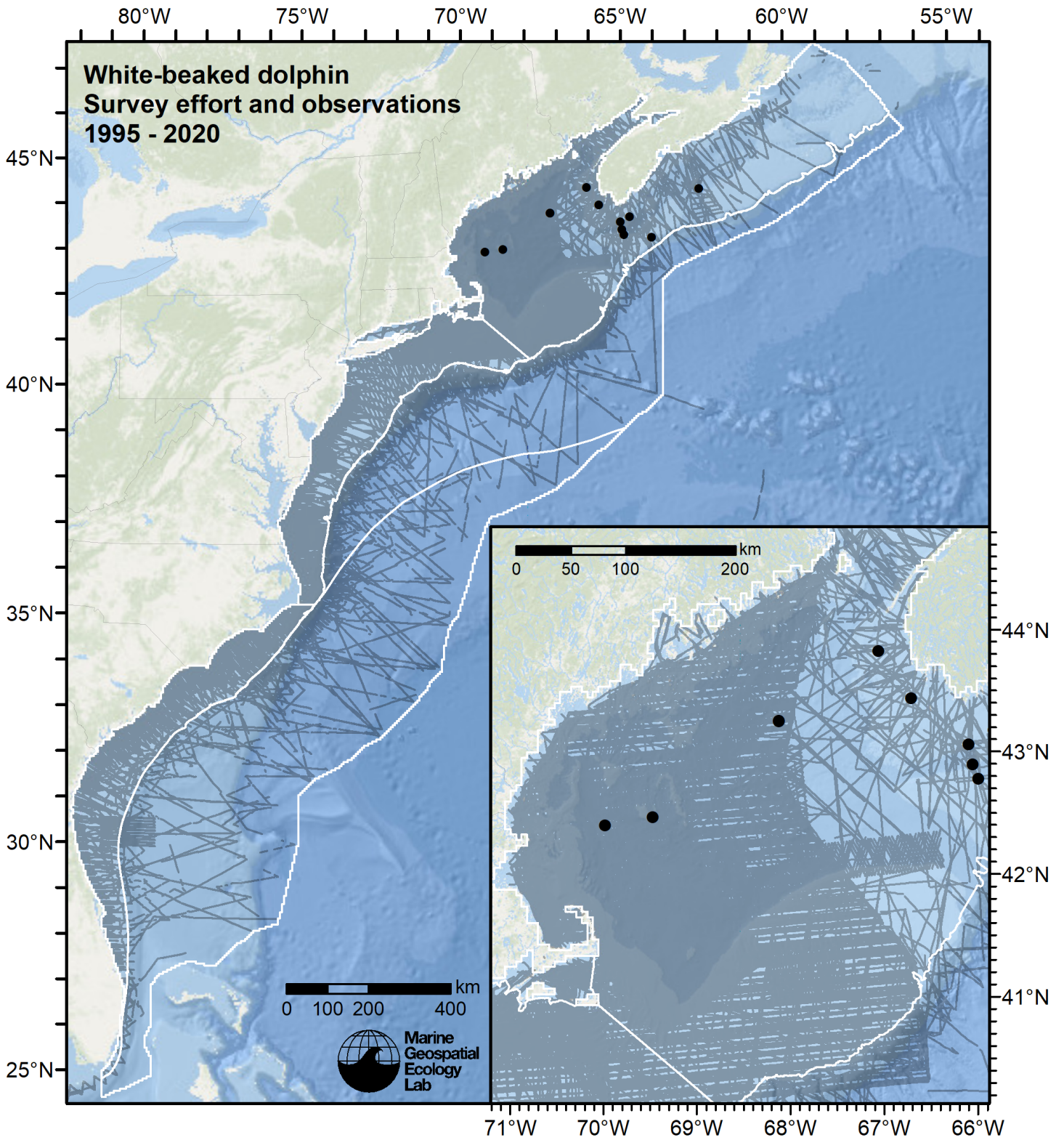


Figure 1: Survey effort and white-beaked dolphin observations available for density modeling, after detection functions were applied, and excluded segments and truncated observations were removed. White outlines show the strata for which density estimates were derived.

## 2 Detection Functions

### 2.1 With a Taxonomic Covariate

We fitted the detection functions in this section to pools of species with similar detectability characteristics and used the taxonomic identification as a covariate (ScientificName) to account for differences between them. We consulted the literature and observer teams to determine appropriate poolings. We usually employed this approach to boost the counts of observations in the detection functions, which increased the chance that other covariates such as Beaufort sea state could be used to account for differences in observing conditions. When defining the taxonomic covariate, we sometimes had too few observations of species to allocate each of them their own level of the covariate and had to group them together, again consulting the literature and observers for advice on species similarity. Also, when species were observed frequently enough to be allocated their own levels but statistical tests indicated no significant difference between the levels, we usually grouped them together into a single level.

#### 2.1.1 Aerial Surveys

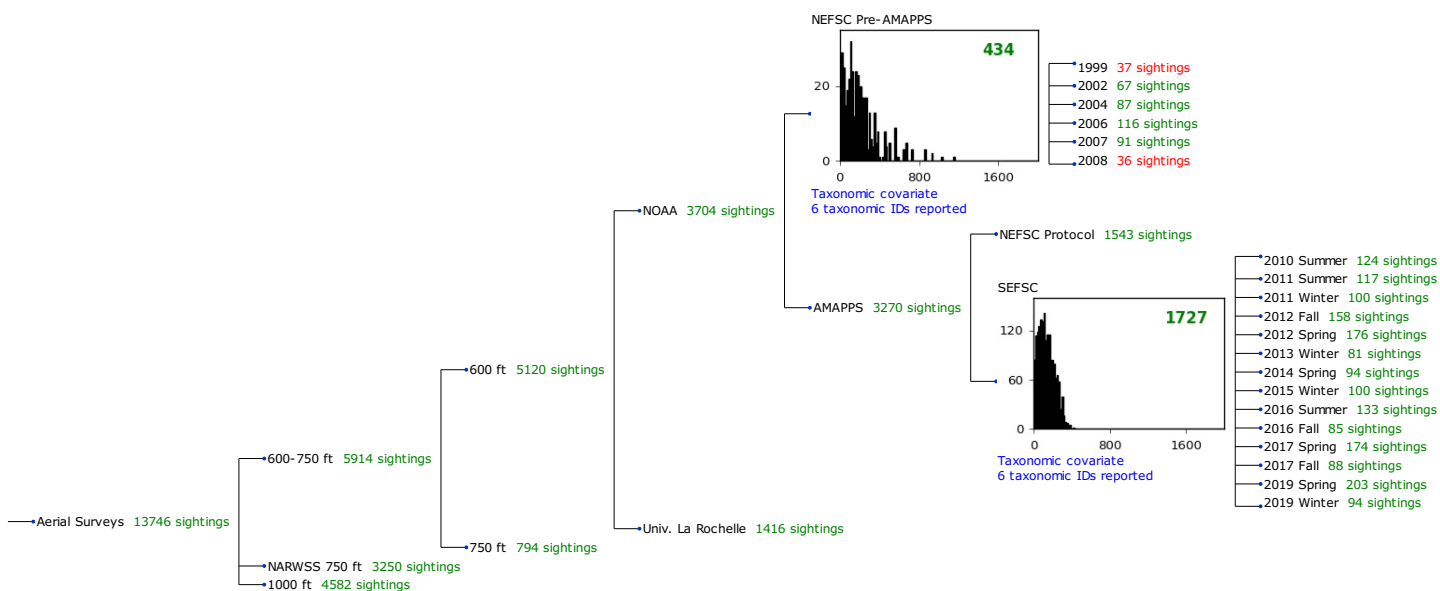


Figure 2: Detection hierarchy for aerial surveys, showing how they were pooled during detectability modeling, for detection functions that pooled multiple taxa and used a taxonomic covariate to account for differences between them. Each histogram represents a detection function and summarizes the perpendicular distances of observations that were pooled to fit it, prior to truncation. Observation counts, also prior to truncation, are shown in green when they met the recommendation of Buckland et al. (2001) that detection functions utilize at least 60 sightings, and red otherwise. For rare taxa, it was not always possible to meet this recommendation, yielding higher statistical uncertainty. During the spatial modeling stage of the analysis, effective strip widths were computed for each survey using the closest detection function above it in the hierarchy (i.e. moving from right to left in the figure). Surveys that do not have a detection function above them in this figure were either addressed by a detection function presented in a different section of this report, or were omitted from the analysis.

##### 2.1.1.1 NEFSC Pre-AMAPPS

After right-truncating observations greater than 600 m, we fitted the detection function to the 413 observations that remained (Table 4). The selected detection function (Figure 3) used a hazard rate key function with Beaufort (Figure 4) and ScientificName (Figure 5) as covariates.

Table 4: Observations used to fit the NEFSC Pre-AMAPPS detection function.

ScientificName	n
Delphinus, Lagenodelphis, Stenella	239
Lagenorhynchus	128
Tursiops, Steno	46
<b>Total</b>	<b>413</b>

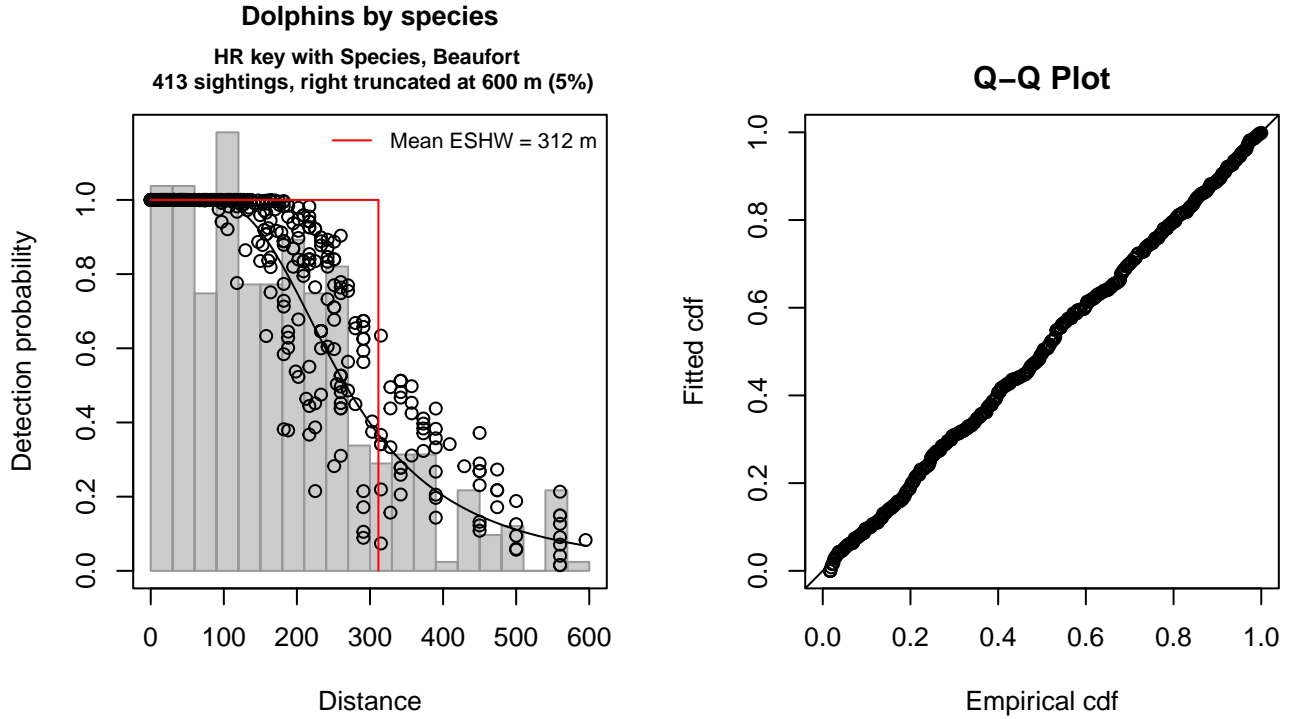


Figure 3: NEFSC Pre-AMAPPS detection function and Q-Q plot showing its goodness of fit.

Statistical output for this detection function:

Summary for ds object

Number of observations : 413  
 Distance range : 0 - 600  
 AIC : 5043.994

Detection function:

Hazard-rate key function

Detection function parameters

Scale coefficient(s):

	estimate	se
(Intercept)	5.3188665	0.15126469
ScientificNameLagenorhynchus	-0.1872175	0.11165678
ScientificNameTursiops, Steno	-0.5457529	0.14785313
Beaufort	0.1451869	0.05844944

Shape coefficient(s):

	estimate	se
(Intercept)	1.107015	0.1176733

Estimate	SE	CV
----------	----	----

Average p 0.4982478 0.02373666 0.04764026  
 N in covered region 828.9047438 49.28440455 0.05945726

Distance sampling Cramer-von Mises test (unweighted)  
 Test statistic = 0.023324 p = 0.992716

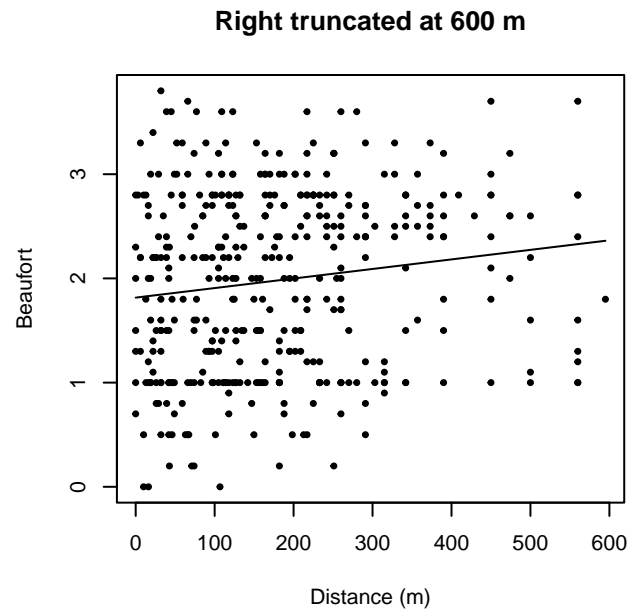
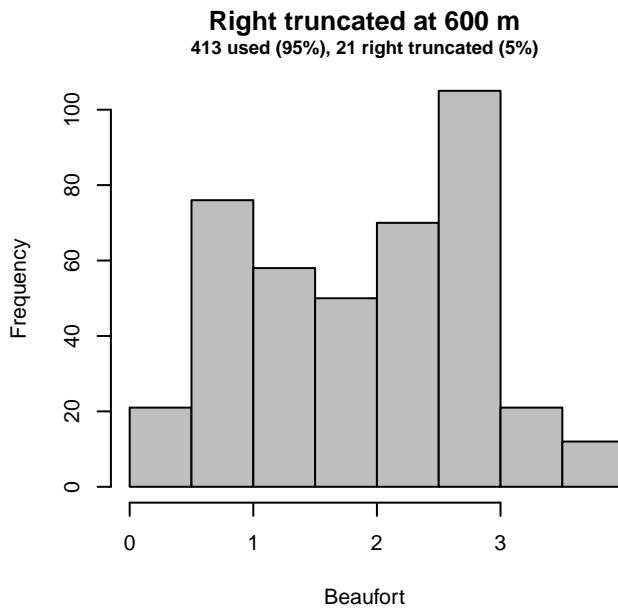
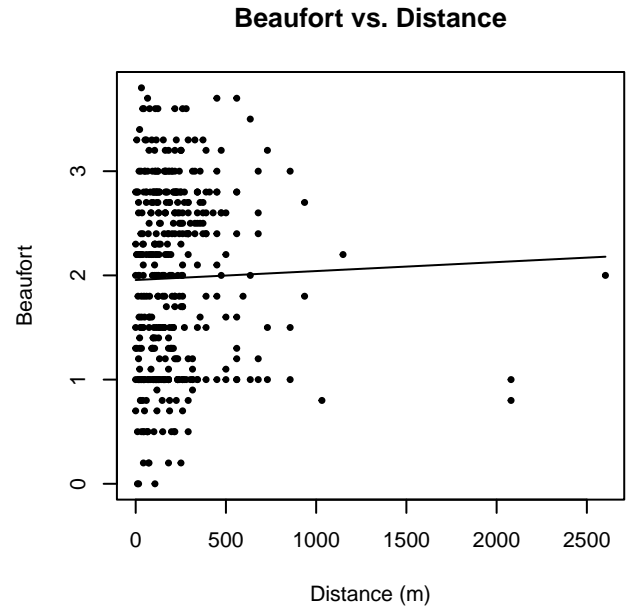
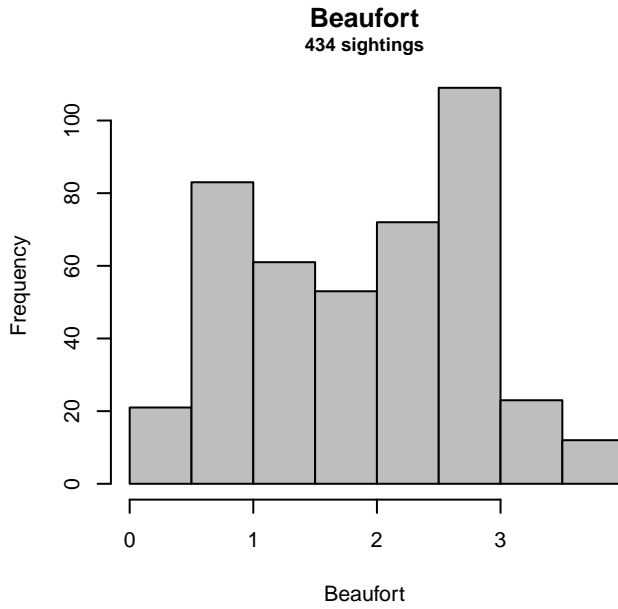


Figure 4: Distribution of the Beaufort covariate before (top row) and after (bottom row) observations were truncated to fit the NEFSC Pre-AMAPPS detection function.

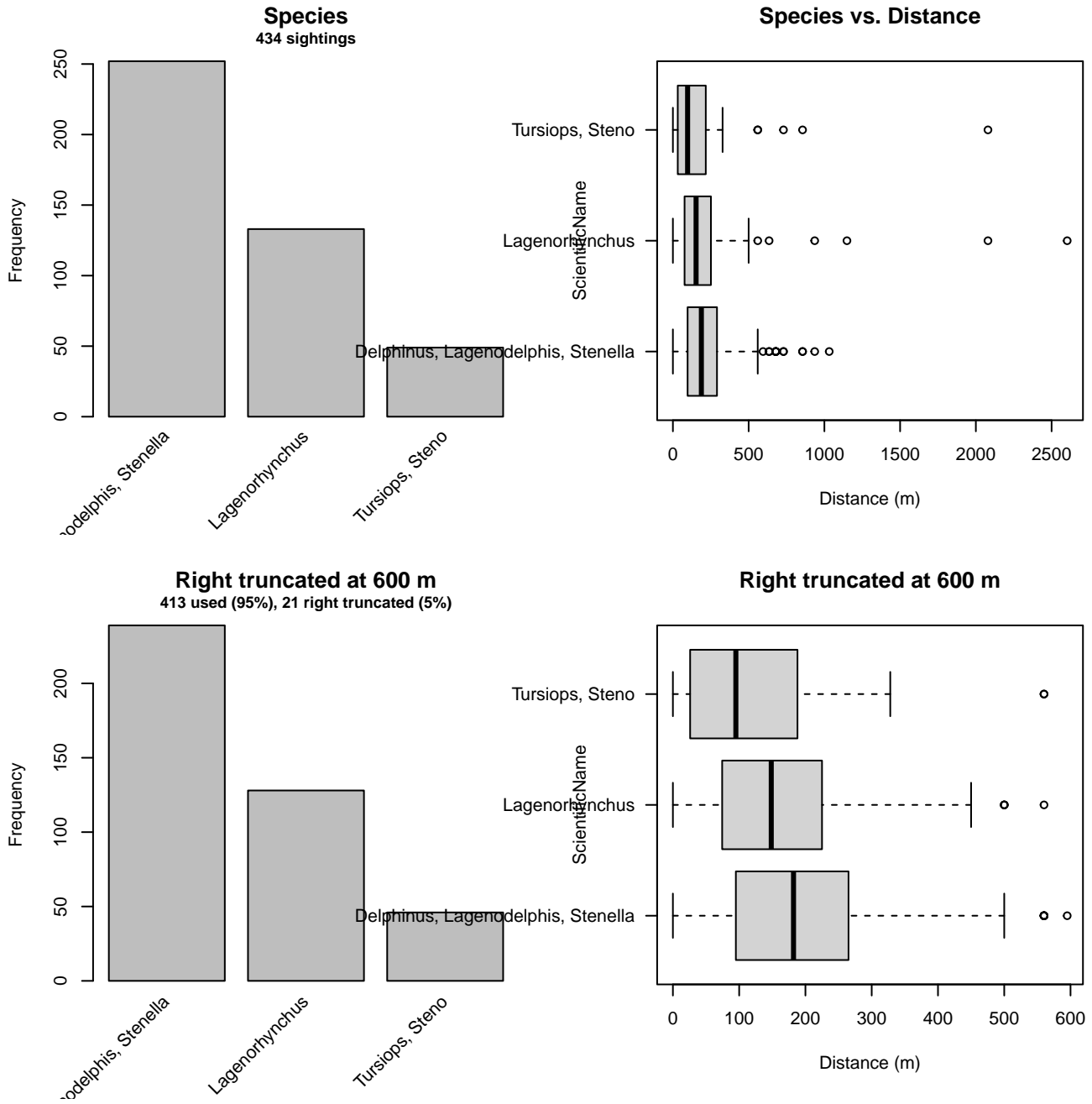


Figure 5: Distribution of the ScientificName covariate before (top row) and after (bottom row) observations were truncated to fit the NEFSC Pre-AMAPPS detection function.

### 2.1.1.2 SEFSC AMAPPS

After right-truncating observations greater than 325 m and left-truncating observations less than 15 m (Figure 7), we fitted the detection function to the 1628 observations that remained (Table 5). The selected detection function (Figure 6) used a hazard rate key function with Beaufort (Figure 8), ScientificName (Figure 9) and Season (Figure 10) as covariates.

Table 5: Observations used to fit the SEFSC AMAPPS detection function.

ScientificName	n
Delphinus, Tursiops, Lagenorhynchus, Steno	1422
Stenella, Lagenodelphis	206
<b>Total</b>	<b>1628</b>

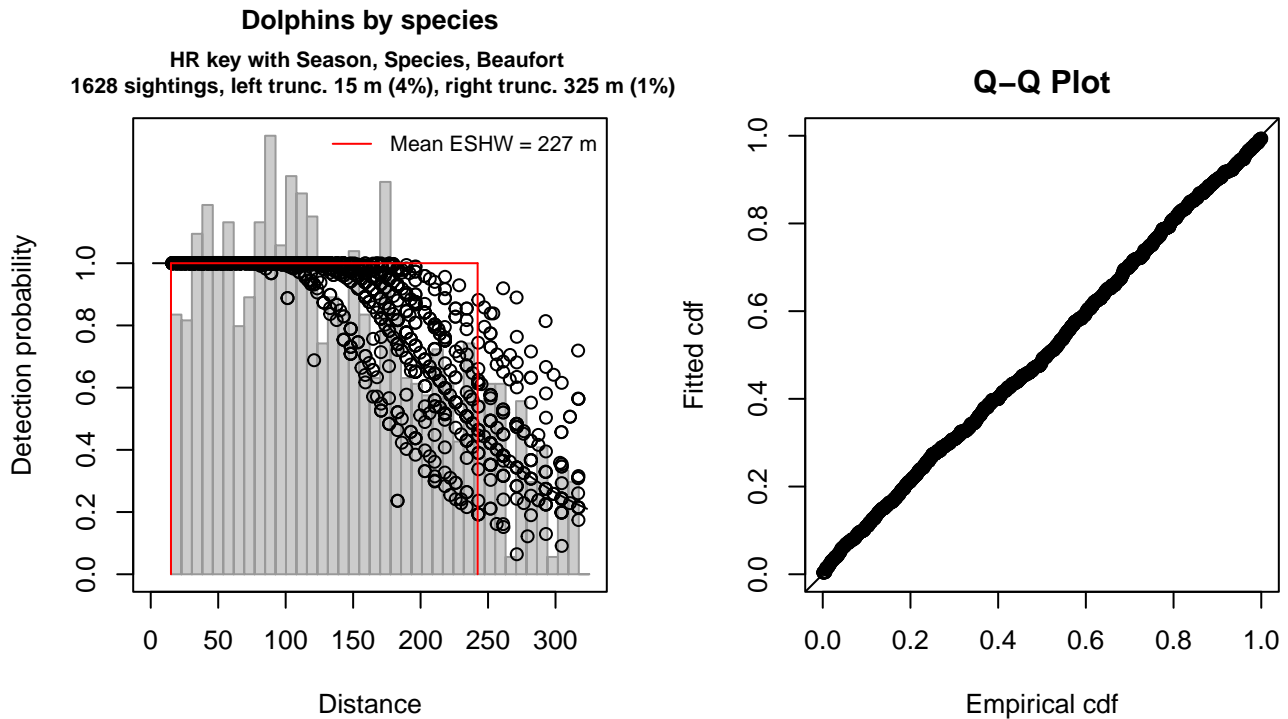


Figure 6: SEFSC AMAPPS detection function and Q-Q plot showing its goodness of fit.

Statistical output for this detection function:

Summary for ds object

Number of observations : 1628  
Distance range : 15 - 325  
AIC : 18351.39

Detection function:

Hazard-rate key function

Detection function parameters

Scale coefficient(s):

	estimate	se
(Intercept)	5.4780735	0.08251975
SeasonSummer	0.1269645	0.06172358
SeasonWinter	-0.2356803	0.06102237
ScientificNameStenella, Lagenodelphis	0.2204074	0.08699872
Beaufort2	-0.1192230	0.08713320
Beaufort3	-0.1846083	0.08971655
Beaufort4	-0.4027356	0.12330363

Shape coefficient(s):

	estimate	se
(Intercept)	1.266688	0.1150367

	Estimate	SE	CV
Average p	0.720161	0.01522909	0.02114679
N in covered region	2260.605761	56.60731047	0.02504077

Distance sampling Cramer-von Mises test (unweighted)

Test statistic = 0.138923 p = 0.425167

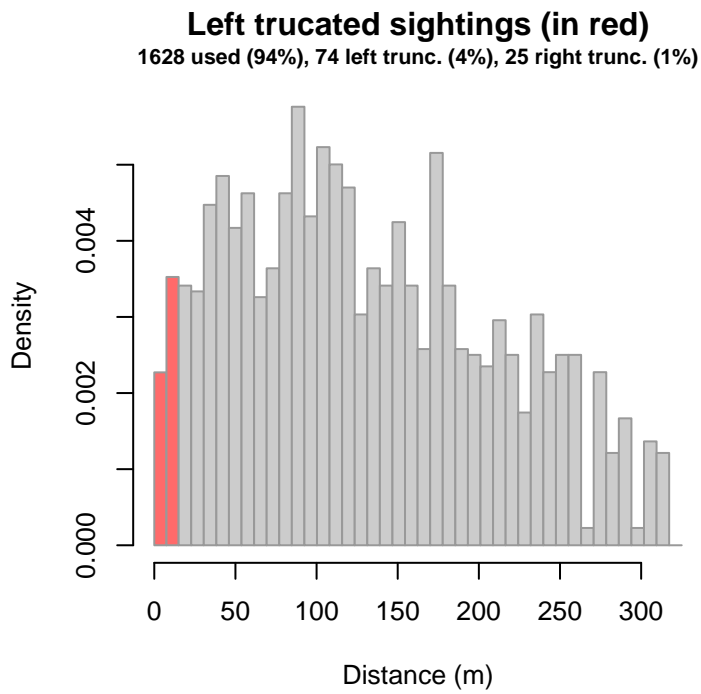


Figure 7: Density histogram of observations used to fit the SEFSC AMAPPS detection function, with the left-most bar showing observations at distances less than 15 m, which were left-truncated and excluded from the analysis [Buckland et al. (2001)]. (This bar may be very short if there were very few left-truncated sightings, or very narrow if the left truncation distance was very small; in either case it may not appear red.)

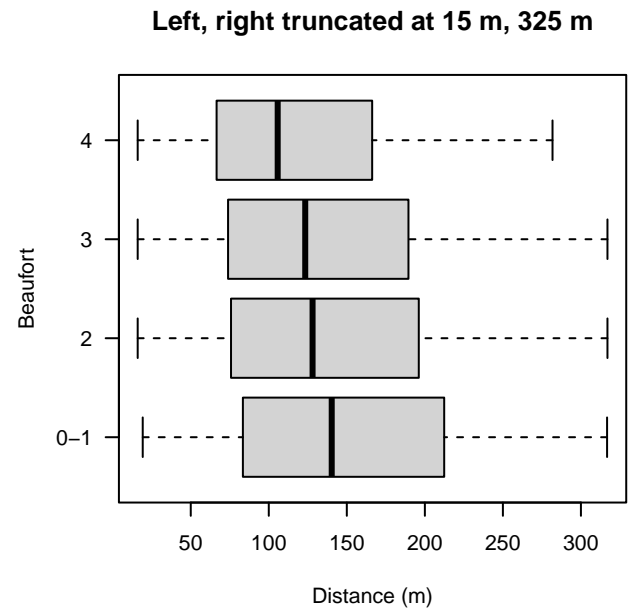
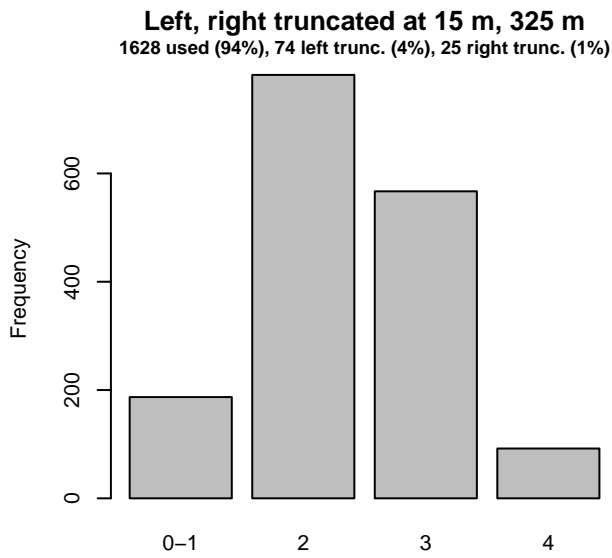
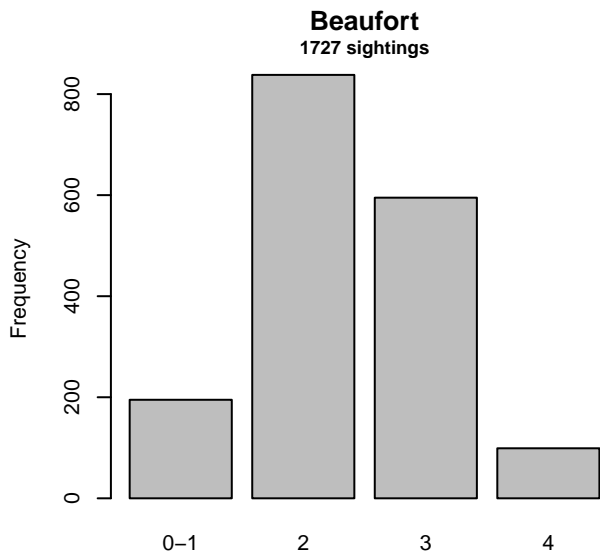


Figure 8: Distribution of the Beaufort covariate before (top row) and after (bottom row) observations were truncated to fit the SEFSC AMAPPS detection function.



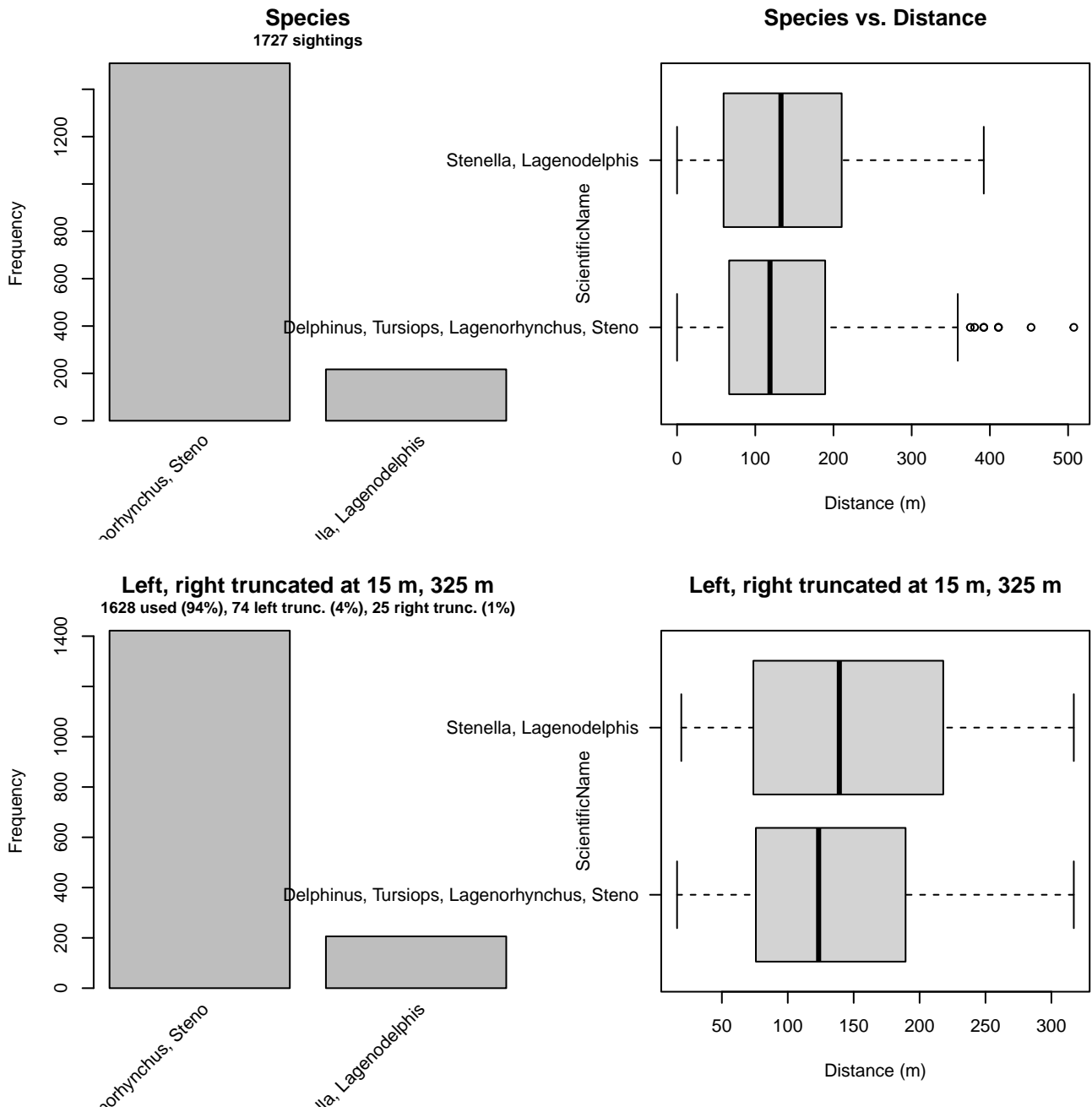


Figure 9: Distribution of the ScientificName covariate before (top row) and after (bottom row) observations were truncated to fit the SEFSC AMAPPS detection function.

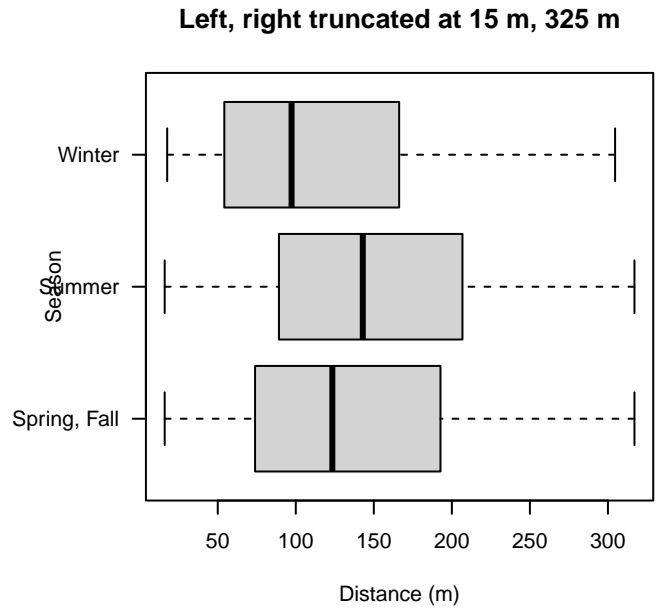
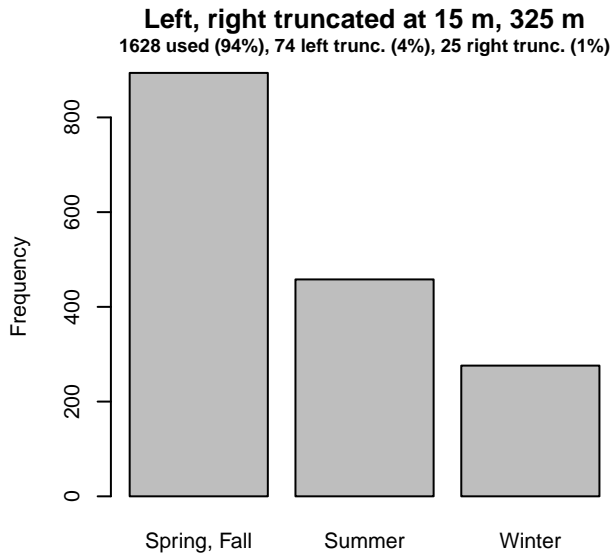
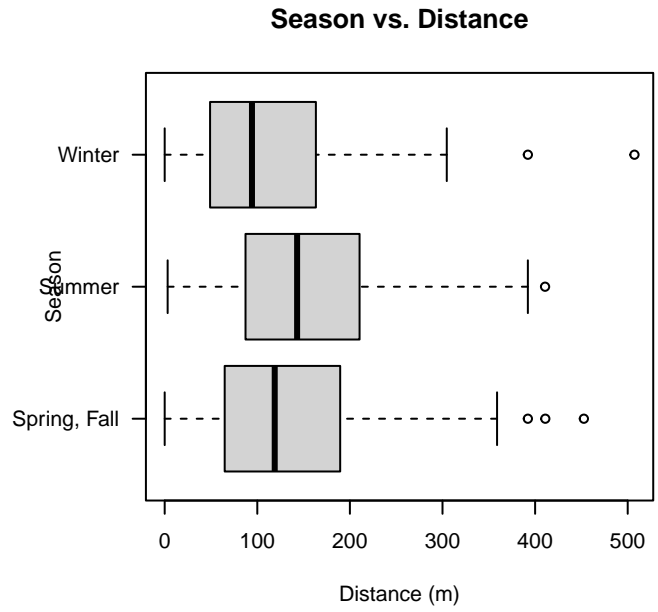
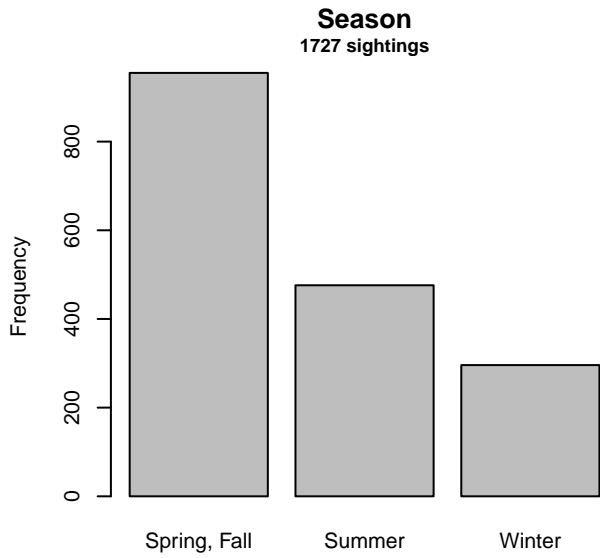


Figure 10: Distribution of the Season covariate before (top row) and after (bottom row) observations were truncated to fit the SEFSC AMAPPS detection function.

## 2.1.2 Shipboard Surveys

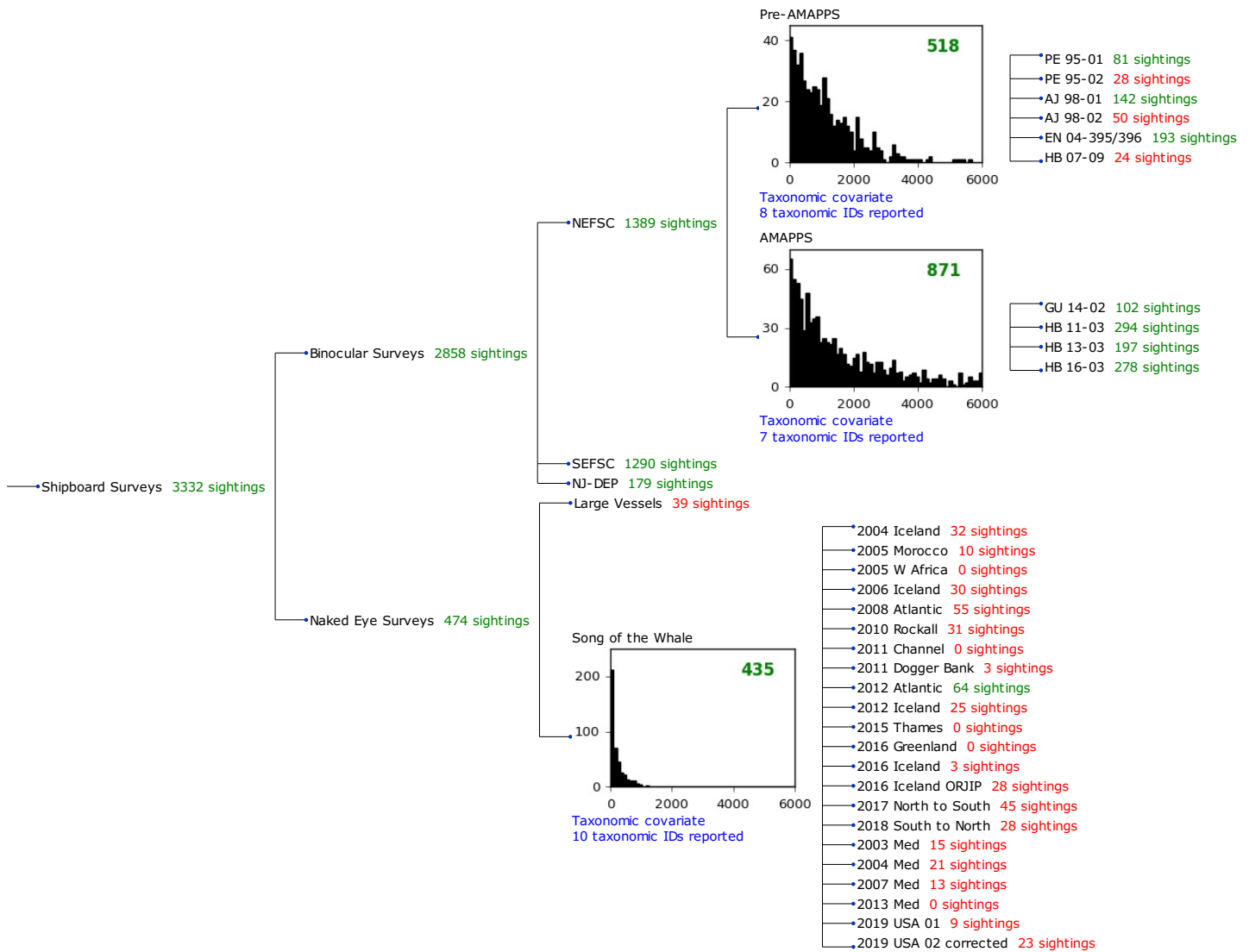


Figure 11: Detection hierarchy for shipboard surveys, showing how they were pooled during detectability modeling, for detection functions that pooled multiple taxa and used a taxonomic covariate to account for differences between them. Each histogram represents a detection function and summarizes the perpendicular distances of observations that were pooled to fit it, prior to truncation. Observation counts, also prior to truncation, are shown in green when they met the recommendation of Buckland et al. (2001) that detection functions utilize at least 60 sightings, and red otherwise. For rare taxa, it was not always possible to meet this recommendation, yielding higher statistical uncertainty. During the spatial modeling stage of the analysis, effective strip widths were computed for each survey using the closest detection function above it in the hierarchy (i.e. moving from right to left in the figure). Surveys that do not have a detection function above them in this figure were either addressed by a detection function presented in a different section of this report, or were omitted from the analysis.

### 2.1.2.1 NEFSC Pre-AMAPPS

After right-truncating observations greater than 4000 m, we fitted the detection function to the 508 observations that remained (Table 6). The selected detection function (Figure 12) used a hazard rate key function with Beaufort (Figure 13), ScientificName (Figure 14) and VesselName (Figure 15) as covariates.

Table 6: Observations used to fit the NEFSC Pre-AMAPPS detection function.

ScientificName	n
Delphinus, Lagenorhynchus, Tursiops, Steno	365
Other Stenella, Lagenodelphis	130
Stenella frontalis	13
<b>Total</b>	<b>508</b>

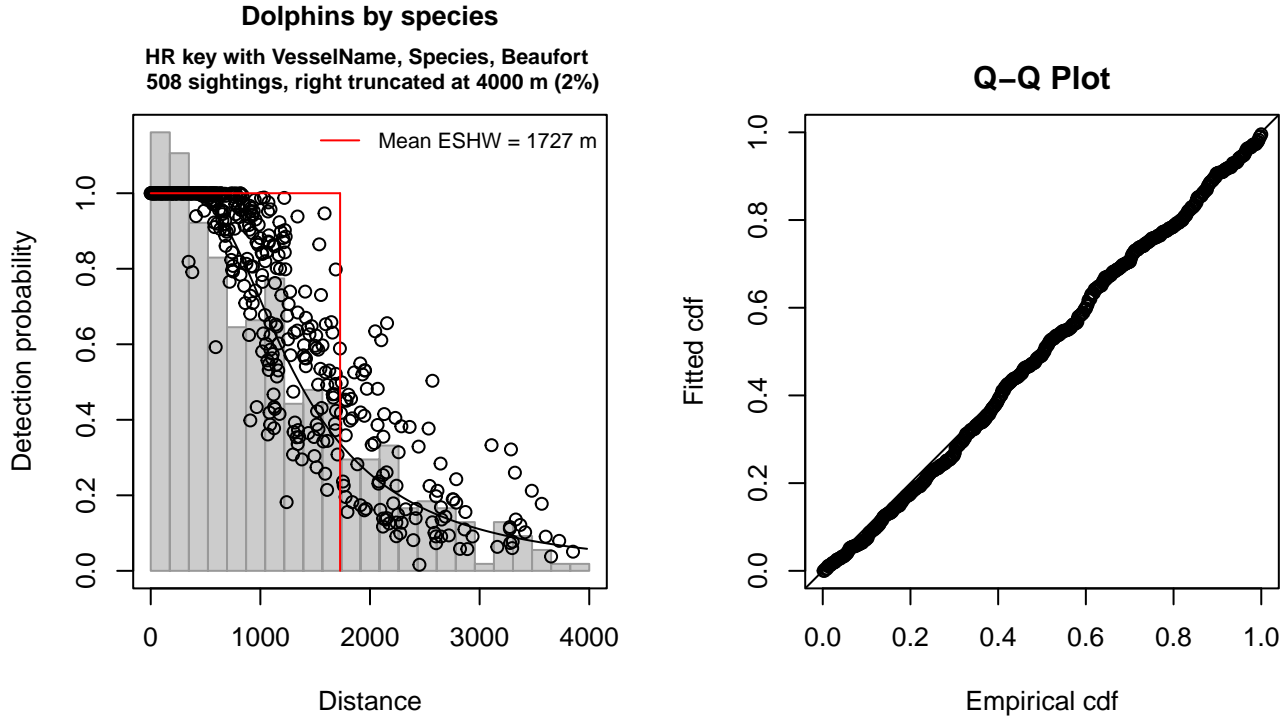


Figure 12: NEFSC Pre-AMAPPS detection function and Q-Q plot showing its goodness of fit.

Statistical output for this detection function:

Summary for ds object

Number of observations : 508  
 Distance range : 0 - 4000  
 AIC : 8058.614

Detection function:

Hazard-rate key function

Detection function parameters

Scale coefficient(s):

	estimate	se
(Intercept)	7.3979634	0.1986065
VesselNameEndeavor, Bigelow	0.2529041	0.1095209
ScientificNameOther Stenella, Lagenodelphis	0.3555978	0.1258179
ScientificNameStenella frontalis	-0.8556981	0.3078540
Beaufort	-0.1897812	0.0694737

Shape coefficient(s):

	estimate	se
(Intercept)	0.8752144	0.1006522

	Estimate	SE	CV
Average p	0.4071518	0.02118698	0.05203705
N in covered region	1247.6919609	78.15195776	0.06263722

Distance sampling Cramer-von Mises test (unweighted)  
 Test statistic = 0.120847 p = 0.492001

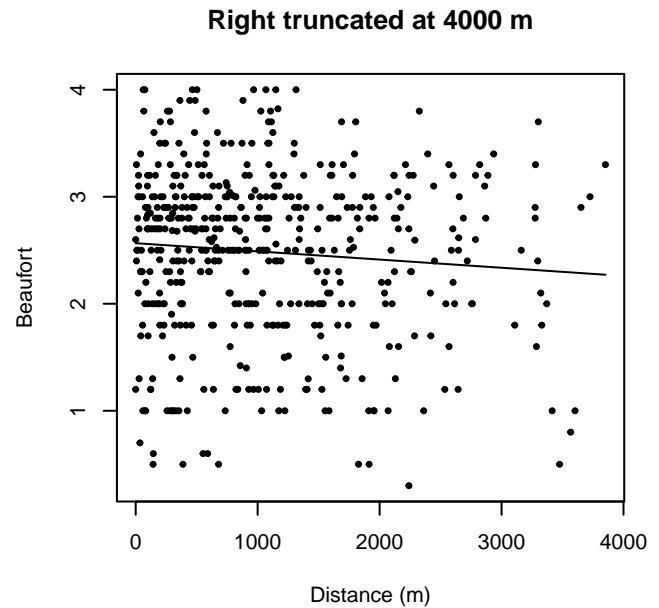
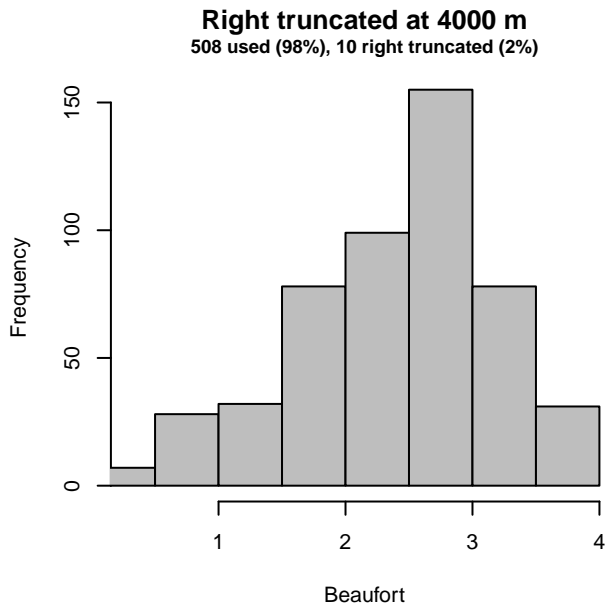
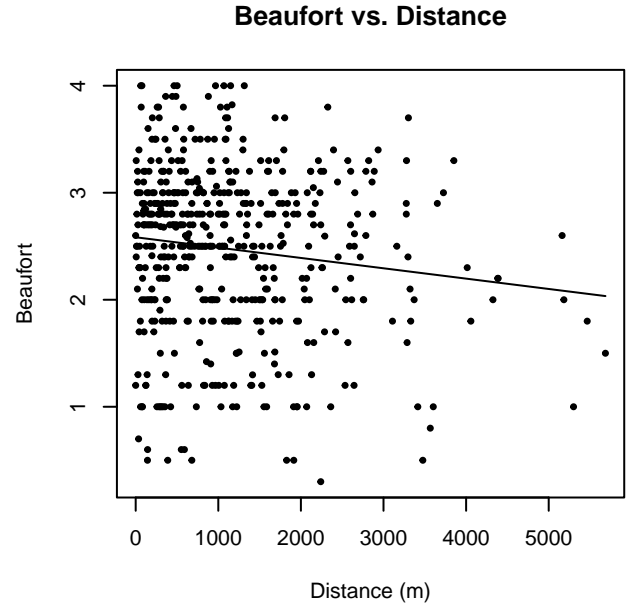
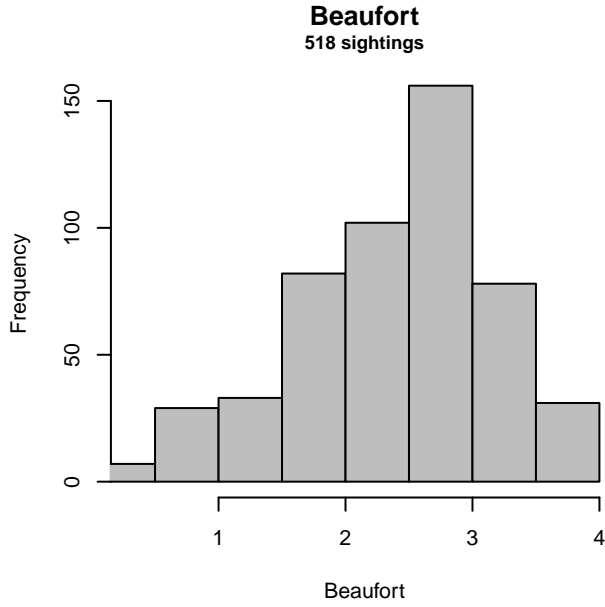


Figure 13: Distribution of the Beaufort covariate before (top row) and after (bottom row) observations were truncated to fit the NEFSC Pre-AMAPPS detection function.

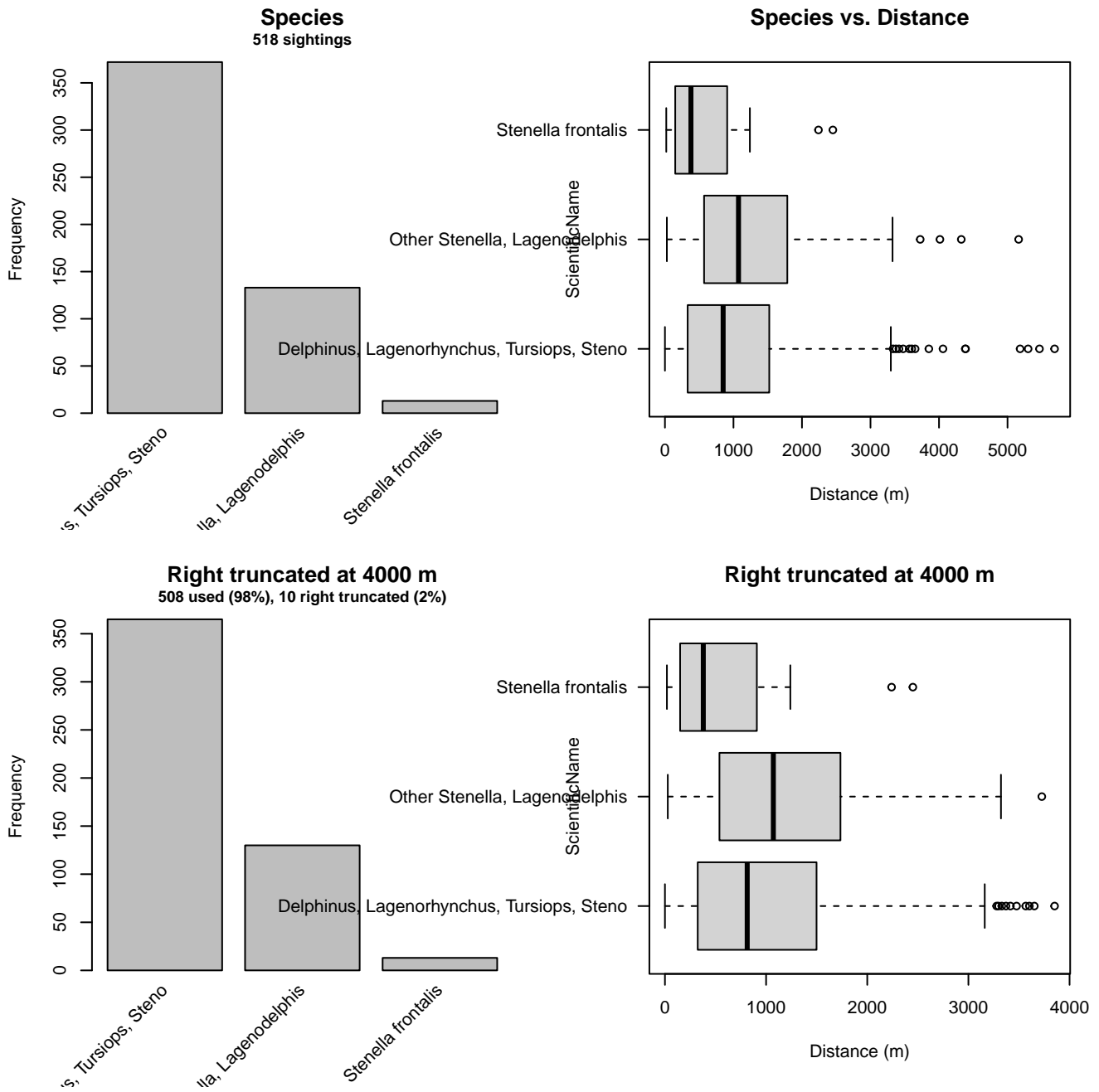


Figure 14: Distribution of the ScientificName covariate before (top row) and after (bottom row) observations were truncated to fit the NEFSC Pre-AMAPPS detection function.

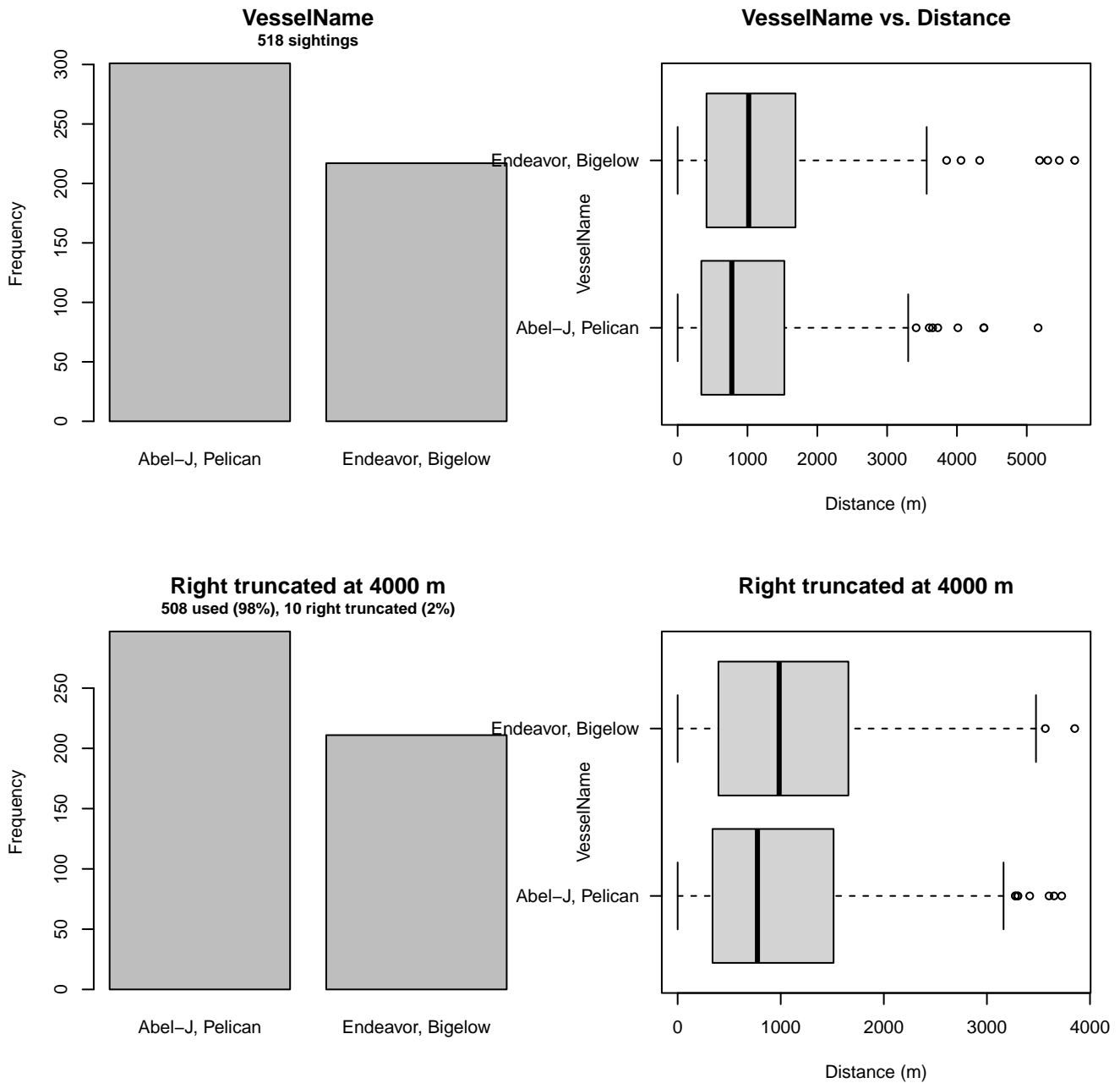


Figure 15: Distribution of the VesselName covariate before (top row) and after (bottom row) observations were truncated to fit the NEFSC Pre-AMAPPS detection function.

### 2.1.2.2 NEFSC AMAPPS

After right-truncating observations greater than 6000 m, we fitted the detection function to the 857 observations that remained (Table 7). The selected detection function (Figure 16) used a hazard rate key function with Beaufort (Figure 17) and ScientificName (Figure 18) as covariates.

Table 7: Observations used to fit the NEFSC AMAPPS detection function.

ScientificName	n
Delphinus, Lagenorhynchus	358
Other Stenella, Lagenodelphis	175
Stenella frontalis	53
Tursiops, Steno	271
<b>Total</b>	<b>857</b>

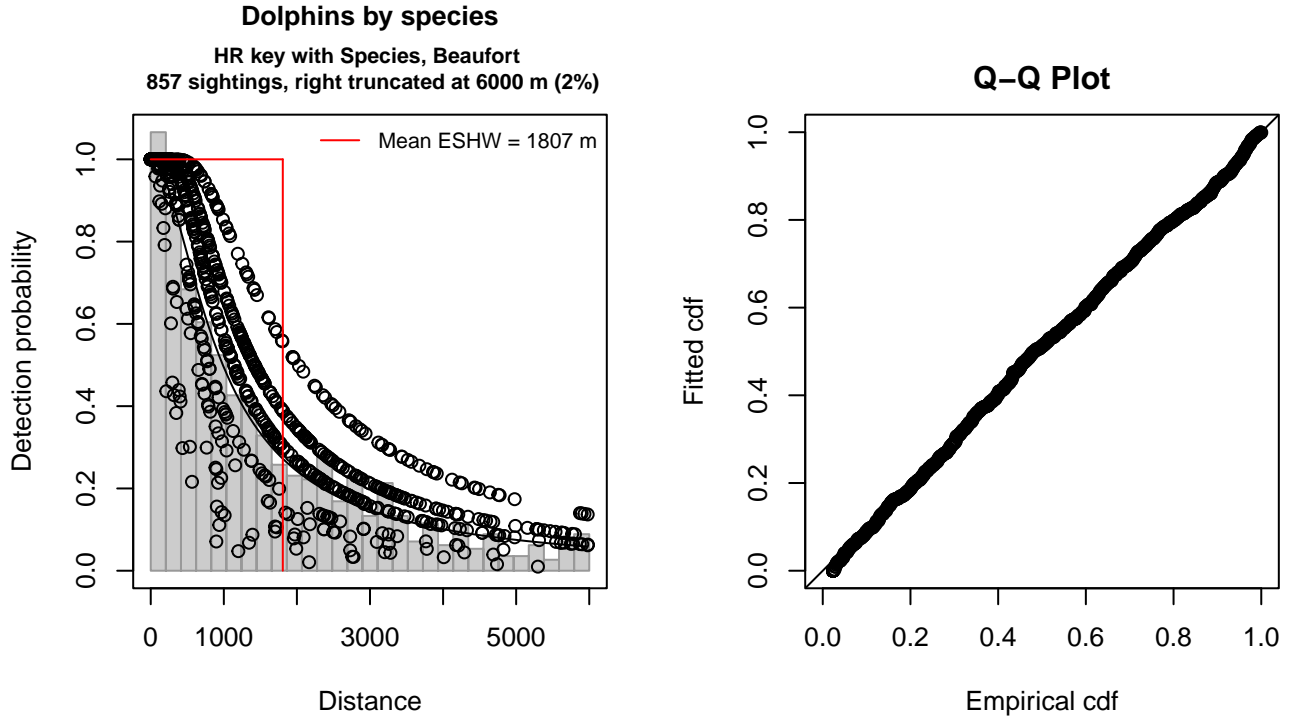


Figure 16: NEFSC AMAPPS detection function and Q-Q plot showing its goodness of fit.

Statistical output for this detection function:

Summary for ds object

Number of observations : 857  
 Distance range : 0 - 6000  
 AIC : 14222.66

Detection function:

Hazard-rate key function

Detection function parameters

Scale coefficient(s):

	estimate	se
(Intercept)	7.0022801	0.1342692
ScientificNameOther Stenella, Lagenodelphis	0.3515378	0.1854896
ScientificNameStenella frontalis	-0.5910499	0.3033455
ScientificNameTursiops, Steno	-0.2176361	0.1602756
Beaufort3-4	-0.5842019	0.1839783
Beaufort4-5	-1.4374209	0.2667762

Shape coefficient(s):

estimate	se
----------	----



(Intercept) 0.356339 0.0663051

	Estimate	SE	CV
Average p	0.2624967	0.01868208	0.07117073
N in covered region	3264.8026106	252.27662296	0.07727163

Distance sampling Cramer-von Mises test (unweighted)  
Test statistic = 0.089267 p = 0.640081

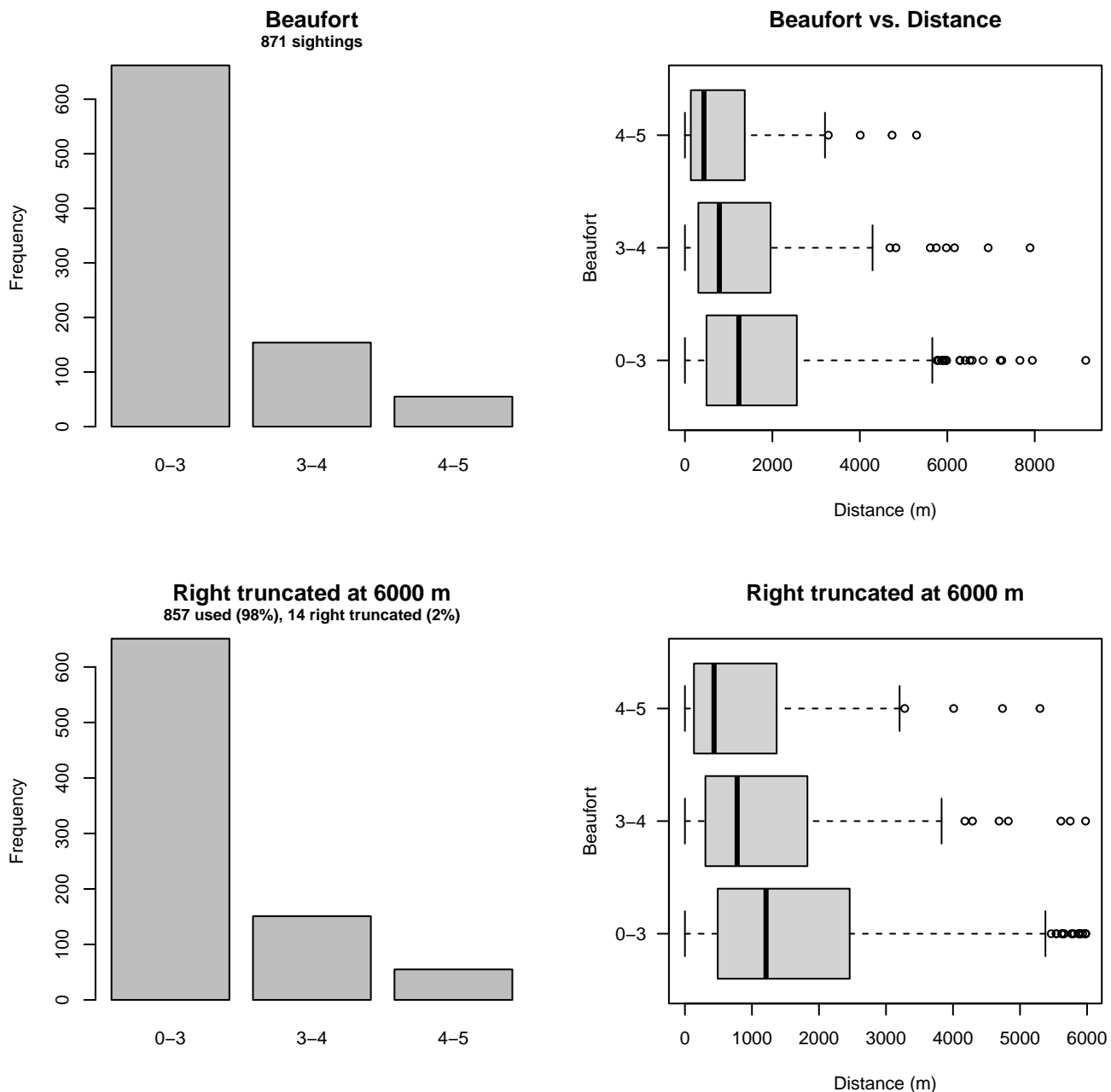


Figure 17: Distribution of the Beaufort covariate before (top row) and after (bottom row) observations were truncated to fit the NEFSC AMAPPS detection function.

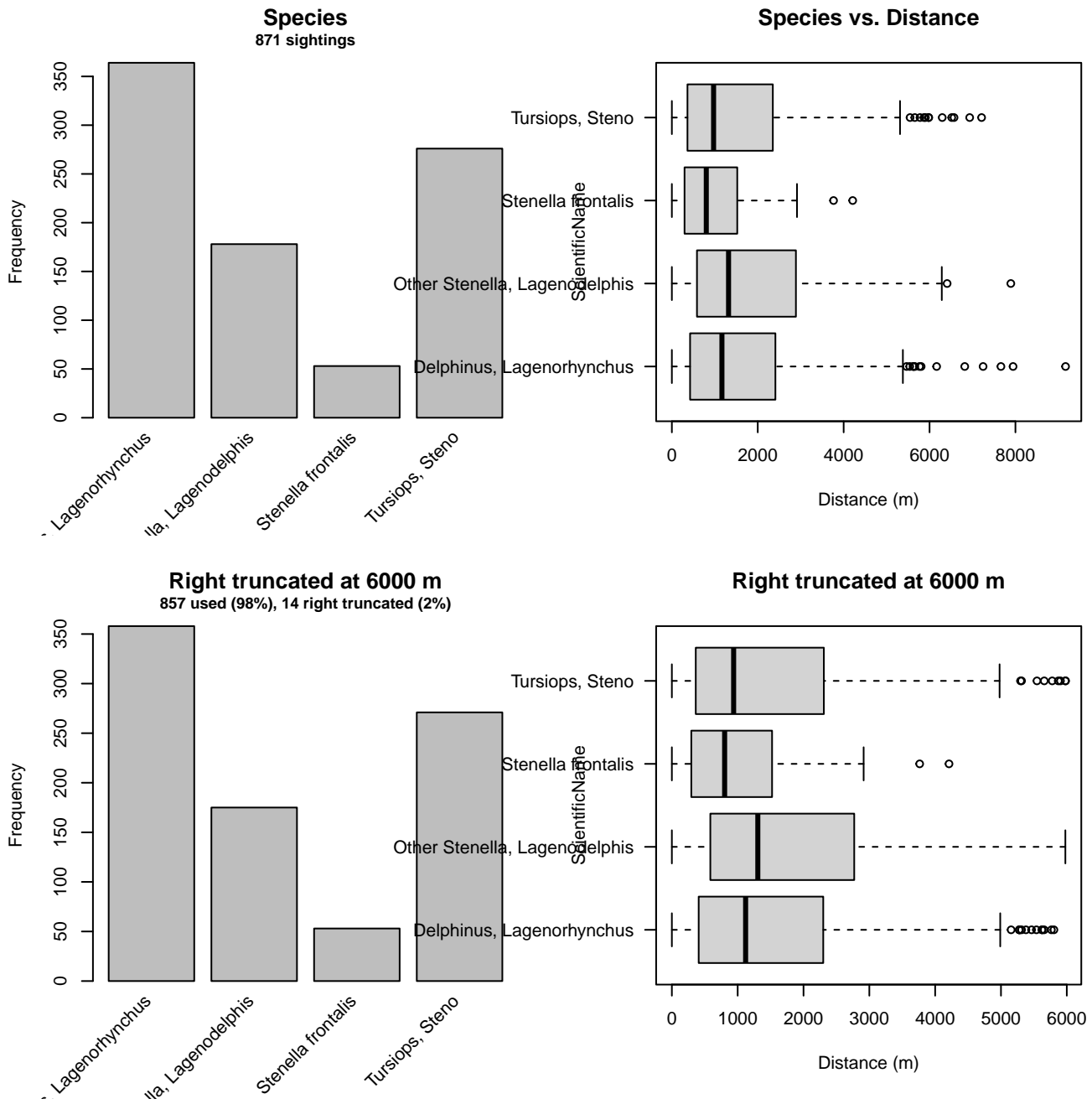


Figure 18: Distribution of the ScientificName covariate before (top row) and after (bottom row) observations were truncated to fit the NEFSC AMAPPS detection function.

### 2.1.2.3 Song of the Whale

After right-truncating observations greater than 700 m and left-truncating observations less than 1 m (Figure 20), we fitted the detection function to the 360 observations that remained (Table 8). The selected detection function (Figure 19) used a hazard rate key function with Beaufort (Figure 21), ScientificName (Figure 22) and Visibility (Figure 23) as covariates.

Table 8: Observations used to fit the Song of the Whale detection function.

ScientificName	n
All others	211
Delphinus	149
<b>Total</b>	<b>360</b>

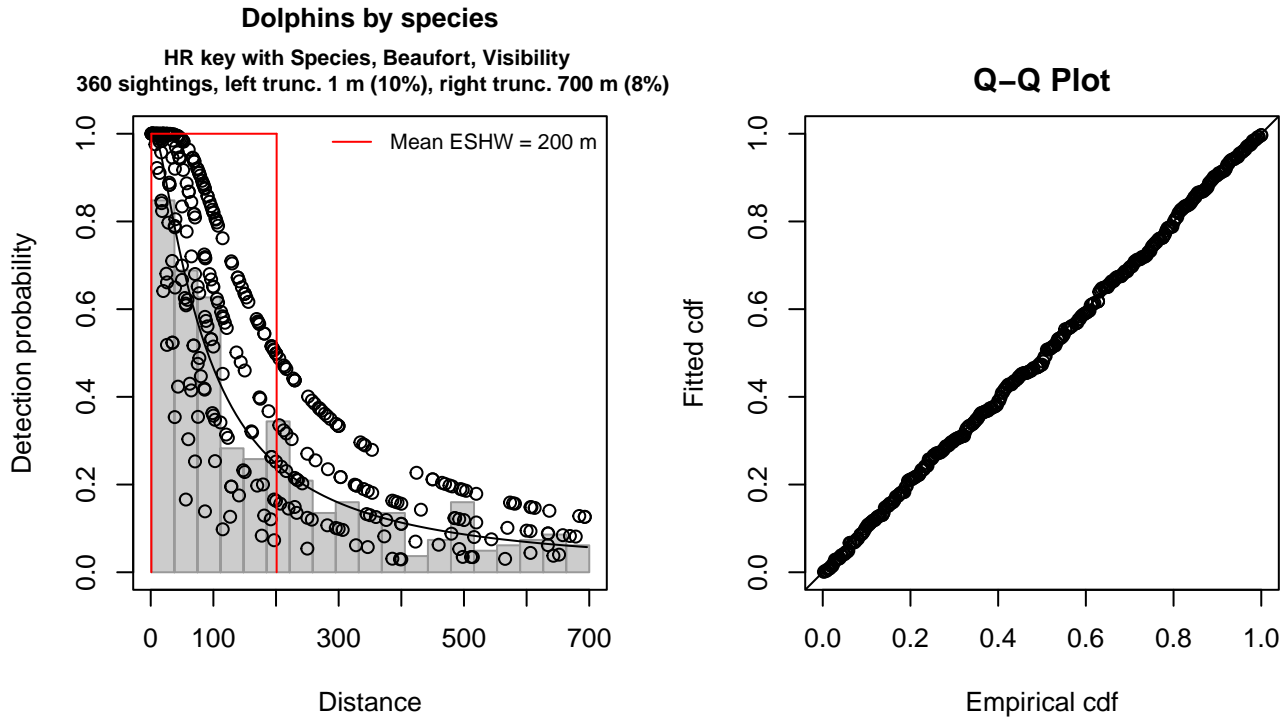


Figure 19: Song of the Whale detection function and Q-Q plot showing its goodness of fit.

Statistical output for this detection function:

Summary for ds object

Number of observations : 360  
 Distance range : 1 - 700  
 AIC : 4434.06

Detection function:

Hazard-rate key function

Detection function parameters

Scale coefficient(s):

	estimate	se
(Intercept)	5.0168382	0.2118228
ScientificNameDelphinus	-0.3746003	0.2526245
Beaufort3	-0.6586604	0.2922112
Beaufort3.5-4	-1.3223280	0.3841776
VisibilityModerate (2-5nmi)	-0.9687696	0.4363084

Shape coefficient(s):

	estimate	se
(Intercept)	0.2728327	0.09542948

	Estimate	SE	CV
Average p	0.232512	0.02944422	0.1266352
N in covered region	1548.306965	209.54903632	0.1353408

Distance sampling Cramer-von Mises test (unweighted)

Test statistic = 0.019198 p = 0.997687

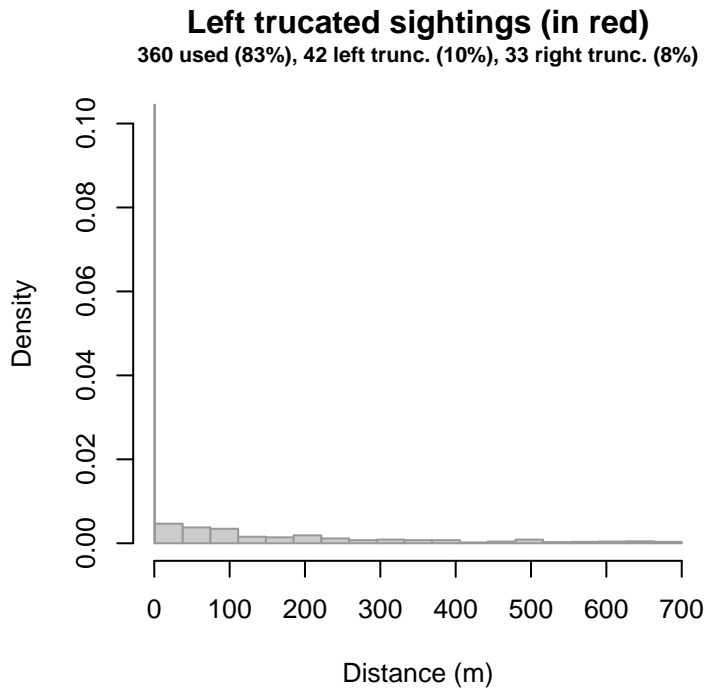


Figure 20: Density histogram of observations used to fit the Song of the Whale detection function, with the left-most bar showing observations at distances less than 1 m, which were left-truncated and not used to fit the detection function. (This bar may be very short if there were very few left-truncated sightings, or very narrow if the left truncation distance was very small; in either case it may not appear red.) These were excluded because they formed a problematic "spike" in detections close to the trackline, suggesting that animals approached the vessel (e.g. to bow-ride) prior to being detected. To address this, we fitted the detection function to the observations beyond the spike and assumed that within it, detection probability was 1, effectively treating it like a strip transect. We then added the left-truncated observations back into the analysis as if they occurred in this strip. This treatment may have resulted in an underestimation of detection probability.

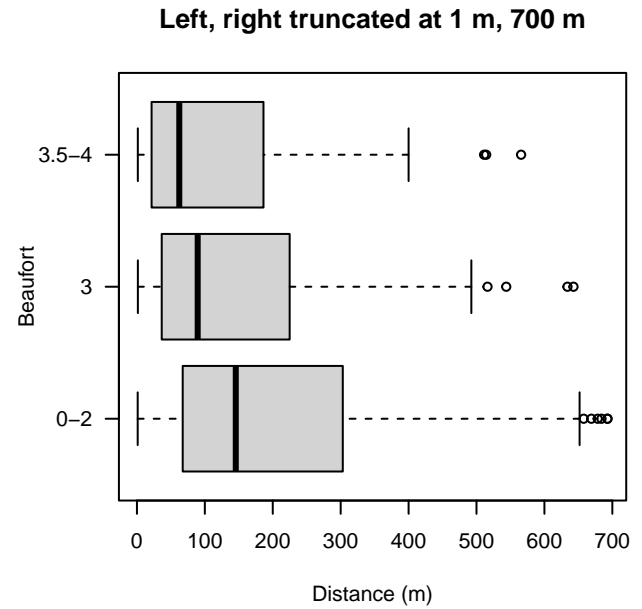
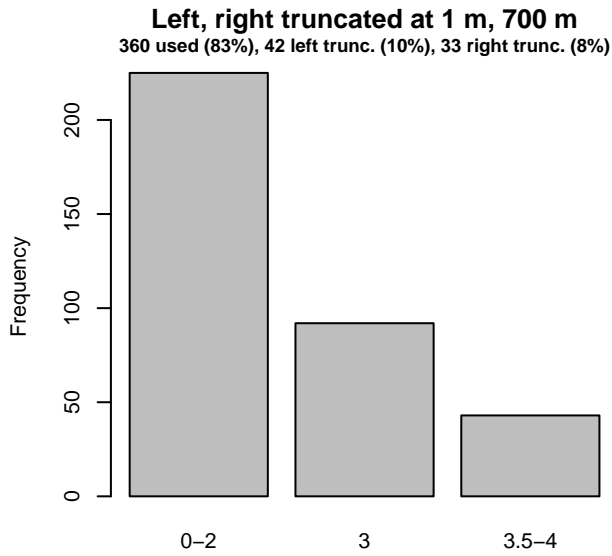
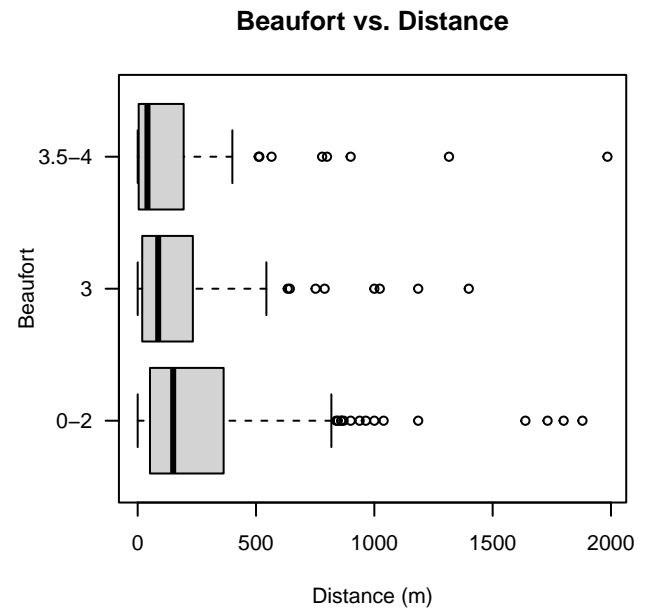
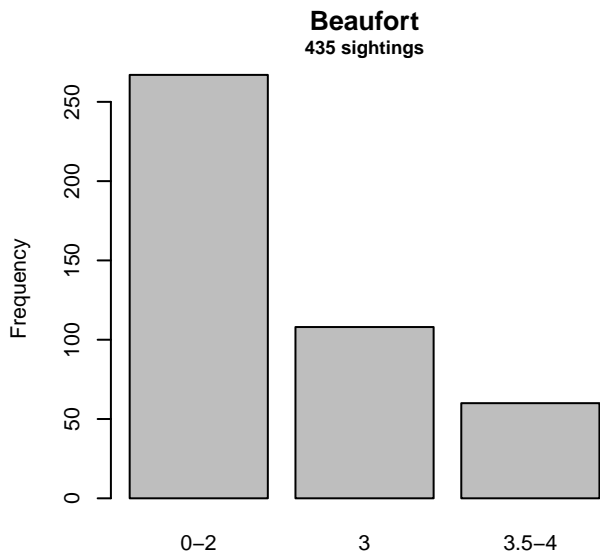


Figure 21: Distribution of the Beaufort covariate before (top row) and after (bottom row) observations were truncated to fit the Song of the Whale detection function.

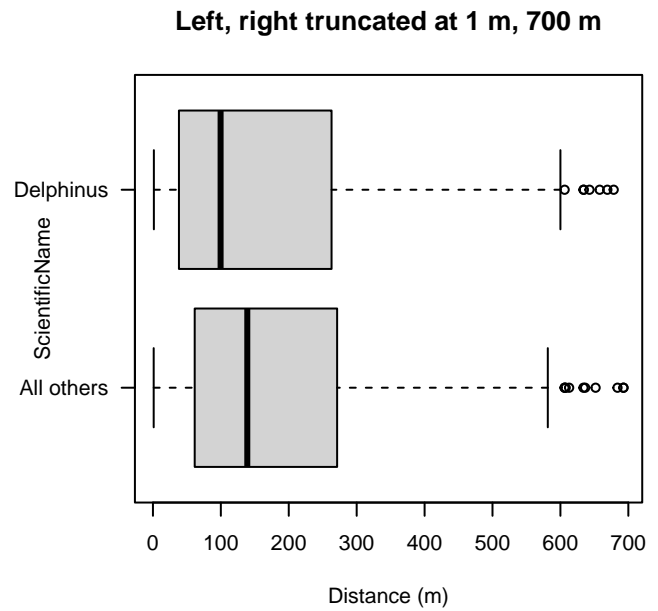
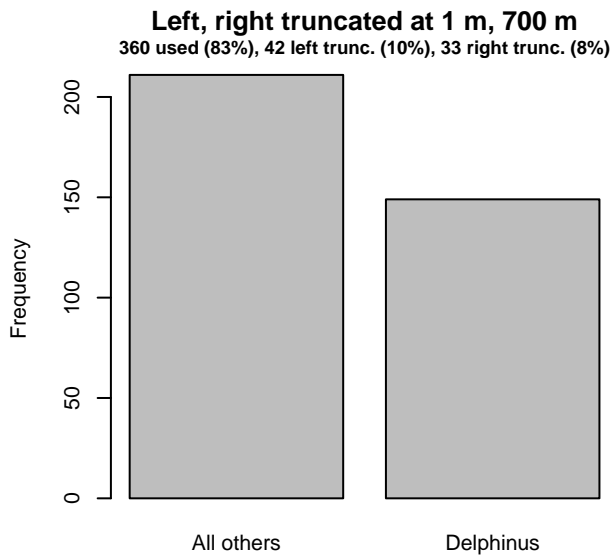
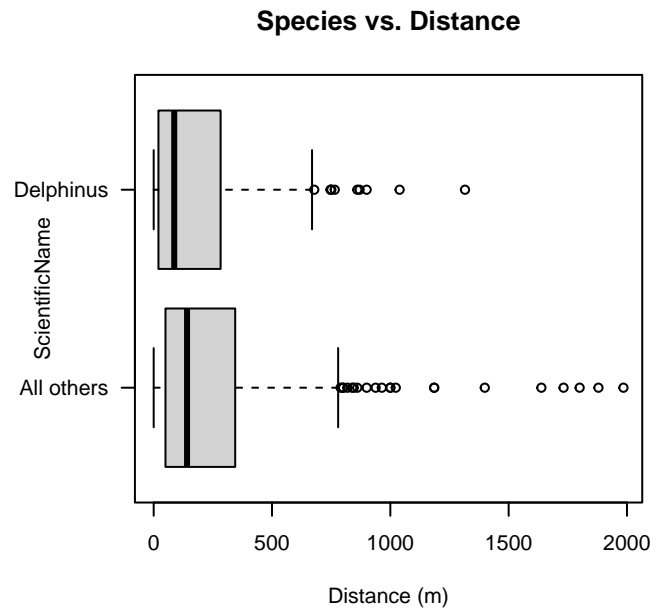
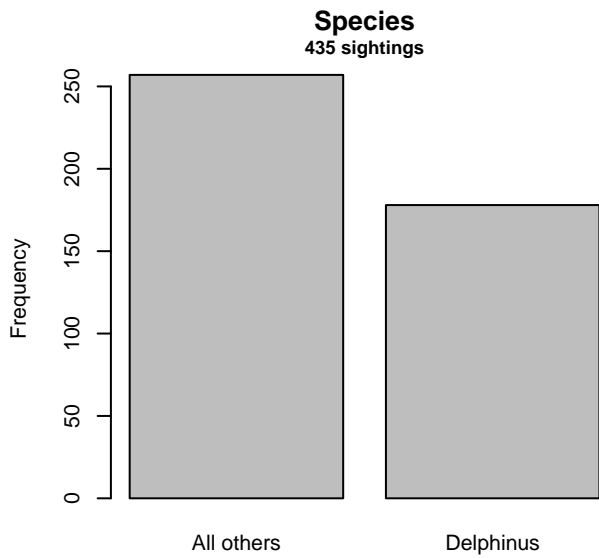


Figure 22: Distribution of the ScientificName covariate before (top row) and after (bottom row) observations were truncated to fit the Song of the Whale detection function.

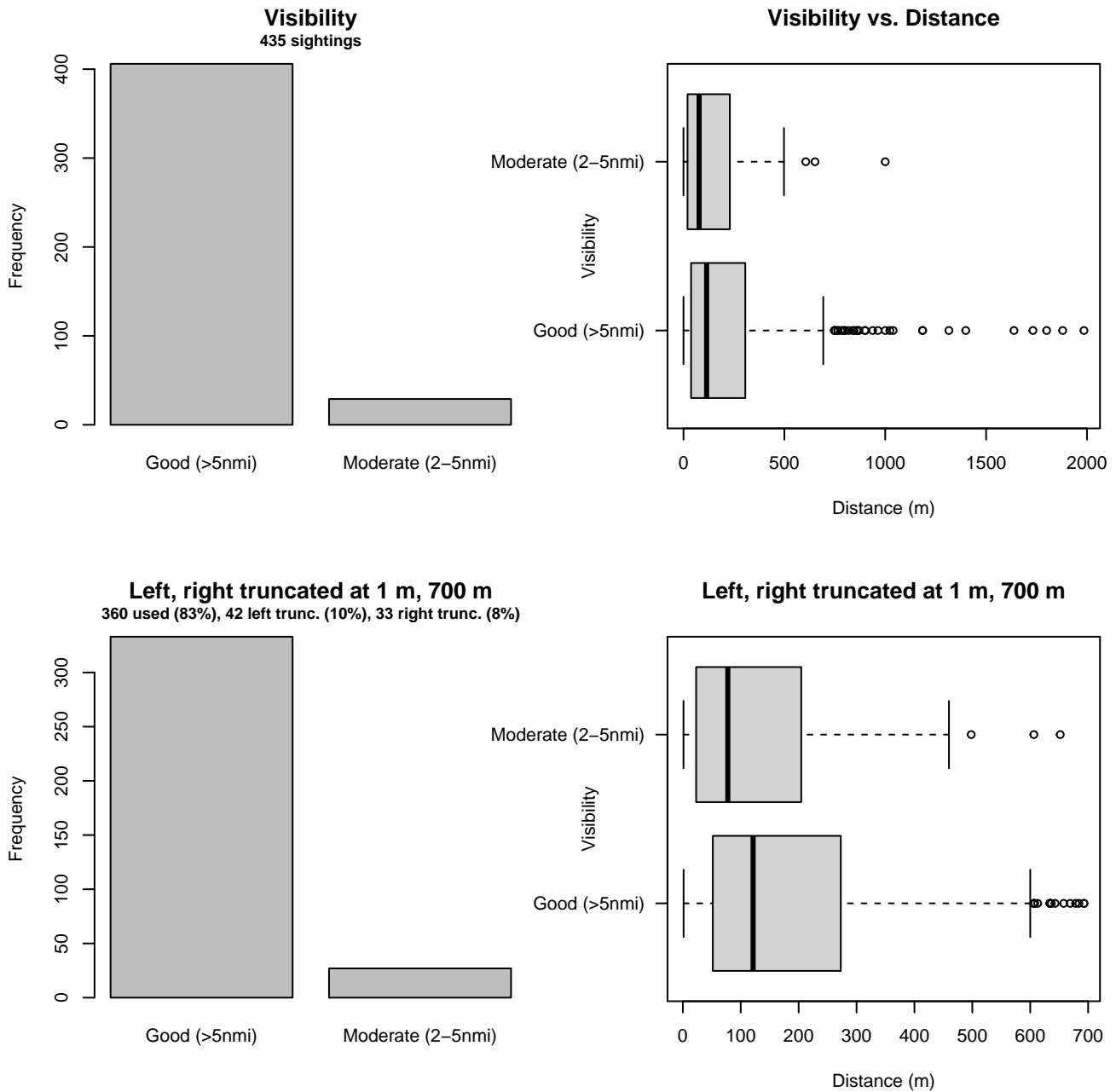


Figure 23: Distribution of the Visibility covariate before (top row) and after (bottom row) observations were truncated to fit the Song of the Whale detection function.

## 2.2 Without a Taxonomic Covariate

We fitted the detection functions in this section to pools of species with similar detectability characteristics but could not use a taxonomic identification as a covariate to account for differences between them. We usually took this approach after trying the taxonomic covariate and finding it had insufficient statistical power to be retained. We also resorted to it when the focal taxon being modeled had too few observations to be allocated its own taxonomic covariate level and was too poorly known for us to confidently determine which other taxa we could group it with.

## 2.2.1 Aerial Surveys

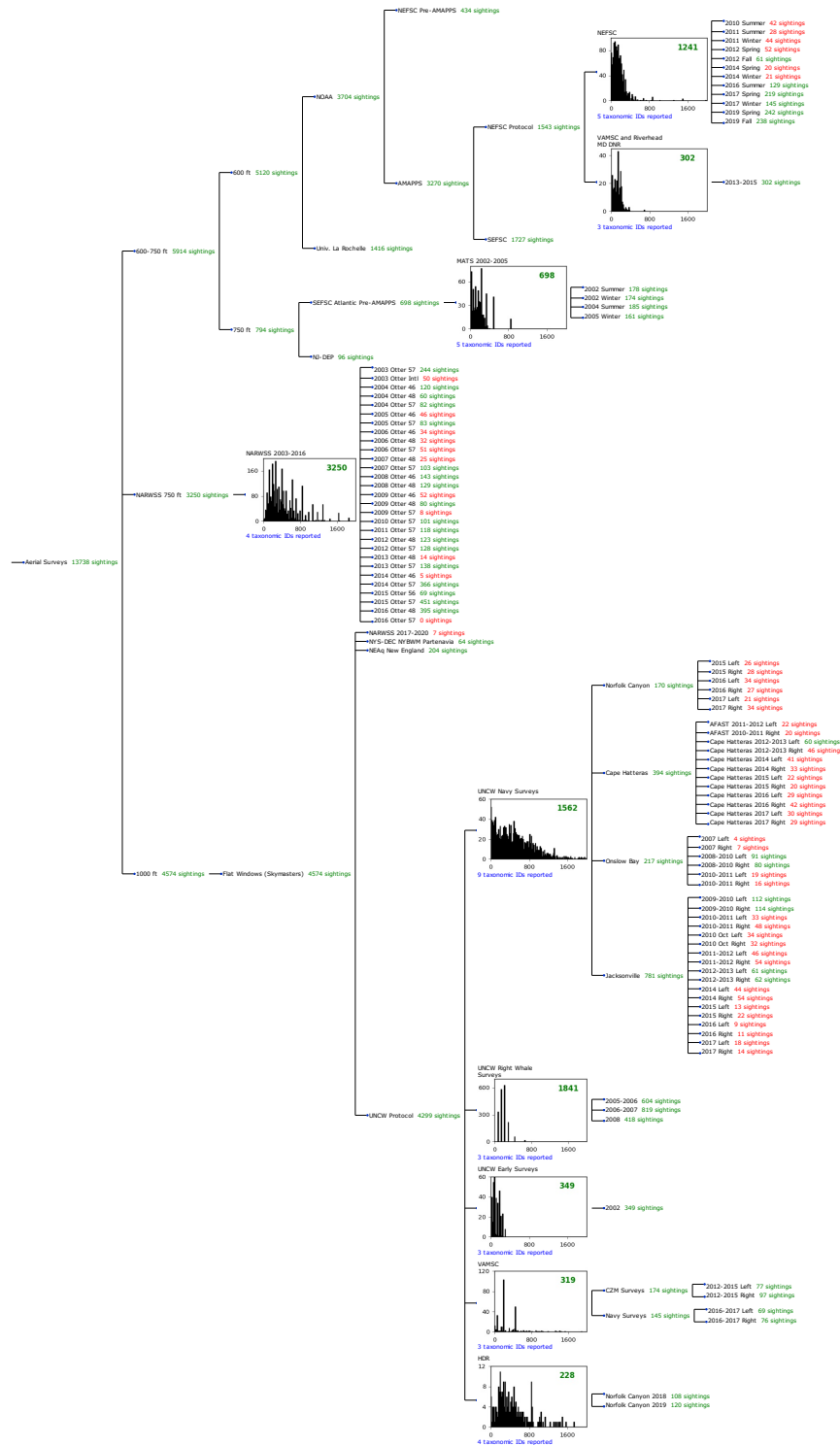


Figure 24: Detection hierarchy for aerial surveys, showing how they were pooled during detectability modeling, for detection functions that pooled multiple taxa but could not use a taxonomic covariate to account for differences between them. Each histogram represents a detection function and summarizes the perpendicular distances of observations that were pooled to fit it, prior to truncation. Observation counts, also prior to truncation, are shown in green when they met the recommendation of Buckland et al. (2001) that detection functions utilize at least 60 sightings, and red otherwise. For rare taxa, it was not always possible to meet this recommendation, yielding higher statistical uncertainty. During the spatial modeling stage of the analysis, effective strip widths were computed for each survey using the closest detection function above it in the hierarchy (i.e. moving from right to left in the figure). Surveys that do not have a detection function above them in this figure were either addressed by a detection function presented in a different section of this report, or were omitted from the analysis.



### 2.2.1.1 NEFSC AMAPPS

After right-truncating observations greater than 600 m, we fitted the detection function to the 1218 observations that remained (Table 9). The selected detection function (Figure 25) used a hazard rate key function with Season (Figure 26) as a covariate.

Table 9: Observations used to fit the NEFSC AMAPPS detection function.

ScientificName	n
Delphinus delphis	817
Lagenorhynchus acutus	280
Lagenorhynchus albirostris	3
Stenella coeruleoalba	13
Tursiops truncatus	105
<b>Total</b>	<b>1218</b>

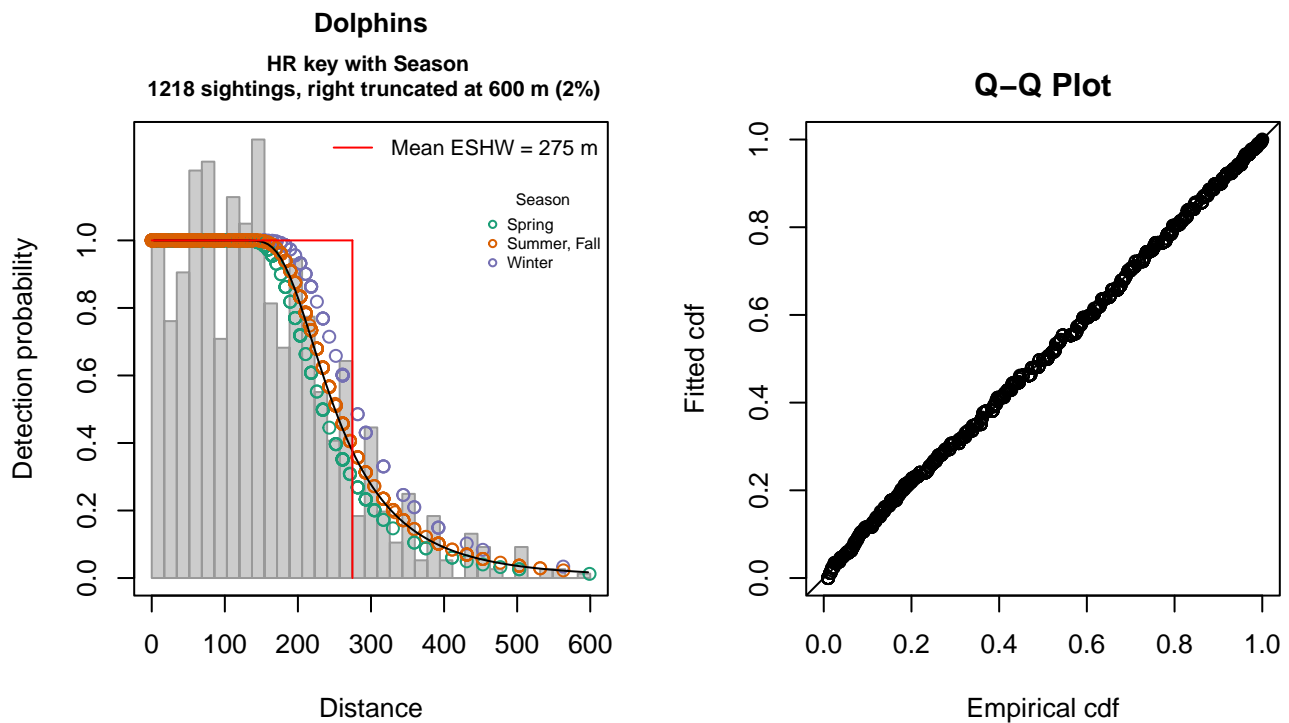


Figure 25: NEFSC AMAPPS detection function and Q-Q plot showing its goodness of fit.

Statistical output for this detection function:

Summary for ds object

Number of observations : 1218  
 Distance range : 0 - 600  
 AIC : 14460.69

Detection function:

Hazard-rate key function

Detection function parameters

Scale coefficient(s):

	estimate	se
(Intercept)	5.36944749	0.04422696
SeasonSummer, Fall	0.08083579	0.04638562
SeasonWinter	0.17600218	0.07702020

Shape coefficient(s):

	estimate	se
(Intercept)	1.452854	0.065484

	Estimate	SE	CV
Average p	0.456561	0.00970389	0.02125431
N in covered region	2667.770370	79.97999993	0.02998009

Distance sampling Cramer-von Mises test (unweighted)  
 Test statistic = 0.126854 p = 0.468488

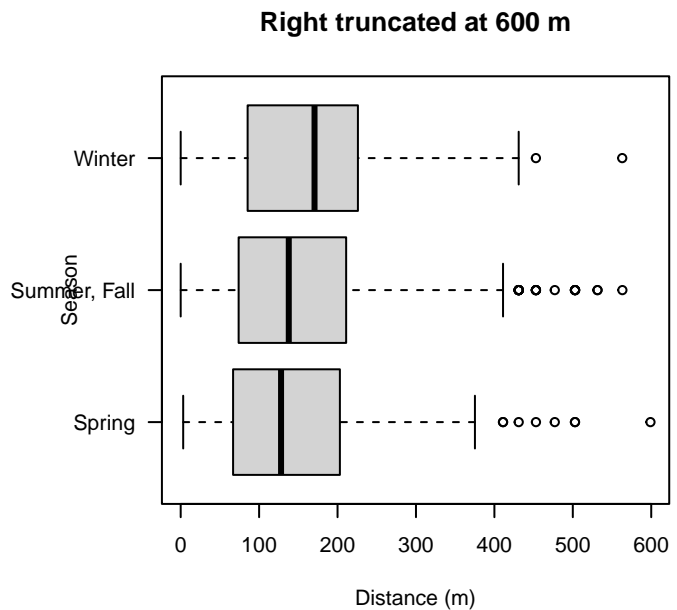
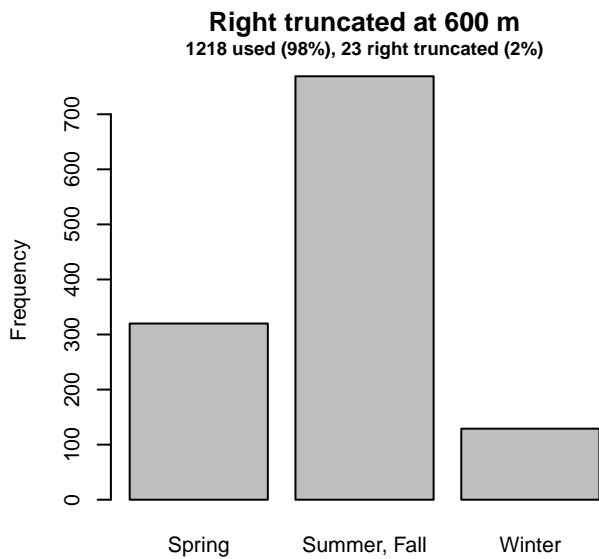
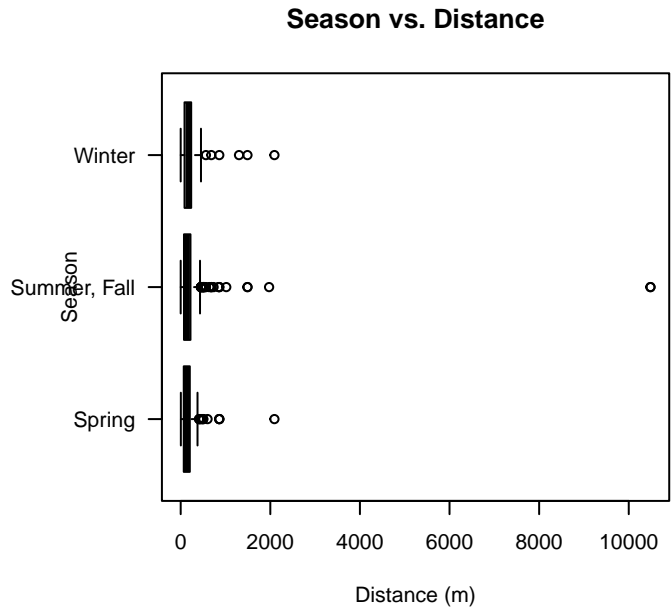
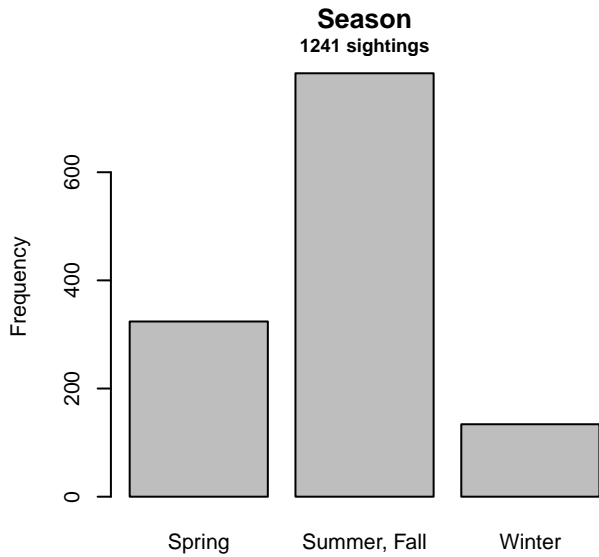


Figure 26: Distribution of the Season covariate before (top row) and after (bottom row) observations were truncated to fit the NEFSC AMAPPS detection function.

### 2.2.1.2 VAMSC and Riverhead MD DNR

After right-truncating observations greater than 400 m, we fitted the detection function to the 301 observations that remained (Table 10). The selected detection function (Figure 27) used a hazard rate key function with no covariates.

Table 10: Observations used to fit the VAMSC and Riverhead MD DNR detection function.

ScientificName	n
Delphinus delphis	22
Stenella frontalis	1
Tursiops truncatus	278
<b>Total</b>	<b>301</b>

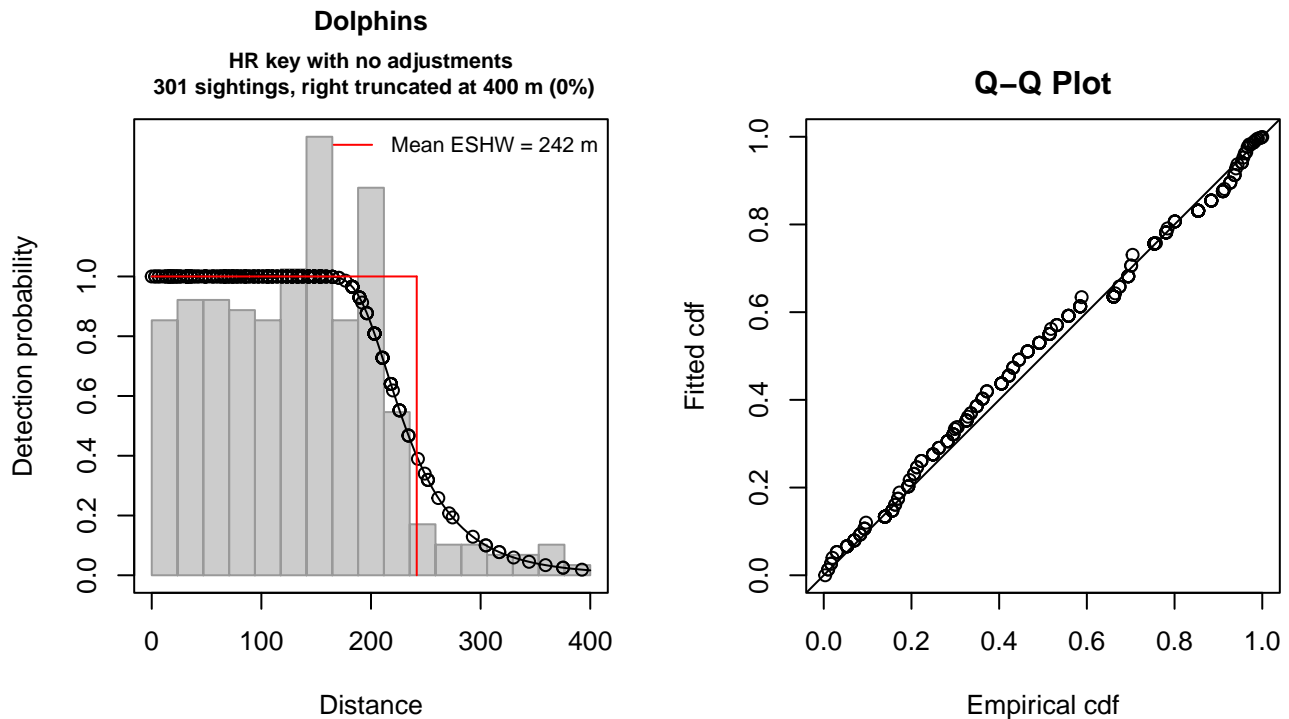


Figure 27: VAMSC and Riverhead MD DNR detection function and Q-Q plot showing its goodness of fit.

Statistical output for this detection function:

```
Summary for ds object
Number of observations : 301
Distance range       : 0 - 400
AIC                  : 3426.124
```

```
Detection function:
Hazard-rate key function
```

```
Detection function parameters
Scale coefficient(s):
      estimate      se
(Intercept) 5.388208 0.04209556
```

```
Shape coefficient(s):
      estimate      se
(Intercept) 1.91525 0.1331166
```

	Estimate	SE	CV
Average p	0.6042969	0.0203517	0.03367831
N in covered region	498.0995265	24.6489147	0.04948592

Distance sampling Cramer-von Mises test (unweighted)  
 Test statistic = 0.302011 p = 0.133421

### 2.2.1.3 MATS 2002-2005

After right-truncating observations greater than 629 m, we fitted the detection function to the 684 observations that remained (Table 11). The selected detection function (Figure 28) used a hazard rate key function with Beaufort (Figure 29) as a covariate.

Table 11: Observations used to fit the MATS 2002-2005 detection function.

ScientificName	n
Delphinus delphis	2
Stenella attenuata	2
Stenella frontalis	104
Tursiops truncatus	576
<b>Total</b>	<b>684</b>

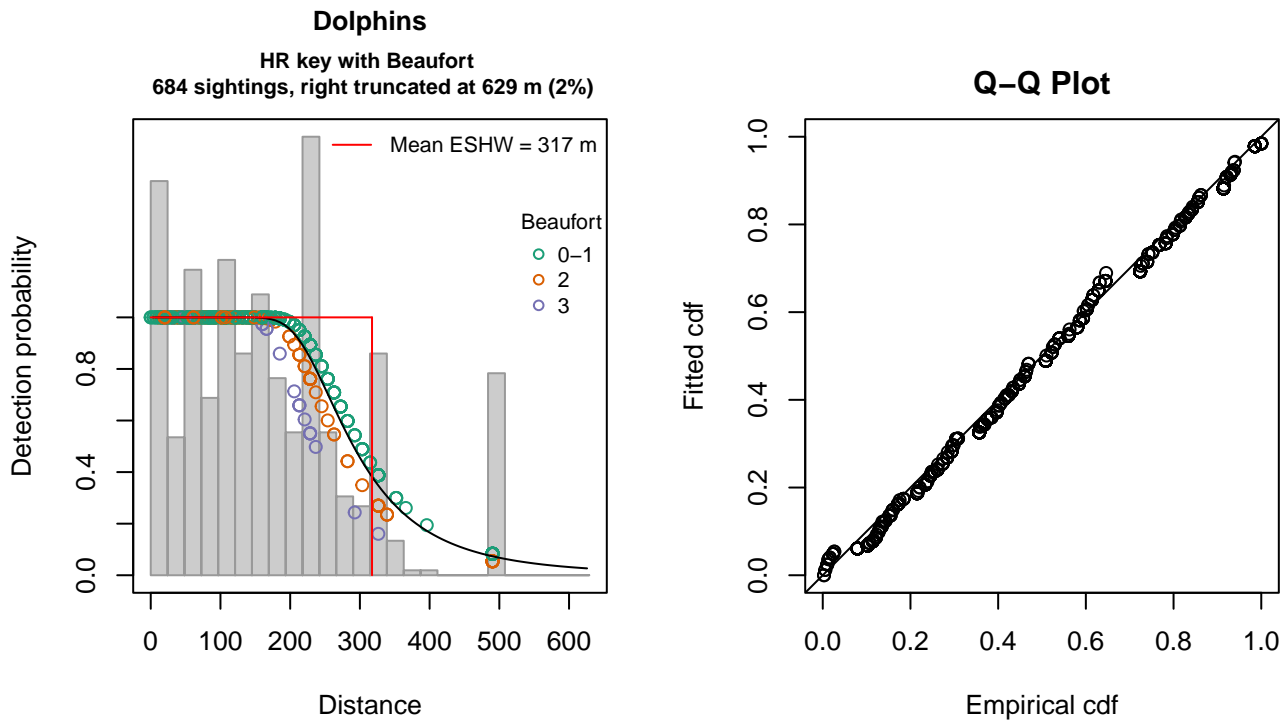


Figure 28: MATS 2002-2005 detection function and Q-Q plot showing its goodness of fit.

Statistical output for this detection function:

```
Summary for ds object
Number of observations : 684
Distance range       : 0 - 629
AIC                  : 8306.088
```

Detection function:

Hazard-rate key function

Detection function parameters

Scale coefficient(s):

	estimate	se
(Intercept)	5.6213531	0.04325709
Beaufort2	-0.1046854	0.06814971
Beaufort3	-0.2421057	0.13060115

Shape coefficient(s):

	estimate	se
(Intercept)	1.449025	0.08965229

	Estimate	SE	CV
Average p	0.5026836	0.0147185	0.02927984
N in covered region	1360.6968013	54.2106880	0.03984039

Distance sampling Cramer-von Mises test (unweighted)

Test statistic = 0.194502 p = 0.278380

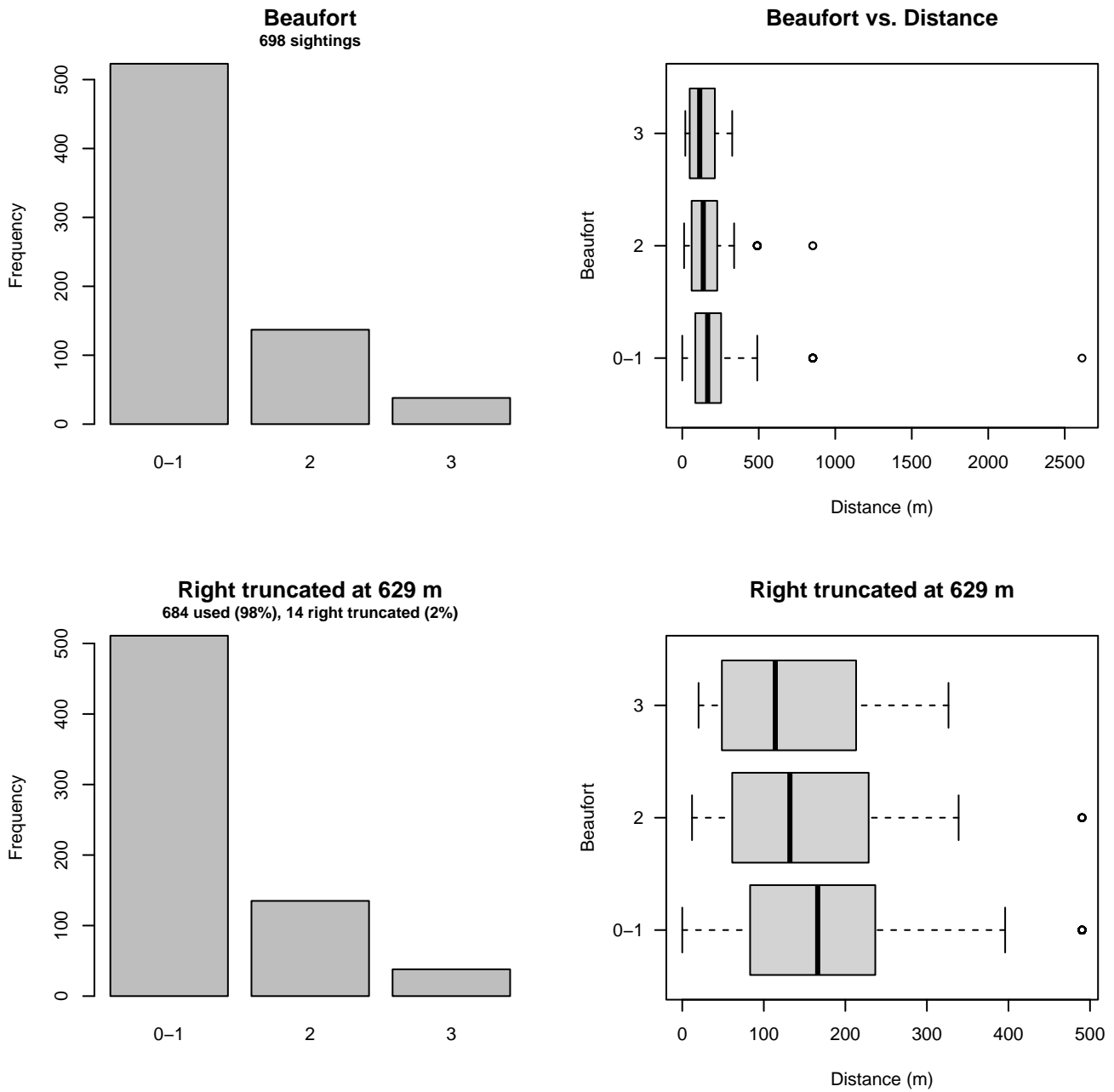


Figure 29: Distribution of the Beaufort covariate before (top row) and after (bottom row) observations were truncated to fit the MATS 2002-2005 detection function.

#### 2.2.1.4 NARWSS 2003-2016

After right-truncating observations greater than 1367 m and left-truncating observations less than 61 m (Figure 31), we fitted the detection function to the 3073 observations that remained (Table 12). The selected detection function (Figure 30) used a hazard rate key function with Beaufort (Figure 32) and Season (Figure 33) as covariates.

Table 12: Observations used to fit the NARWSS 2003-2016 detection function.

ScientificName	n
Delphinus delphis	607
Lagenorhynchus acutus	2404
Lagenorhynchus albirostris	6
Tursiops truncatus	56
<b>Total</b>	<b>3073</b>

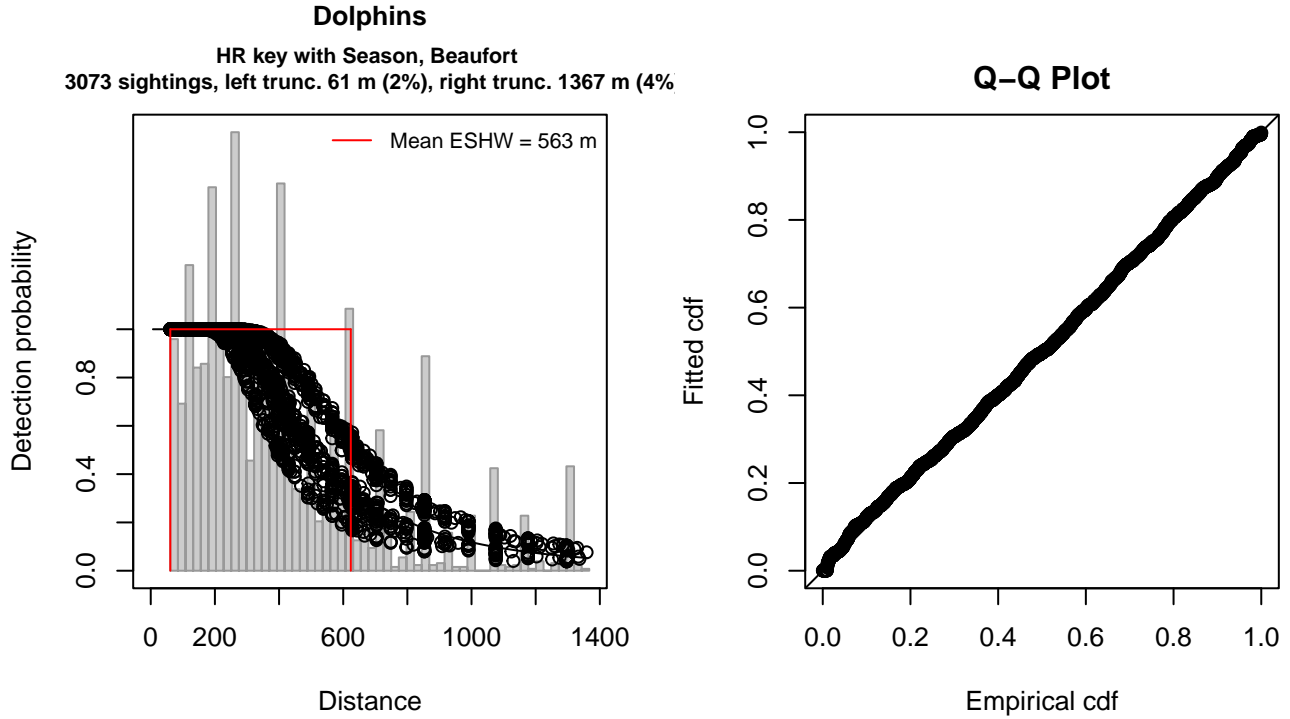


Figure 30: NARWSS 2003-2016 detection function and Q-Q plot showing its goodness of fit.

Statistical output for this detection function:

Summary for ds object

Number of observations : 3073  
 Distance range : 61 - 1367  
 AIC : 41850.8

Detection function:

Hazard-rate key function

Detection function parameters

Scale coefficient(s):

	estimate	se
(Intercept)	6.10469263	0.07579397
SeasonSpring	0.06689438	0.05622050
SeasonSummer	0.29278056	0.05383279
SeasonWinter	-0.15259970	0.06804643
Beaufort	-0.03572691	0.02383833

Shape coefficient(s):

	estimate	se
(Intercept)	1.009361	0.0398862

	Estimate	SE	CV
Average p	0.4196247	8.827249e-03	0.02103606
N in covered region	7323.2113220	1.845410e+02	0.02519946

Distance sampling Cramer-von Mises test (unweighted)  
 Test statistic = 0.246036 p = 0.193531

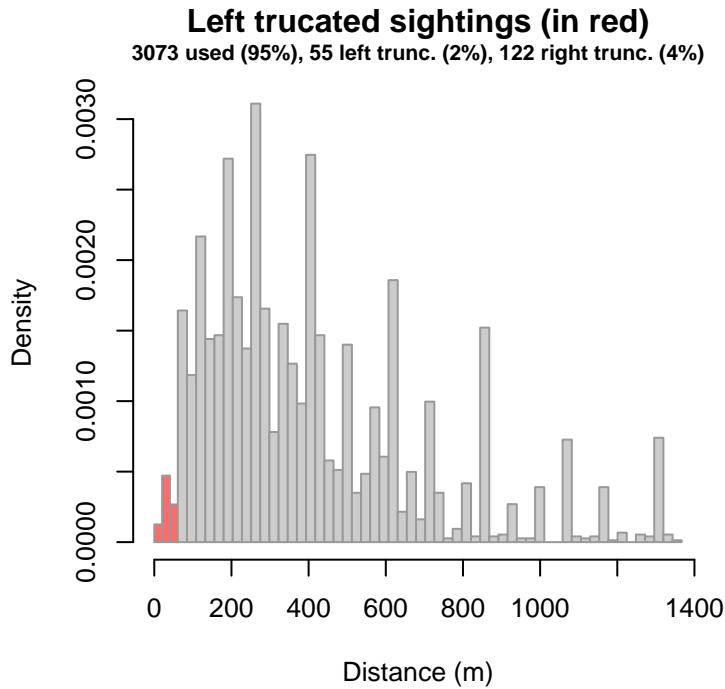


Figure 31: Density histogram of observations used to fit the NARWSS 2003-2016 detection function, with the left-most bar showing observations at distances less than 61 m, which were left-truncated and excluded from the analysis [Buckland et al. (2001)]. (This bar may be very short if there were very few left-truncated sightings, or very narrow if the left truncation distance was very small; in either case it may not appear red.)



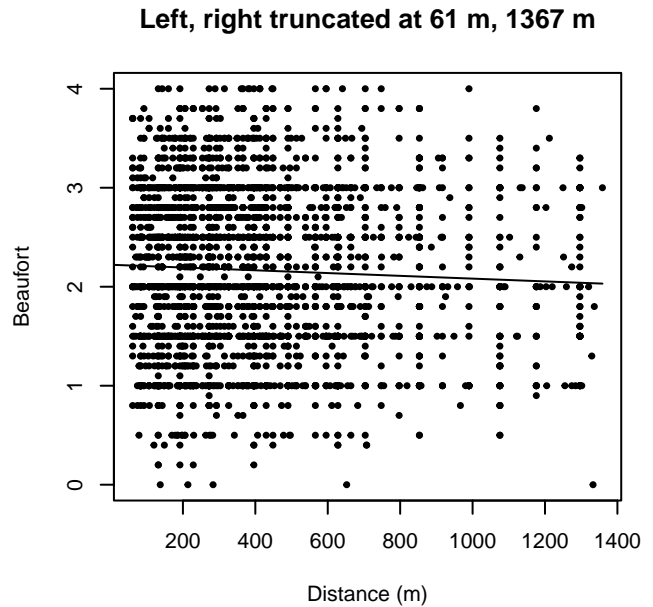
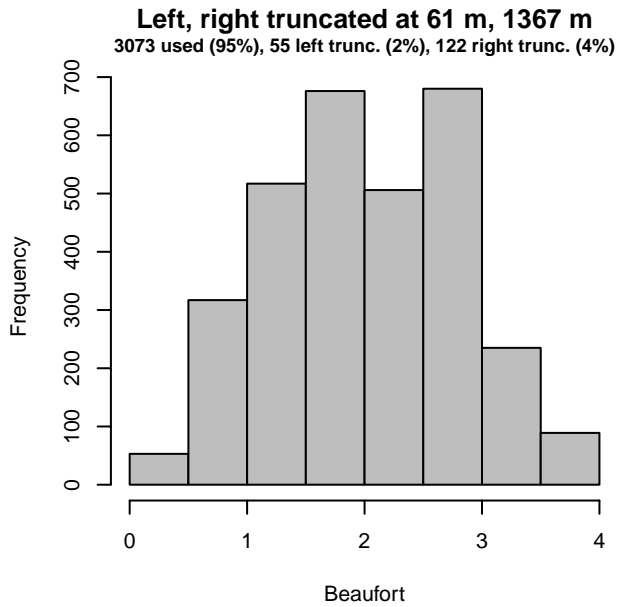
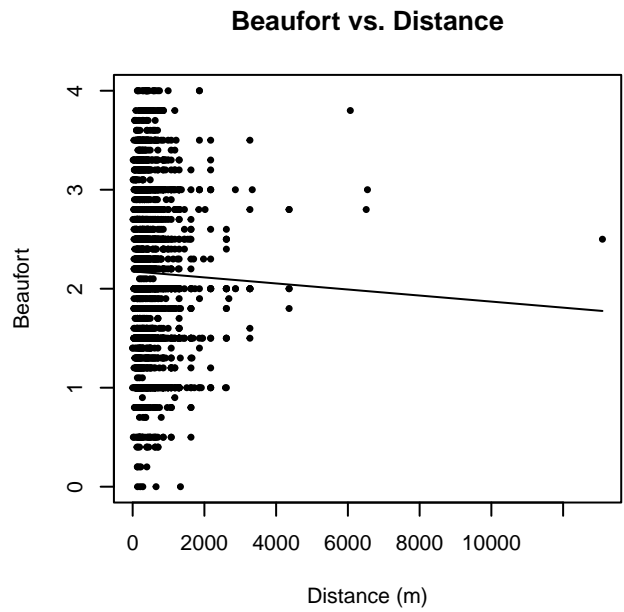
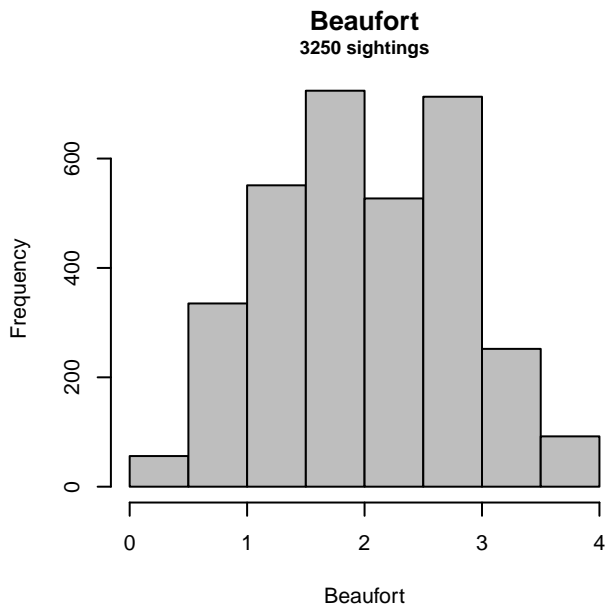


Figure 32: Distribution of the Beaufort covariate before (top row) and after (bottom row) observations were truncated to fit the NARWSS 2003-2016 detection function.

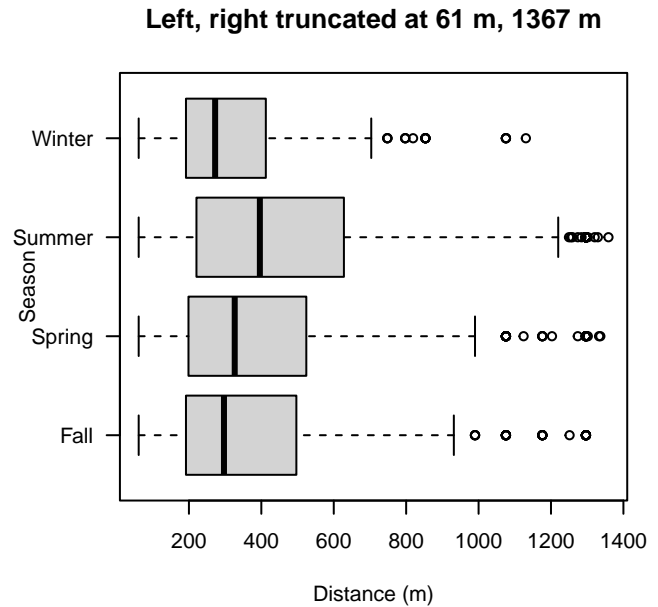
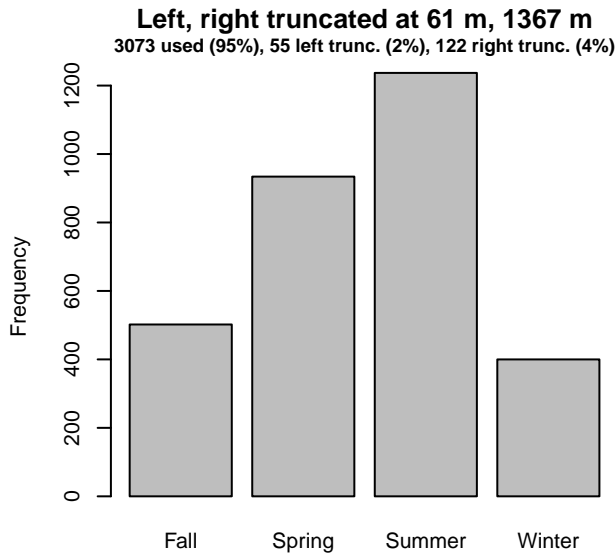
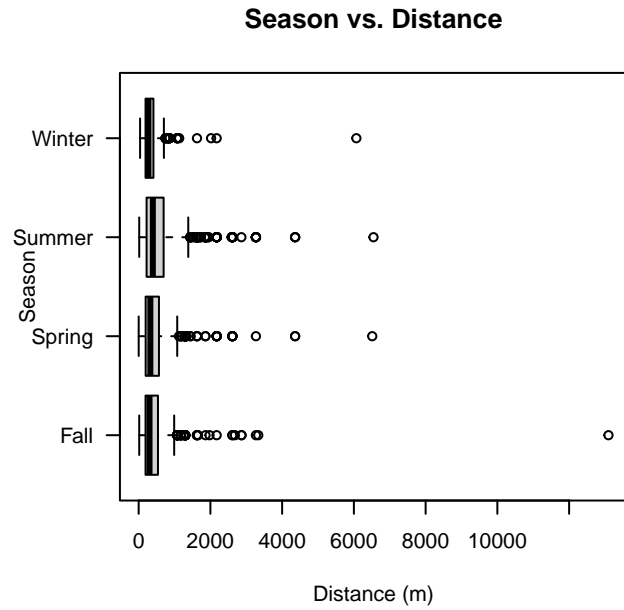
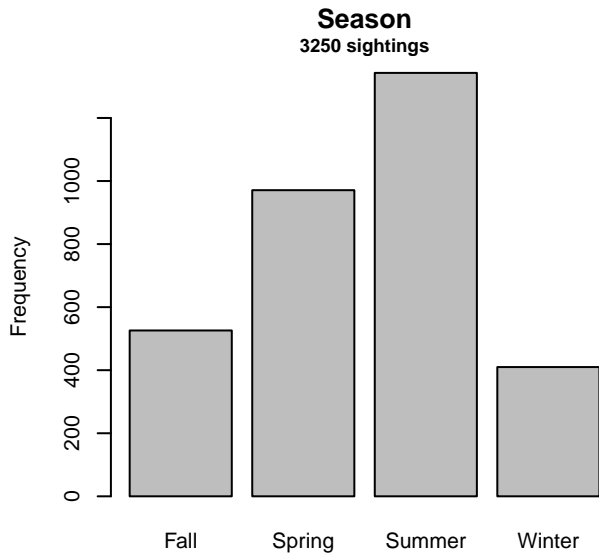


Figure 33: Distribution of the Season covariate before (top row) and after (bottom row) observations were truncated to fit the NARWSS 2003-2016 detection function.

### 2.2.1.5 UNCW Navy Surveys

After right-truncating observations greater than 1600 m, we fitted the detection function to the 1523 observations that remained (Table 13). The selected detection function (Figure 34) used a half normal key function with Glare (Figure 35) and Visibility (Figure 36) as covariates.

Table 13: Observations used to fit the UNCW Navy Surveys detection function.

ScientificName	n
Delphinus delphis	77
Lagenodelphis hosei	1
Stenella attenuata	2
Stenella clymene	11
Stenella coeruleoalba	19
Stenella frontalis	480
Stenella longirostris	1
Steno bredanensis	14
Tursiops truncatus	918
<b>Total</b>	<b>1523</b>

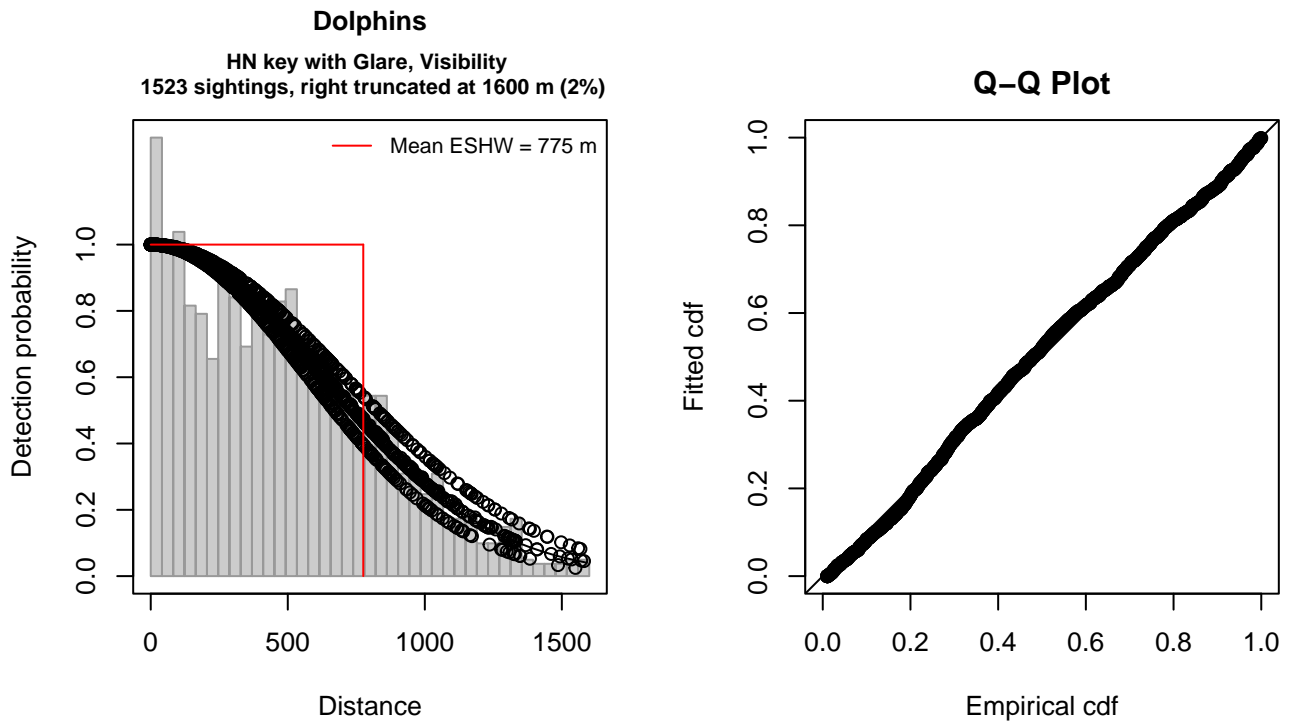


Figure 34: UNCW Navy Surveys detection function and Q-Q plot showing its goodness of fit.

Statistical output for this detection function:

Summary for ds object

Number of observations : 1523  
 Distance range : 0 - 1600  
 AIC : 21665.78

Detection function:

Half-normal key function

Detection function parameters

Scale coefficient(s):

	estimate	se
(Intercept)	6.55223233	0.04798577
GlareNone, 0-25%, Unk.	-0.10934970	0.05247015
VisibilityHalf	-0.09759271	0.04601702

	Estimate	SE	CV
Average p	0.4827398	0.01003395	0.02078542
N in covered region	3154.9084328	87.71221948	0.02780183

Distance sampling Cramer-von Mises test (unweighted)  
 Test statistic = 0.331909 p = 0.110182

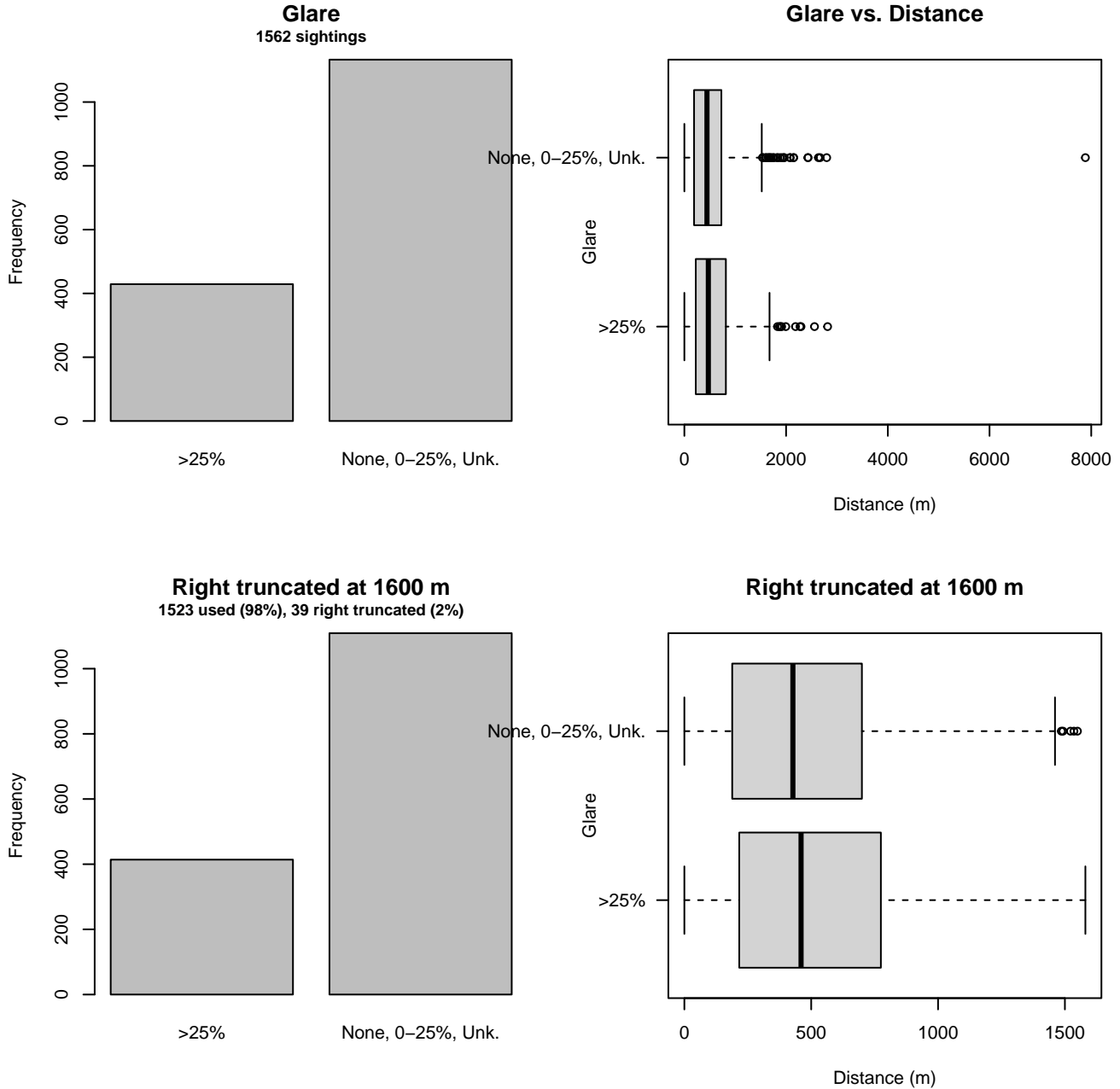


Figure 35: Distribution of the Glare covariate before (top row) and after (bottom row) observations were truncated to fit the UNCW Navy Surveys detection function.

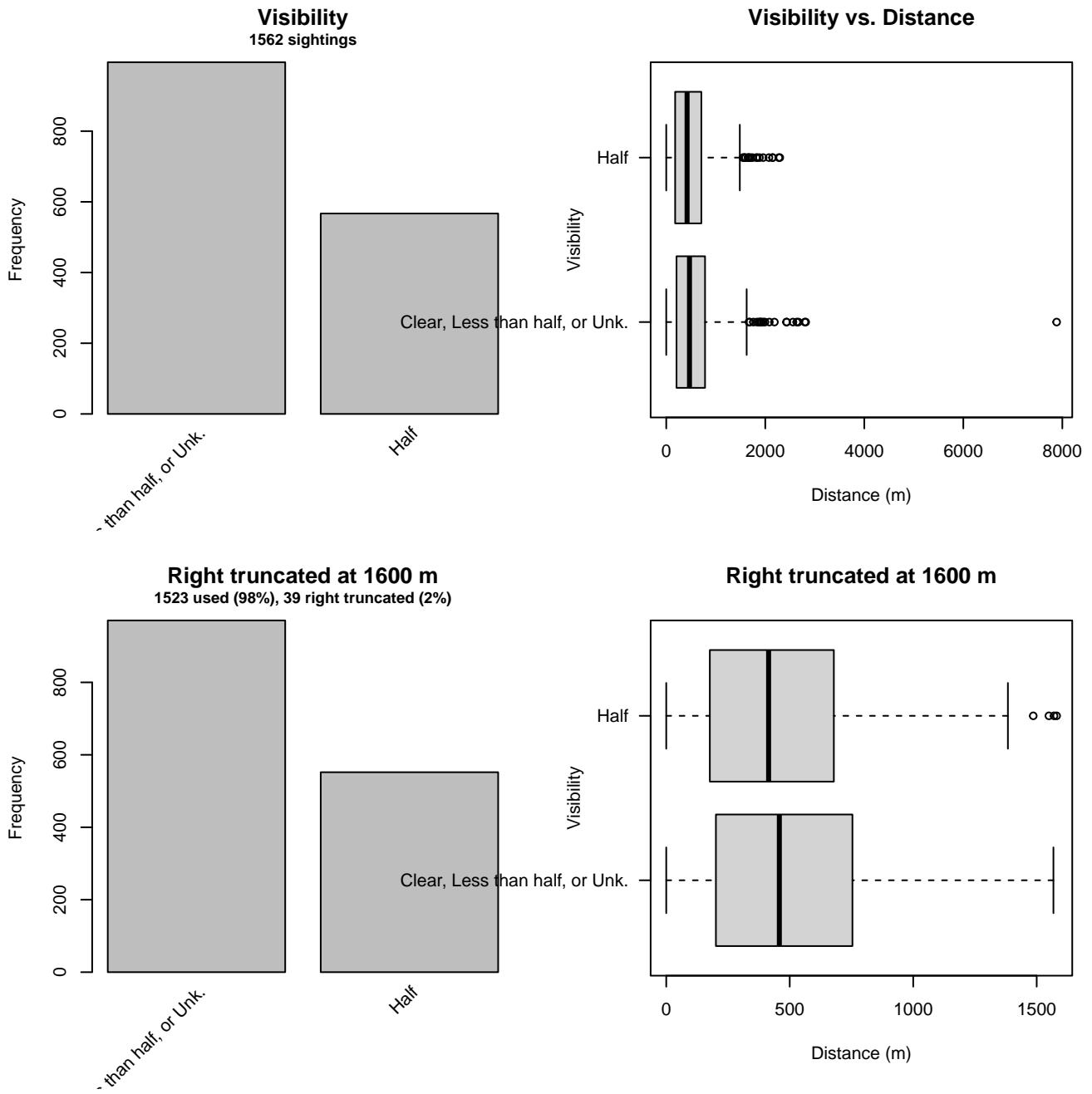


Figure 36: Distribution of the Visibility covariate before (top row) and after (bottom row) observations were truncated to fit the UNCW Navy Surveys detection function.

### 2.2.1.6 UNCW Right Whale Surveys

After right-truncating observations greater than 528 m and left-truncating observations less than 54 m (Figure 38), we fitted the detection function to the 1821 observations that remained (Table 14). The selected detection function (Figure 37) used a hazard rate key function with no covariates.

Table 14: Observations used to fit the UNCW Right Whale Surveys detection function.

ScientificName	n
Delphinus delphis	26
Stenella frontalis	4
Tursiops truncatus	1791
<b>Total</b>	<b>1821</b>

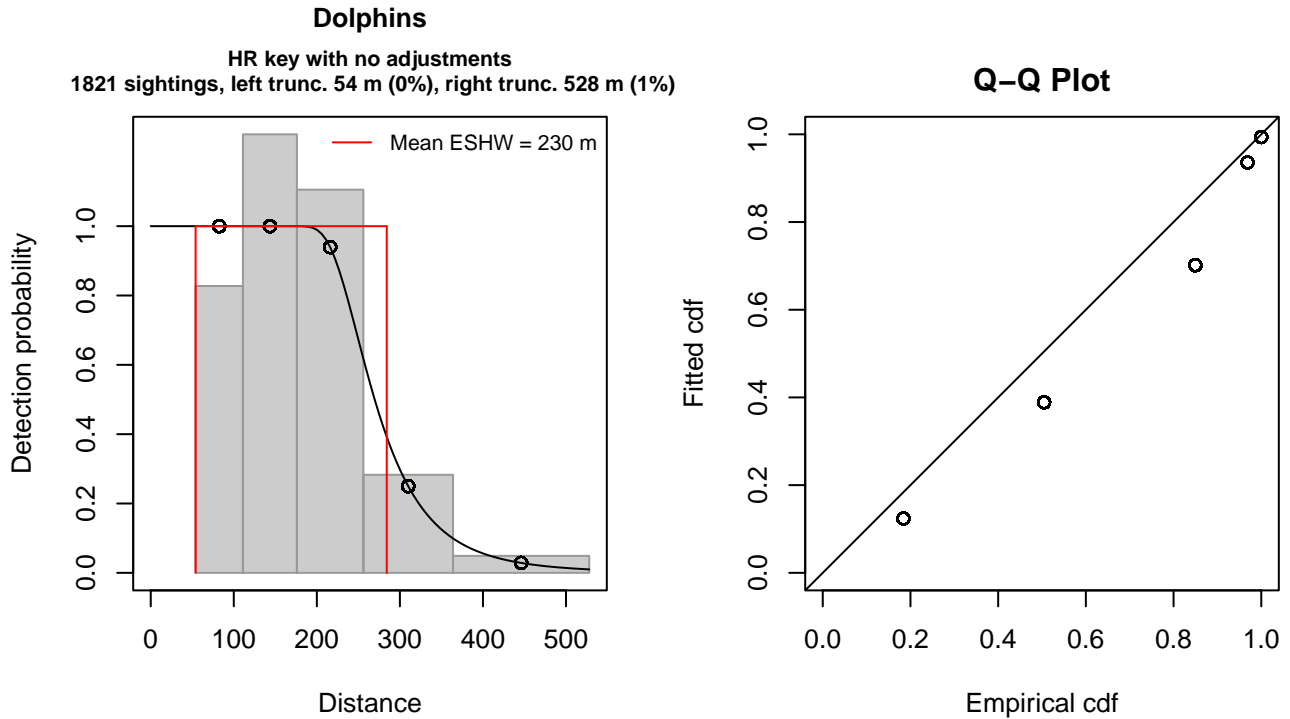


Figure 37: UNCW Right Whale Surveys detection function and Q-Q plot showing its goodness of fit.

Statistical output for this detection function:

Summary for ds object

Number of observations : 1821  
 Distance range : 54 - 528  
 AIC : 5176.116

Detection function:

Hazard-rate key function

Detection function parameters

Scale coefficient(s):

	estimate	se
(Intercept)	5.538954	0.02098751

Shape coefficient(s):

	estimate	se
(Intercept)	1.841299	0.06464608

	Estimate	SE	CV
Average p	0.4855453	0.009233858	0.01901750
N in covered region	3750.4226341	95.188173832	0.02538065

Distance sampling Cramer-von Mises test (unweighted)  
 Test statistic = 14.468539 p = 0.010416

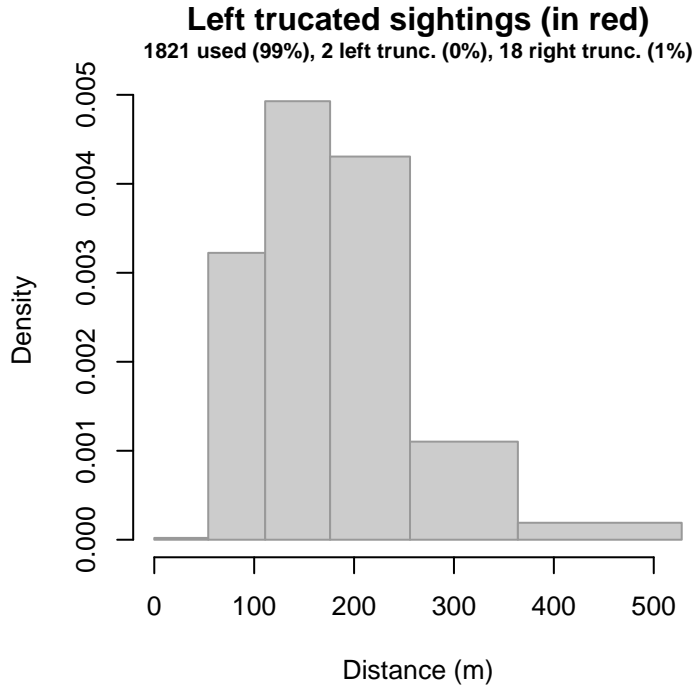


Figure 38: Density histogram of observations used to fit the UNCW Right Whale Surveys detection function, with the left-most bar showing observations at distances less than 54 m, which were left-truncated and excluded from the analysis [Buckland et al. (2001)]. (This bar may be very short if there were very few left-truncated sightings, or very narrow if the left truncation distance was very small; in either case it may not appear red.)

### 2.2.1.7 UNCW Early Surveys

After right-truncating observations greater than 333 m and left-truncating observations less than 14 m (Figure 40), we fitted the detection function to the 349 observations that remained (Table 15). The selected detection function (Figure 39) used a half normal key function with Beaufort (Figure 41) as a covariate.

Table 15: Observations used to fit the UNCW Early Surveys detection function.

ScientificName	n
Delphinus delphis	5
Stenella frontalis	1
Tursiops truncatus	343
<b>Total</b>	<b>349</b>

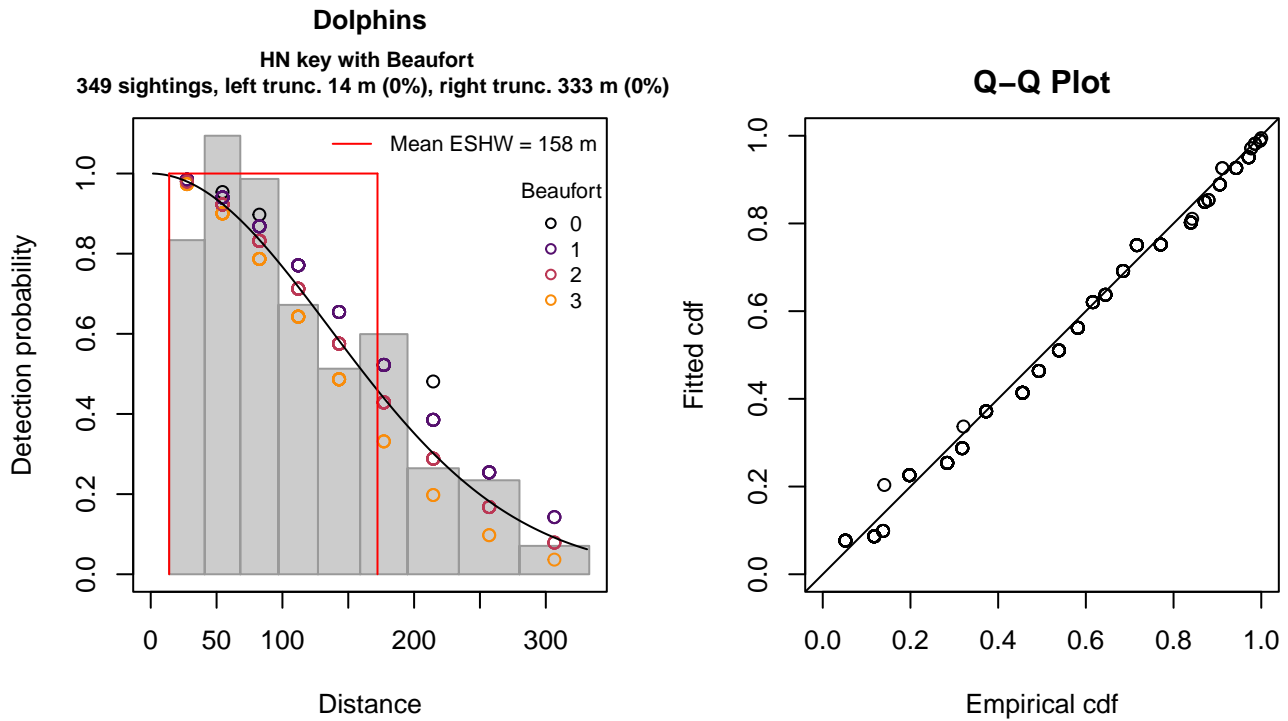


Figure 39: UNCW Early Surveys detection function and Q-Q plot showing its goodness of fit.

Statistical output for this detection function:

Summary for ds object

Number of observations : 349  
 Distance range : 14 - 333  
 AIC : 1464.597

Detection function:

Half-normal key function

Detection function parameters

Scale coefficient(s):

	estimate	se
(Intercept)	5.1778911	0.14575211
Beaufort	-0.1325498	0.07066838

	Estimate	SE	CV
Average p	0.4915207	0.02352103	0.04785360
N in covered region	710.0413079	43.53534195	0.06131382

Distance sampling Cramer-von Mises test (unweighted)

Test statistic = 0.278162 p = 0.155953



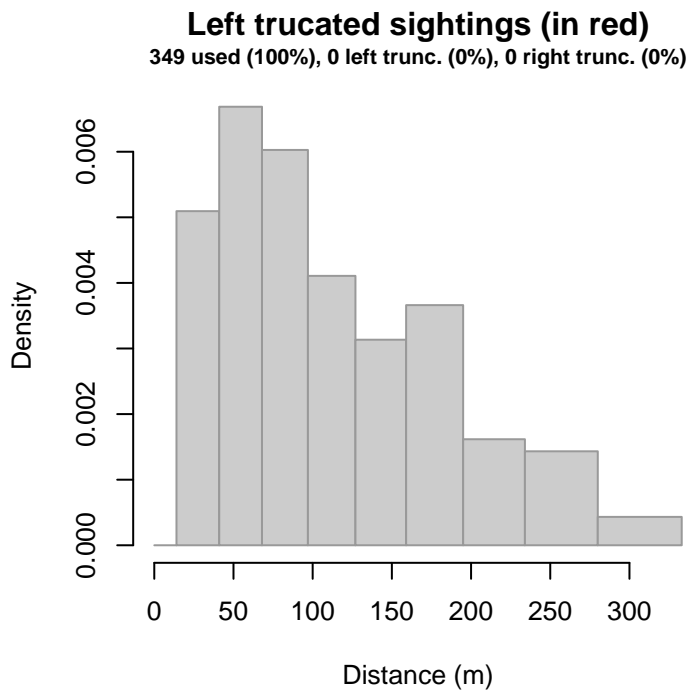


Figure 40: Density histogram of observations used to fit the UNCW Early Surveys detection function, with the left-most bar showing observations at distances less than 14 m, which were left-truncated and excluded from the analysis [Buckland et al. (2001)]. (This bar may be very short if there were very few left-truncated sightings, or very narrow if the left truncation distance was very small; in either case it may not appear red.)

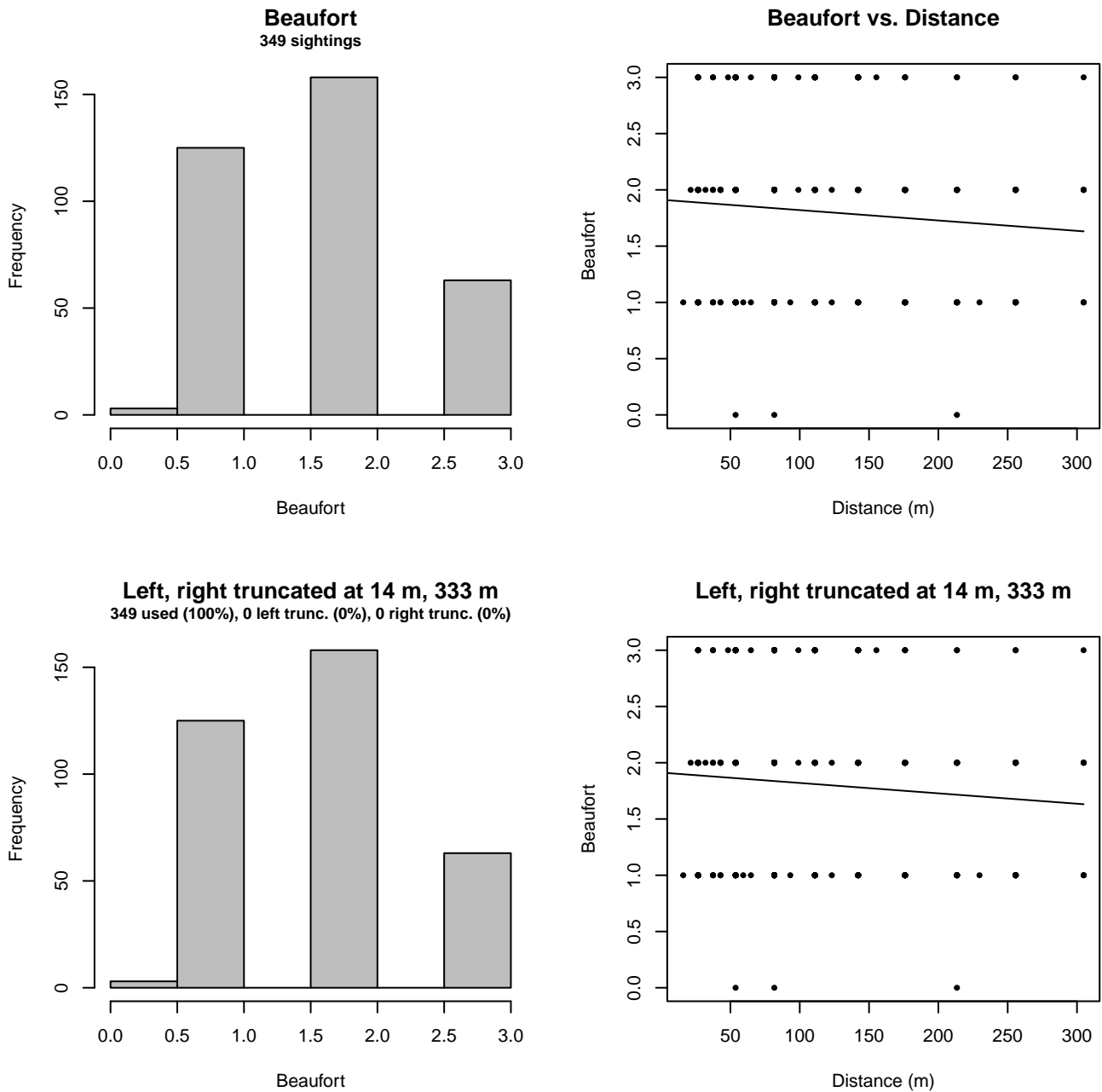


Figure 41: Distribution of the Beaufort covariate before (top row) and after (bottom row) observations were truncated to fit the UNCW Early Surveys detection function.

### 2.2.1.8 VAMSC

After right-truncating observations greater than 1000 m, we fitted the detection function to the 303 observations that remained (Table 16). The selected detection function (Figure 42) used a hazard rate key function with no covariates.

Table 16: Observations used to fit the VAMSC detection function.

ScientificName	n
Delphinus delphis	30
Stenella frontalis	4
Tursiops truncatus	269
<b>Total</b>	<b>303</b>

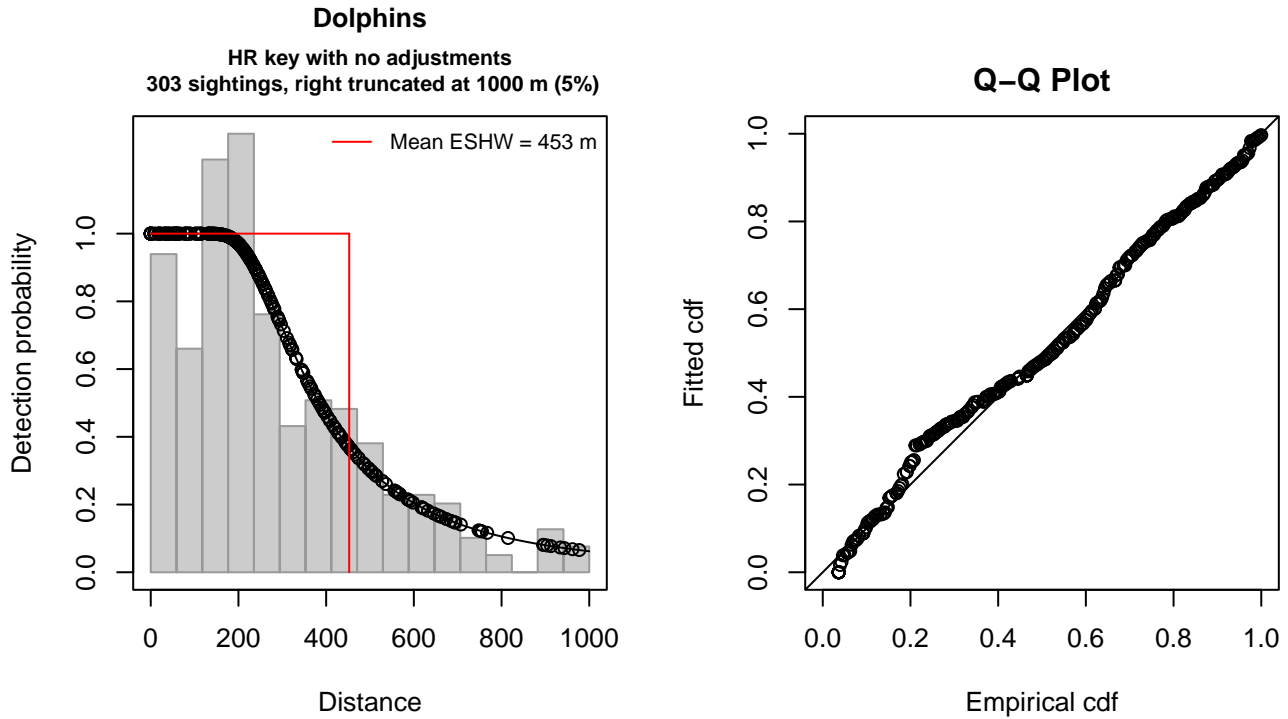


Figure 42: VAMSC detection function and Q-Q plot showing its goodness of fit.

Statistical output for this detection function:

Summary for ds object

Number of observations : 303  
 Distance range : 0 - 1000  
 AIC : 3992.632

Detection function:

Hazard-rate key function

Detection function parameters

Scale coefficient(s):  
 estimate se  
 (Intercept) 5.803823 0.1019737

Shape coefficient(s):  
 estimate se  
 (Intercept) 0.9119562 0.1438459

	Estimate	SE	CV
Average p	0.4525805	0.02853931	0.06305908
N in covered region	669.4942067	50.91287837	0.07604678

Distance sampling Cramer-von Mises test (unweighted)  
 Test statistic = 0.212402 p = 0.244680

### 2.2.1.9 HDR

After right-truncating observations greater than 1500 m and left-truncating observations less than 111 m (Figure 44), we fitted the detection function to the 203 observations that remained (Table 17). The selected detection function (Figure 43) used a hazard rate key function with Season (Figure 45) and Swell (Figure 46) as covariates.

Table 17: Observations used to fit the HDR detection function.

ScientificName	n
Delphinus delphis	47
Stenella coeruleoalba	14
Stenella frontalis	19
Tursiops truncatus	123
<b>Total</b>	<b>203</b>

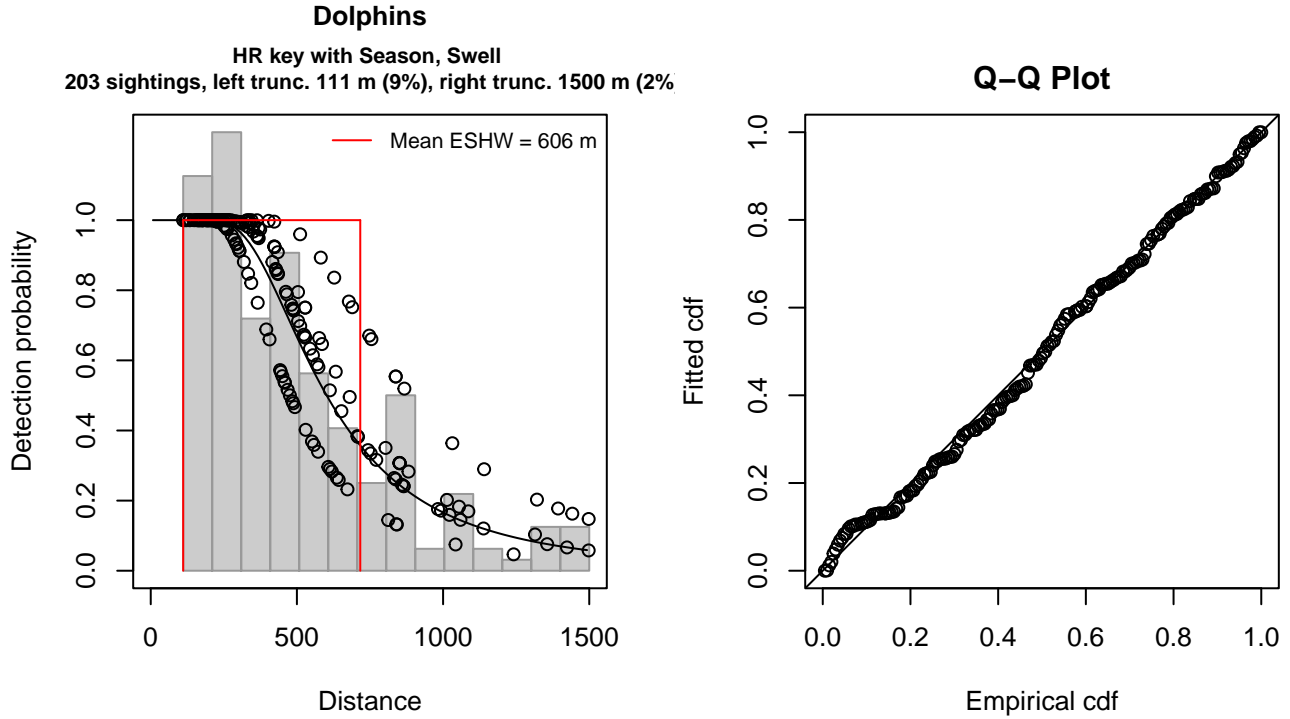


Figure 43: HDR detection function and Q-Q plot showing its goodness of fit.

Statistical output for this detection function:

Summary for ds object

Number of observations : 203  
 Distance range : 111 - 1500  
 AIC : 2802.845

Detection function:

Hazard-rate key function

Detection function parameters

Scale coefficient(s):

	estimate	se
(Intercept)	6.3015171	0.1328018
SeasonWinter, Spring	-0.2671651	0.1458664
Swell3-4	0.3527933	0.1530784

Shape coefficient(s):

	estimate	se
(Intercept)	1.026101	0.1620057

Estimate	SE	CV
----------	----	----

Average p 0.419883 0.03654238 0.08702991  
N in covered region 483.467993 49.56848062 0.10252691

Distance sampling Cramer-von Mises test (unweighted)  
Test statistic = 0.059652 p = 0.816171

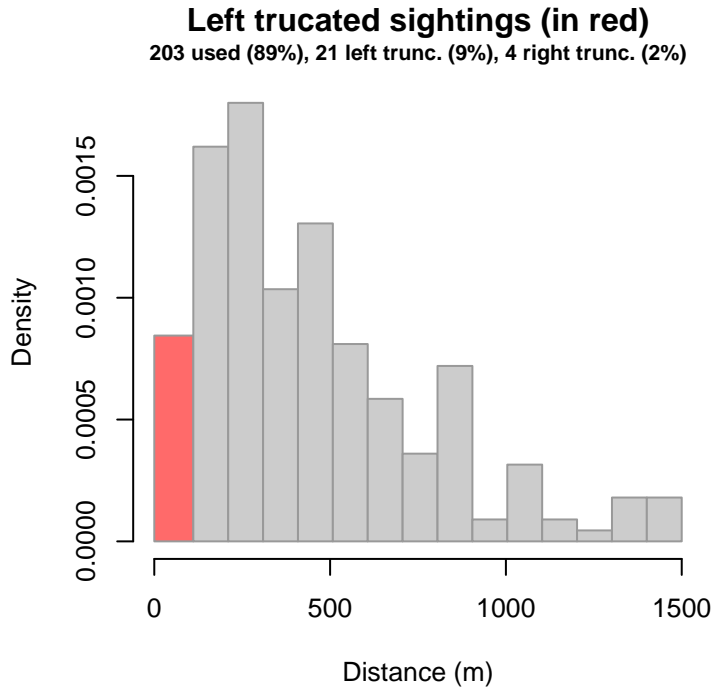


Figure 44: Density histogram of observations used to fit the HDR detection function, with the left-most bar showing observations at distances less than 111 m, which were left-truncated and excluded from the analysis [Buckland et al. (2001)]. (This bar may be very short if there were very few left-truncated sightings, or very narrow if the left truncation distance was very small; in either case it may not appear red.)

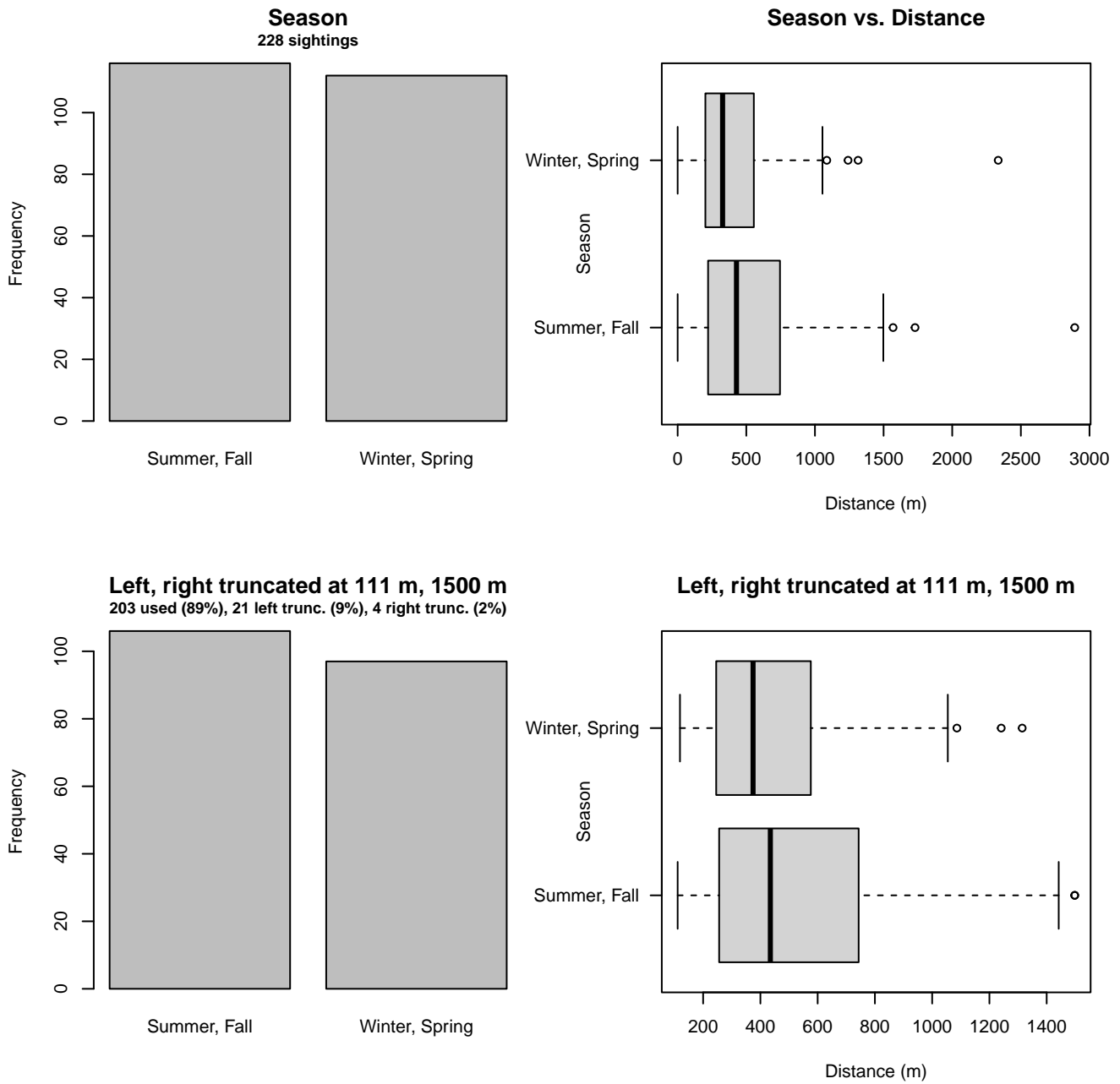


Figure 45: Distribution of the Season covariate before (top row) and after (bottom row) observations were truncated to fit the HDR detection function.

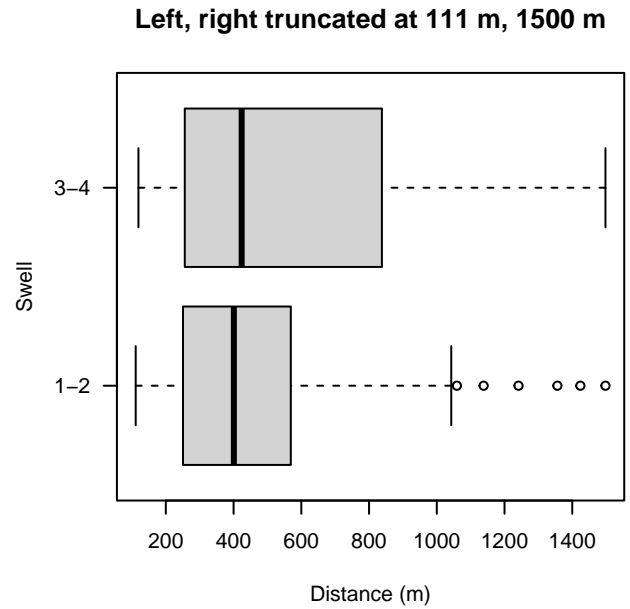
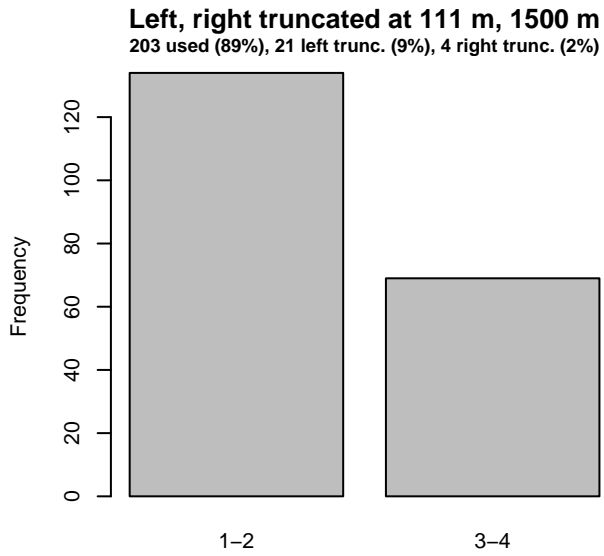
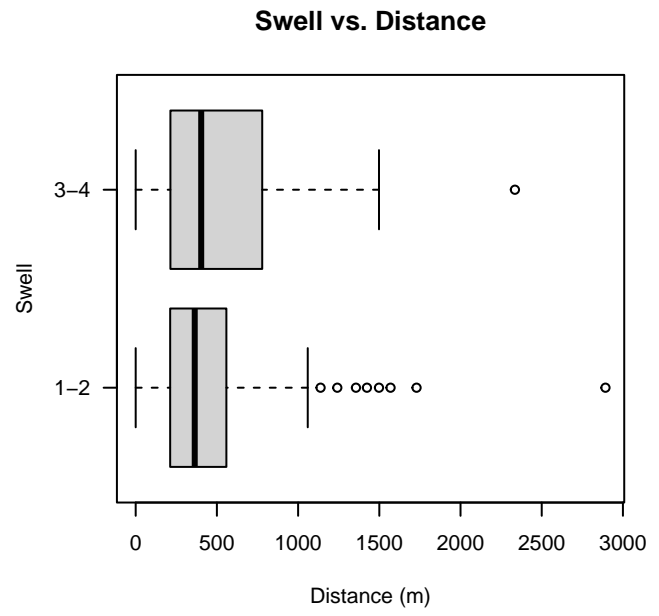
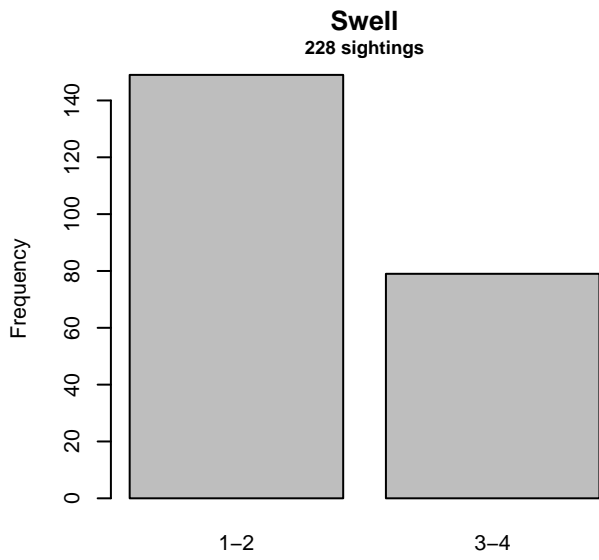


Figure 46: Distribution of the Swell covariate before (top row) and after (bottom row) observations were truncated to fit the HDR detection function.

## 2.2.2 Shipboard Surveys

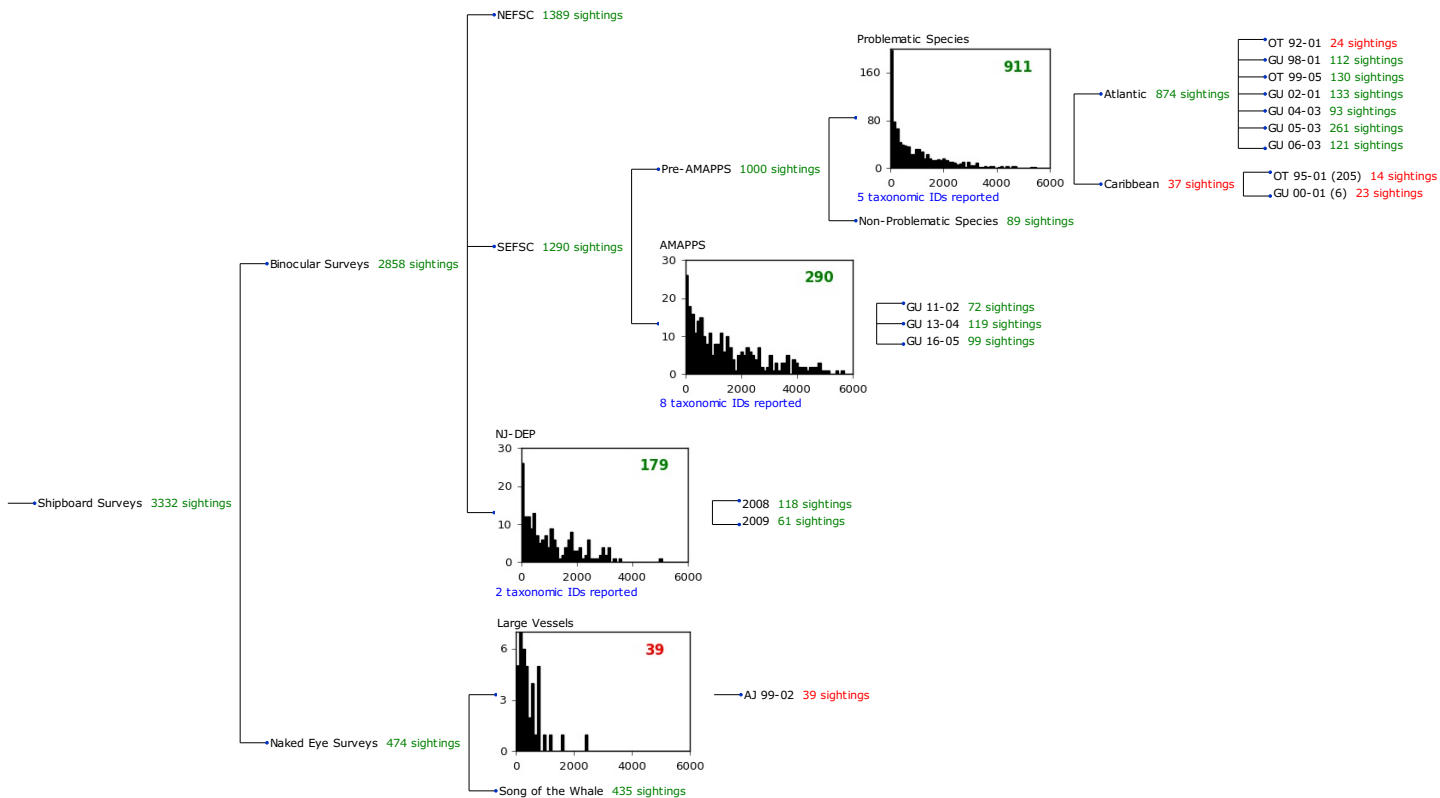


Figure 47: Detection hierarchy for shipboard surveys, showing how they were pooled during detectability modeling, for detection functions that pooled multiple taxa but could not use a taxonomic covariate to account for differences between them. Each histogram represents a detection function and summarizes the perpendicular distances of observations that were pooled to fit it, prior to truncation. Observation counts, also prior to truncation, are shown in green when they met the recommendation of Buckland et al. (2001) that detection functions utilize at least 60 sightings, and red otherwise. For rare taxa, it was not always possible to meet this recommendation, yielding higher statistical uncertainty. During the spatial modeling stage of the analysis, effective strip widths were computed for each survey using the closest detection function above it in the hierarchy (i.e. moving from right to left in the figure). Surveys that do not have a detection function above them in this figure were either addressed by a detection function presented in a different section of this report, or were omitted from the analysis.

### 2.2.2.1 SEFSC Pre-AMAPPS Problematic Species

After right-truncating observations greater than 4000 m and left-truncating observations less than 200 m (Figure 49), we fitted the detection function to the 616 observations that remained (Table 18). The selected detection function (Figure 48) used a hazard rate key function with Beaufort (Figure 50) and VesselName (Figure 51) as covariates.

Table 18: Observations used to fit the SEFSC Pre-AMAPPS Problematic Species detection function.

ScientificName	n
Delphinus delphis	34
Stenella attenuata	14
Stenella frontalis	262
Steno bredanensis	4
Tursiops truncatus	302
<b>Total</b>	<b>616</b>



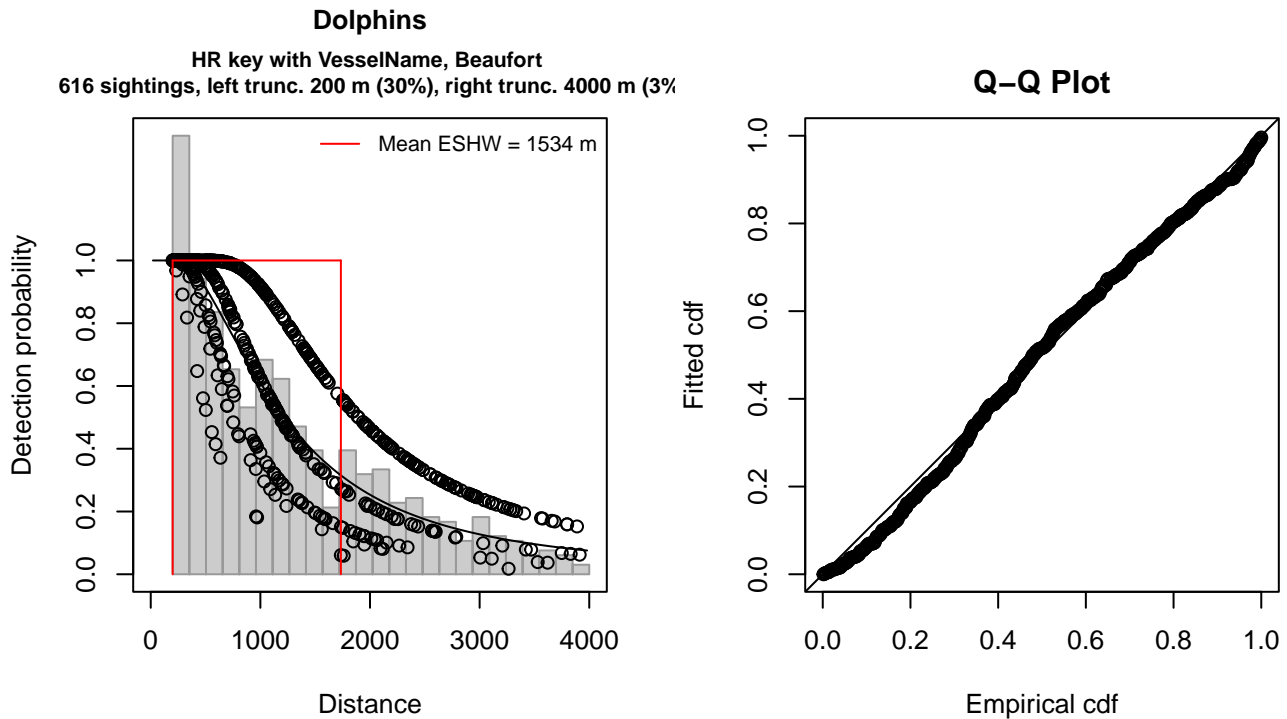


Figure 48: SEFSC Pre-AMAPPS Problematic Species detection function and Q-Q plot showing its goodness of fit.

Statistical output for this detection function:

Summary for ds object

Number of observations : 616  
Distance range : 200 - 4000  
AIC : 9753.004

Detection function:

Hazard-rate key function

Detection function parameters

Scale coefficient(s):

	estimate	se
(Intercept)	7.3628462	0.09422017
VesselNameOregon II	-0.4793018	0.17480366
Beaufort3	-0.4668391	0.14302976
Beaufort4-5	-0.8137669	0.16103824

Shape coefficient(s):

	estimate	se
(Intercept)	0.689867	0.09372714

	Estimate	SE	CV
Average p	0.3555714	0.02671315	0.07512737
N in covered region	1732.4228173	142.52885613	0.08227140

Distance sampling Cramer-von Mises test (unweighted)

Test statistic = 0.313292 p = 0.124062

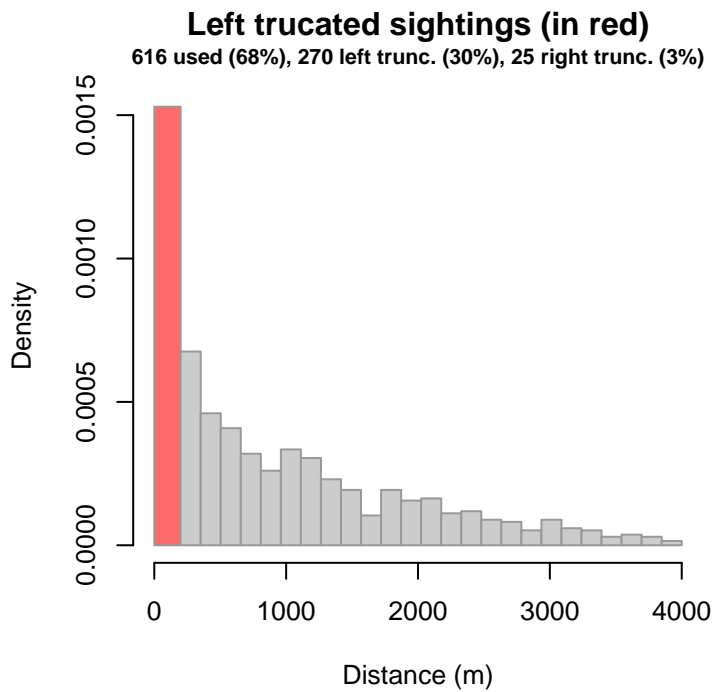


Figure 49: Density histogram of observations used to fit the SEFSC Pre-AMAPPS Problematic Species detection function, with the left-most bar showing observations at distances less than 200 m, which were left-truncated and not used to fit the detection function. (This bar may be very short if there were very few left-truncated sightings, or very narrow if the left truncation distance was very small; in either case it may not appear red.) These were excluded because they formed a problematic "spike" in detections close to the trackline, suggesting that animals approached the vessel (e.g. to bow-ride) prior to being detected. To address this, we fitted the detection function to the observations beyond the spike and assumed that within it, detection probability was 1, effectively treating it like a strip transect. We then added the left-truncated observations back into the analysis as if they occurred in this strip. This treatment may have resulted in an underestimation of detection probability.

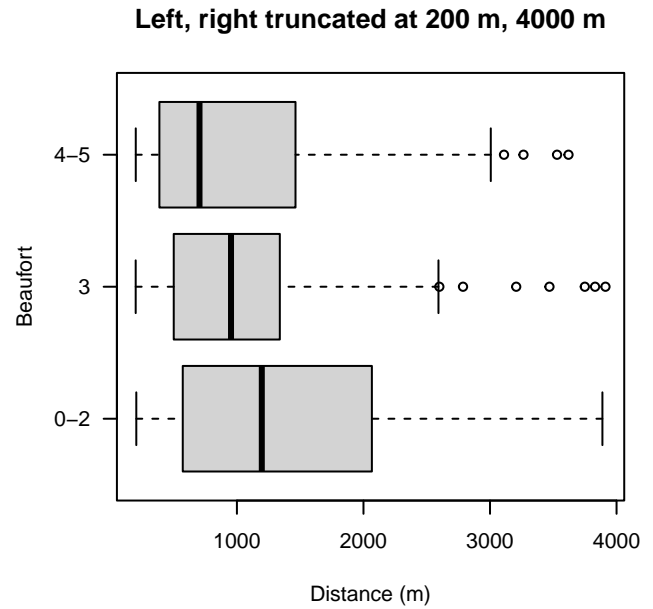
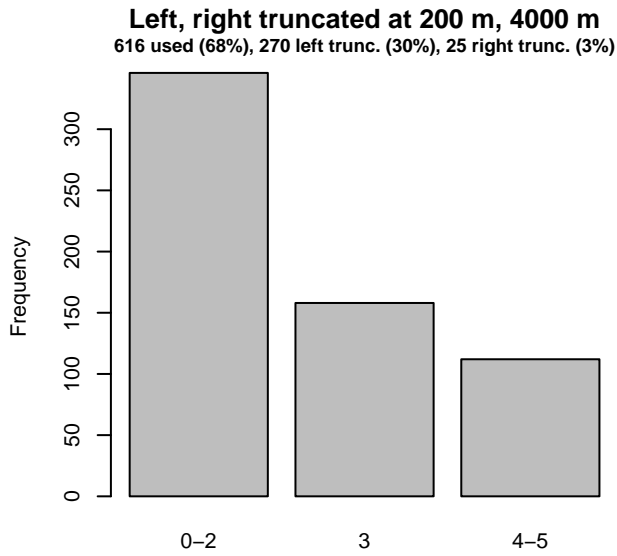
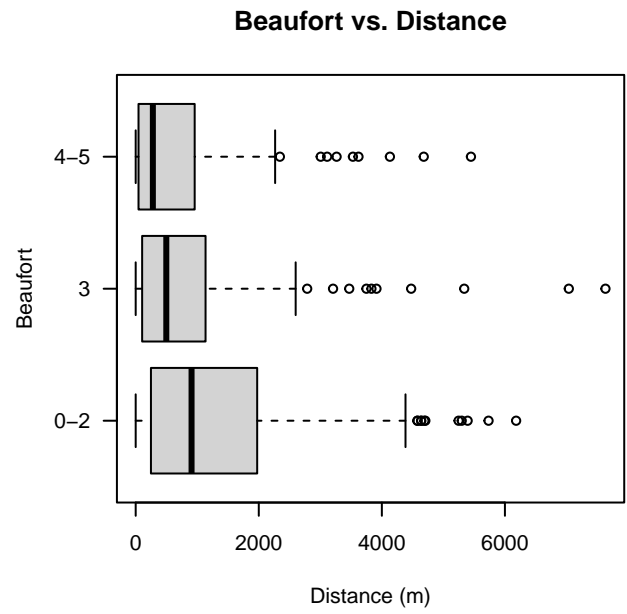
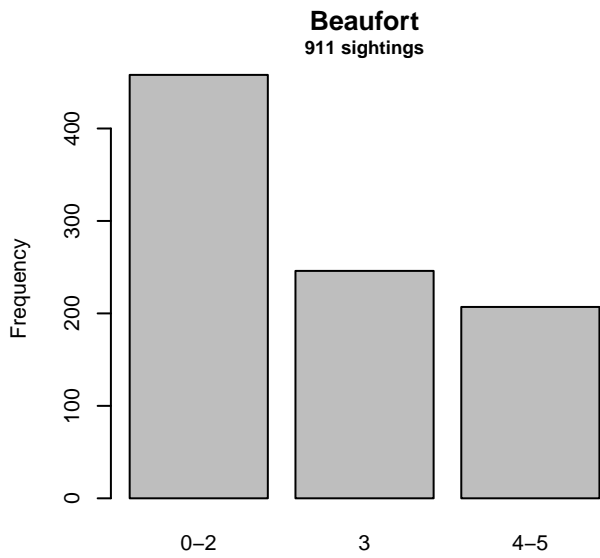


Figure 50: Distribution of the Beaufort covariate before (top row) and after (bottom row) observations were truncated to fit the SEFSC Pre-AMAPPS Problematic Species detection function.

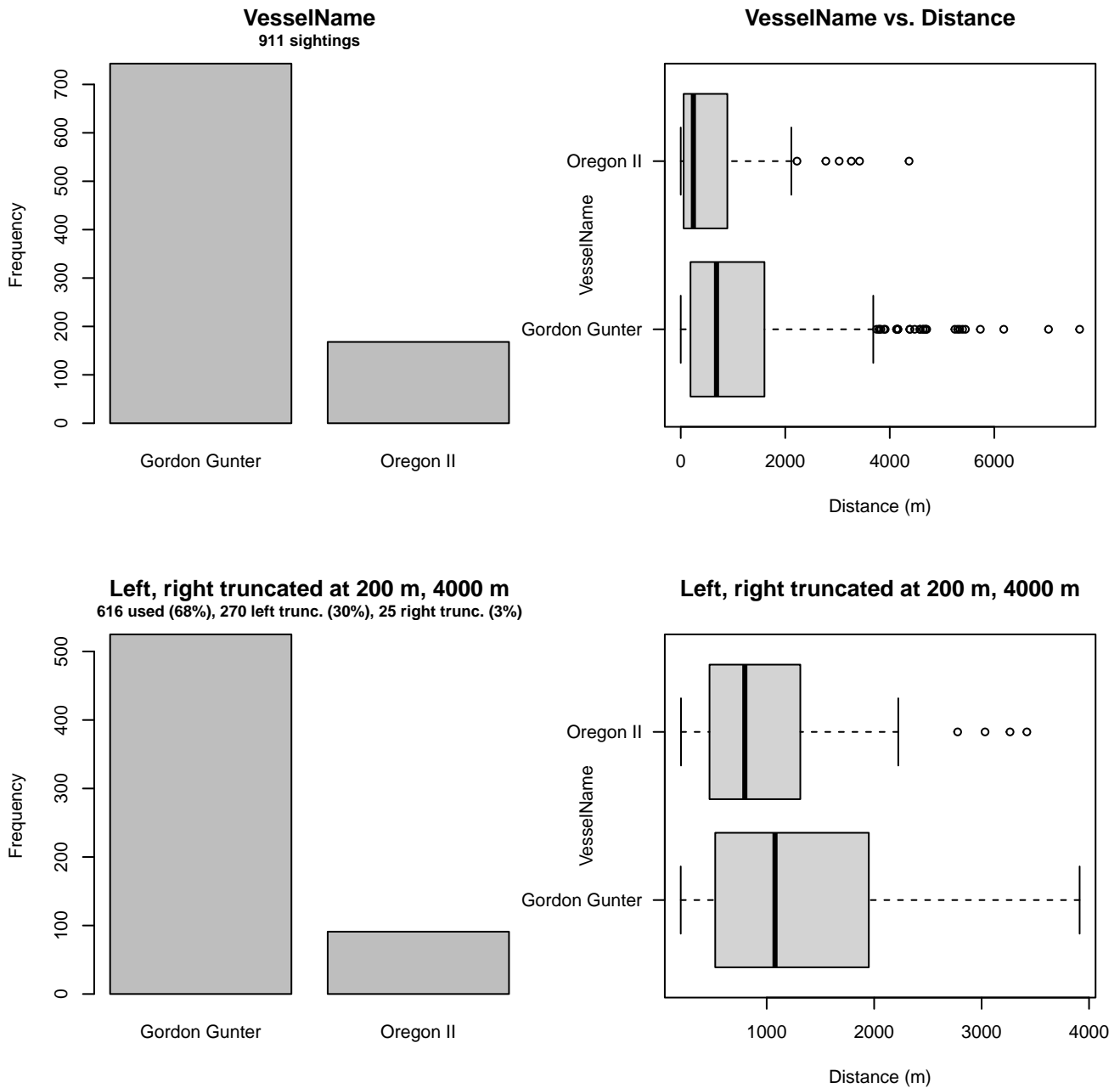


Figure 51: Distribution of the VesselName covariate before (top row) and after (bottom row) observations were truncated to fit the SEFSC Pre-AMAPPS Problematic Species detection function.

### 2.2.2.2 SEFSC AMAPPS

After right-truncating observations greater than 5000 m, we fitted the detection function to the 284 observations that remained (Table 19). The selected detection function (Figure 52) used a hazard rate key function with Beaufort (Figure 53) as a covariate.

Table 19: Observations used to fit the SEFSC AMAPPS detection function.

ScientificName	n
Delphinus delphis	2
Stenella attenuata	10
Stenella clymene	3
Stenella coeruleoalba	11
Stenella frontalis	84
Stenella longirostris	1
Steno bredanensis	2
Tursiops truncatus	171
<b>Total</b>	<b>284</b>

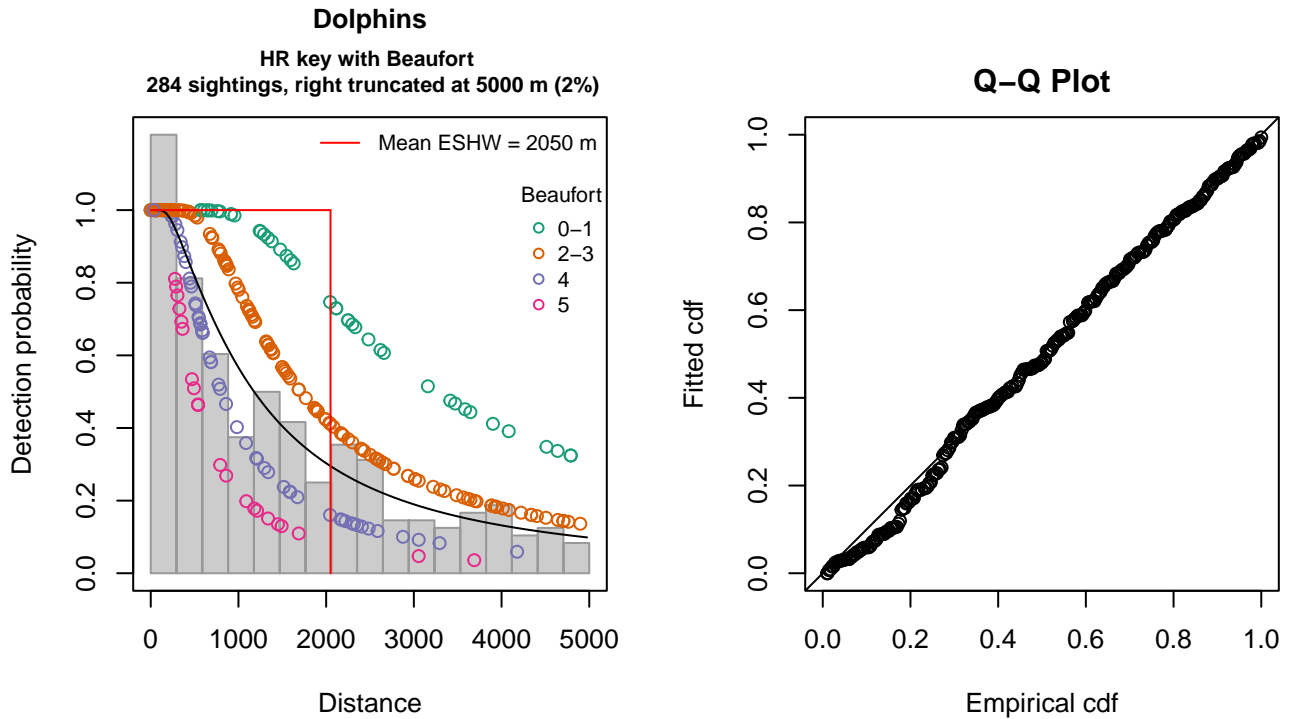


Figure 52: SEFSC AMAPPS detection function and Q-Q plot showing its goodness of fit.

Statistical output for this detection function:

```
Summary for ds object
Number of observations : 284
Distance range       : 0 - 5000
AIC                  : 4678.464
```

```
Detection function:
Hazard-rate key function
```

```
Detection function parameters
Scale coefficient(s):
      estimate      se
(Intercept) 7.8386611 0.3487749
Beaufort2-3 -0.6450433 0.3816484
Beaufort4   -1.3990617 0.4441169
Beaufort5   -1.8689041 0.5186901
```

Shape coefficient(s):

	estimate	se
(Intercept)	0.3878689	0.1380351

	Estimate	SE	CV
Average p	0.3478259	0.03965009	0.1139941
N in covered region	816.5004271	101.68622285	0.1245391

Distance sampling Cramer-von Mises test (unweighted)

Test statistic = 0.107898 p = 0.547527

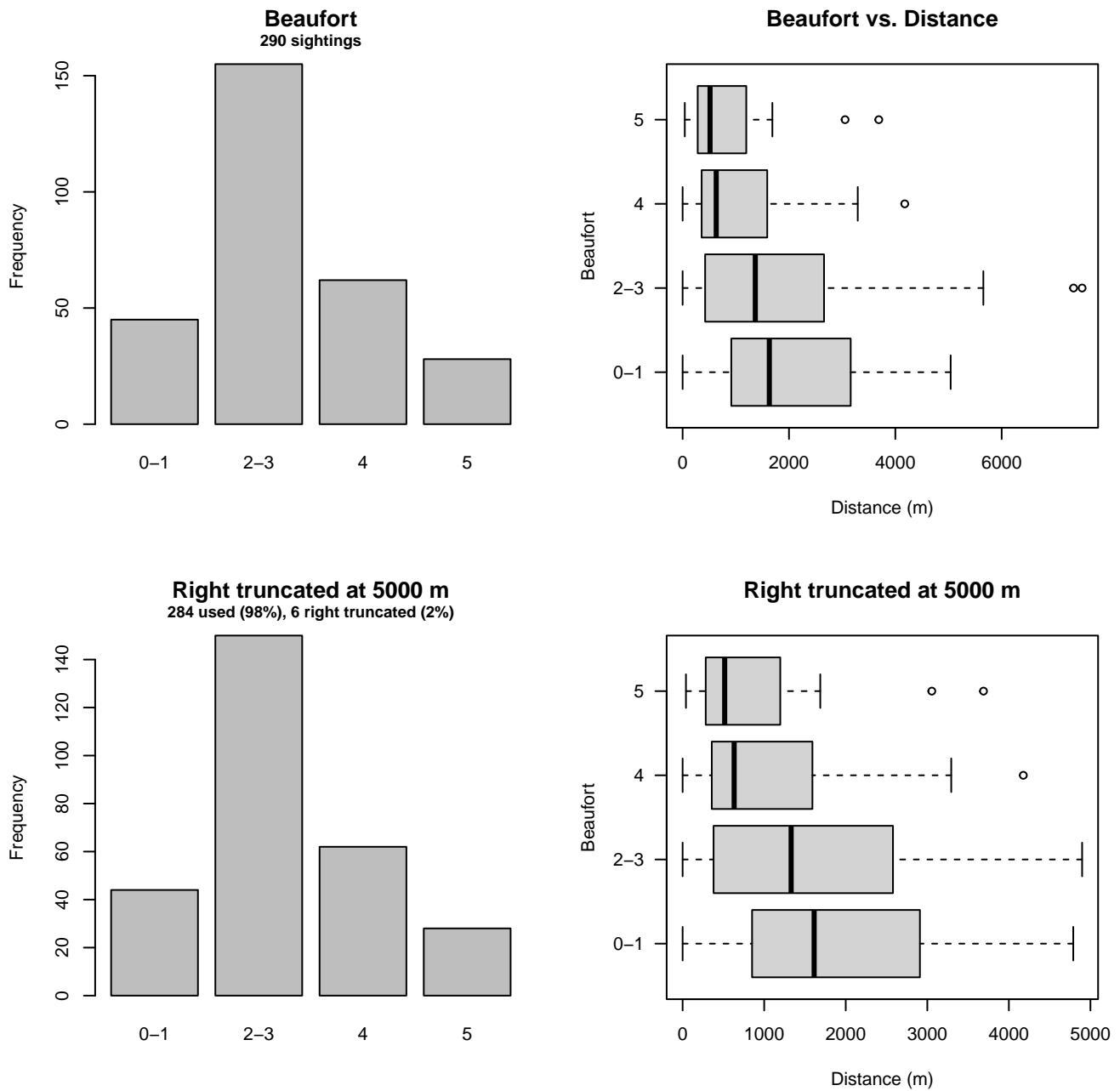


Figure 53: Distribution of the Beaufort covariate before (top row) and after (bottom row) observations were truncated to fit the SEFSC AMAPPS detection function.

### 2.2.2.3 NJ-DEP

After right-truncating observations greater than 3200 m, we fitted the detection function to the 175 observations that remained (Table 20). The selected detection function (Figure 54) used a hazard rate key function with no covariates.

Table 20: Observations used to fit the NJ-DEP detection function.

ScientificName	n
Delphinus delphis	19
Tursiops truncatus	156
<b>Total</b>	<b>175</b>

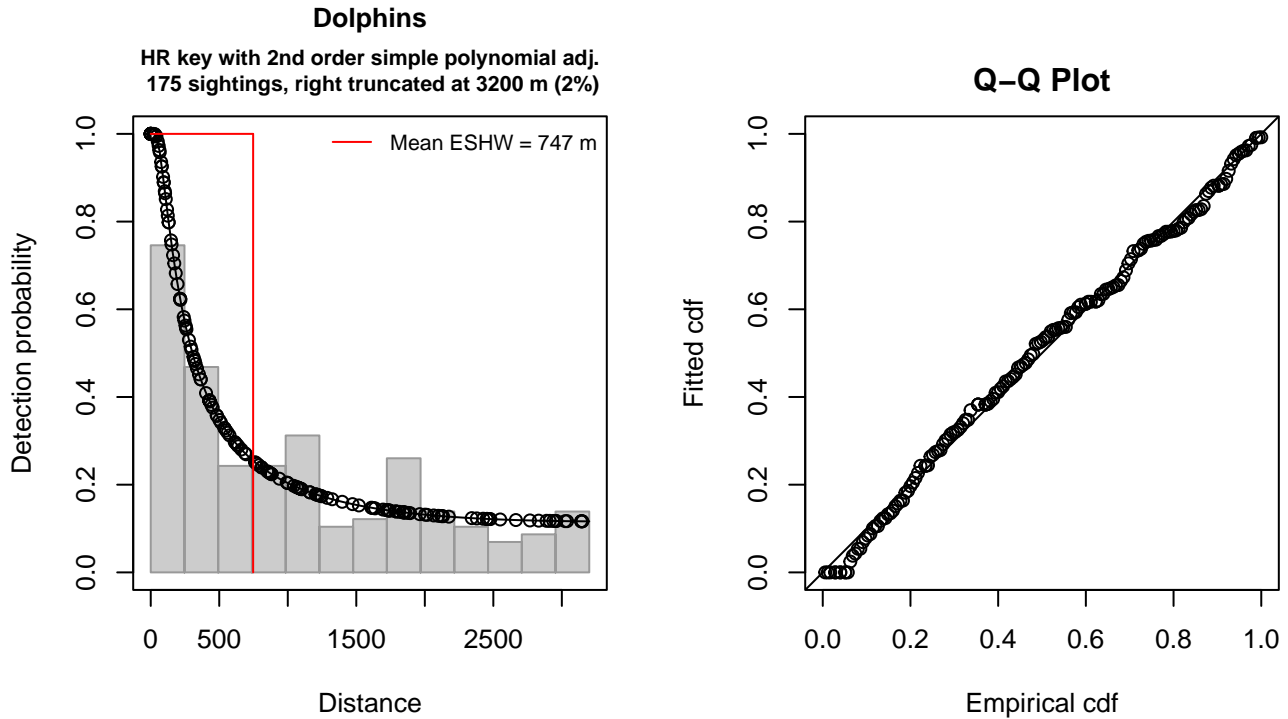


Figure 54: NJ-DEP detection function and Q-Q plot showing its goodness of fit.

Statistical output for this detection function:

Summary for ds object

Number of observations : 175  
 Distance range : 0 - 3200  
 AIC : 2750.547

Detection function:

Hazard-rate key function with simple polynomial adjustment term of order 2

Detection function parameters

Scale coefficient(s):  
 estimate se  
 (Intercept) 5.340225 0.502875

Shape coefficient(s):

estimate se  
 (Intercept) 2.663565e-07 0.3025183

Adjustment term coefficient(s):  
 estimate se  
 poly, order 2 0.8448098 1.306568

Monotonicity constraints were enforced.

	Estimate	SE	CV
Average p	0.2335197	0.05159473	0.2209438
N in covered region	749.4013460	172.84391894	0.2306427

Monotonicity constraints were enforced.

Distance sampling Cramer-von Mises test (unweighted)  
 Test statistic = 0.069450 p = 0.754942

### 2.2.2.4 Large Vessels

After right-truncating observations greater than 1100 m, we fitted the detection function to the 36 observations that remained (Table 21). The selected detection function (Figure 55) used a half normal key function with no covariates.

Table 21: Observations used to fit the Large Vessels detection function.

ScientificName	n
Lagenorhynchus acutus	36
<b>Total</b>	<b>36</b>

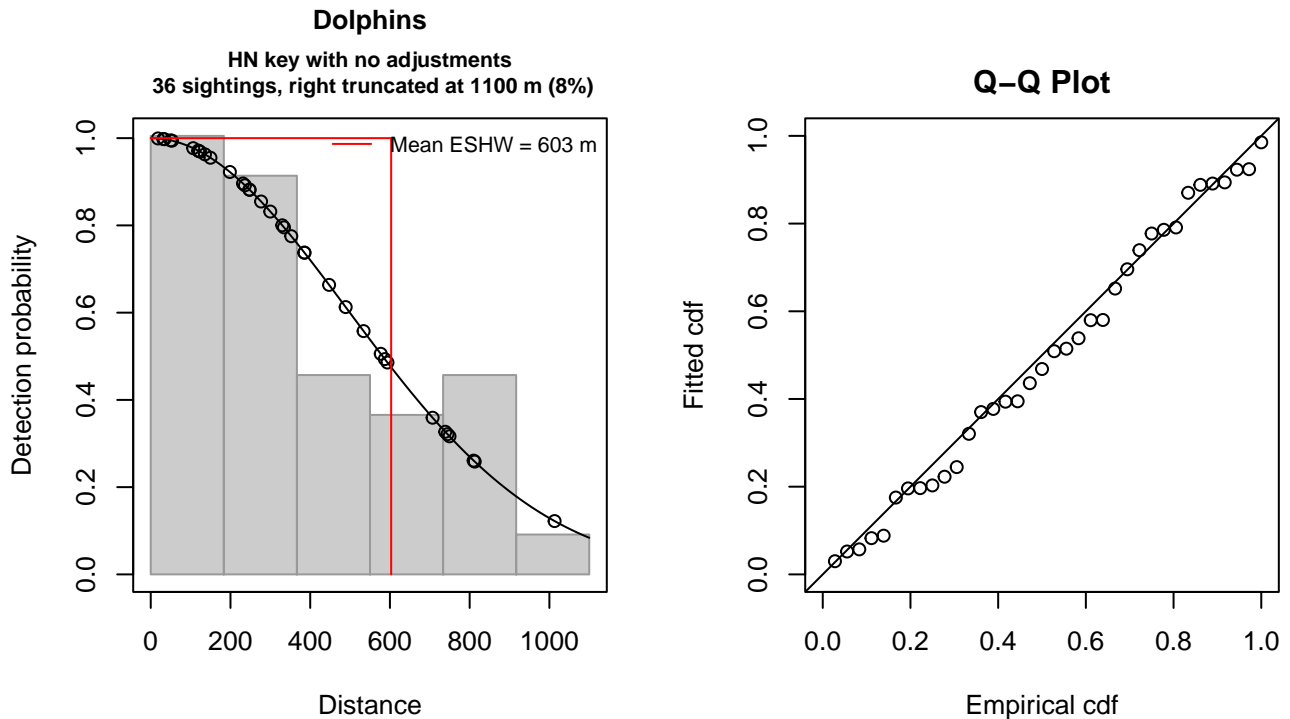


Figure 55: Large Vessels detection function and Q-Q plot showing its goodness of fit.

Statistical output for this detection function:

```
Summary for ds object
Number of observations : 36
Distance range       : 0 - 1100
```



AIC : 493.4472

Detection function:  
Half-normal key function

Detection function parameters  
Scale coefficient(s):  
                  estimate      se  
(Intercept) 6.202683 0.1646341

	Estimate	SE	CV
Average p	0.5483057	0.07646146	0.1394504
N in covered region	65.6568085	11.74385160	0.1788672

Distance sampling Cramer-von Mises test (unweighted)  
Test statistic = 0.026241 p = 0.986825

### 3 Bias Corrections

Density surface modeling methodology uses *distance sampling* (Buckland et al. 2001) to model the probability that an observer on a line transect survey will detect an animal given the perpendicular distance to it from the transect line. Distance sampling assumes that detection probability is 1 when perpendicular distance is 0. When this assumption is not met, detection probability is biased high, leading to an underestimation of density and abundance. This is known as the  $g_0 < 1$  problem, where  $g_0$  refers to the detection probability at distance 0. Modelers often try to address this problem by estimating  $g_0$  empirically and dividing it into estimated density or abundance, thereby correcting those estimates to account for the animals that were presumed missed.

Two important sources of bias for visual surveys are known as *availability bias*, in which an animal was present on the transect line but impossible to detect, e.g. because it was under water, and *perception bias*, in which an animal was present and available but not noticed, e.g. because of its small size or cryptic coloration or behavior (Marsh and Sinclair 1989). Modelers often estimate the influence of these two sources of bias on detection probability independently, yielding two estimates of  $g_0$ , hereafter referred to as  $g_{0A}$  and  $g_{0P}$ , and multiply them together to obtain a final, combined estimate:  $g_0 = g_{0A} \cdot g_{0P}$ .

Our overall approach was to perform this correction on a per-observation basis, to have the flexibility to account for many factors such as platform type, surveyor institution, group size, group composition (e.g. singleton, mother-calf pair, or surface active group), and geographic location (e.g. feeding grounds vs. calving grounds). The level of complexity of the corrections varied by species according to the amount of information available, with North Atlantic right whale having the most elaborate corrections, derived from a substantial set of publications documenting its behavior, and various lesser known odontocetes having corrections based only on platform type (aerial or shipboard), derived from comparatively sparse information. Here we document the corrections used for white-beaked dolphin.

#### 3.1 Aerial Surveys

Reflecting the northerly distribution of the species, the only collaborating institution that reported sightings of white-beaked dolphins during aerial surveys that were suited to modeling small cetaceans was NOAA NEFSC (Table 1). The maximum group size of aerial sightings retained for analysis was 25; one sighting of 35 animals was right-truncated during detection modeling.

Palka et al. (2021) developed perception bias corrections using two team, mark recapture distance sampling (MRDS) methodology (Burt et al. 2014) for aerial surveys conducted in 2010-2017 by NEFSC during the AMAPPS program. We applied this correction to all aerial sightings (all were from NEFSC), including those prior to the AMAPPS program and from the NARWSS program. Palka previously developed a correction for the pre-AMAPPS surveys (Palka 2006) but it utilized older methods and less data than the 2021 analysis, so we used the 2021 analysis instead.

No perception bias estimate was available for NARWSS, but that program used the same aircraft and many of the same observers as the AMAPPS program. However, it flew at a higher altitude and had a searching strategy designed to maximize detections of large whales, so it is possible the AMAPPS estimate undercorrected the NARWSS data (i.e.  $g_{0P}$  for NARWSS should have been less than  $g_{0P}$  for AMAPPS). If so, it is possible this led to an underestimation of density, as about half of the sightings were reported by NARWSS.

We estimated availability bias corrections using the Laake et al. (1997) estimator and dive intervals reported by Palka et al. (2017) (Table 23). We could not locate any dive intervals in the literature for white-beaked dolphin so we used Palka’s estimates for Atlantic white-sided dolphin (*Lagenorhynchus acutus*) as the best available proxy. To estimate time in view, needed by the Laake estimator, we used results reported by Robertson et al. (2015), rescaled linearly for each survey program according to its target altitude and speed.

To address the influence of group size on availability bias, we applied the group availability estimator of McLellan et al. (2018) on a per-observation basis. Following Palka et al. (2021), who also used that method, we assumed that individuals in the group dived asynchronously. The resulting  $g_{0A}$  corrections ranged from about 0.5 to 1 (Figure 56). We caution that the assumption of asynchronous diving can lead to an underestimation of density and abundance if diving is actually synchronous; see McLellan et al. (2018) for an exploration of this effect. However, if future research finds that this species conducts synchronous dives and characterizes the degree of synchronicity, the model can be updated to account for this knowledge.

Table 22: Perception bias corrections for white-beaked dolphin applied to aerial surveys.

Surveys	Group Size	$g_{0P}$	$g_{0P}$	Source
All	$\leq 25$	0.57		Palka et al. (2021): NEFSC

Table 23: Surface and dive intervals for white-beaked dolphin used to estimate availability bias corrections.

Surface Interval (s)	Dive Interval (s)	Source
4.8	38.8	Palka et al. (2017): Atlantic white-sided dolphin

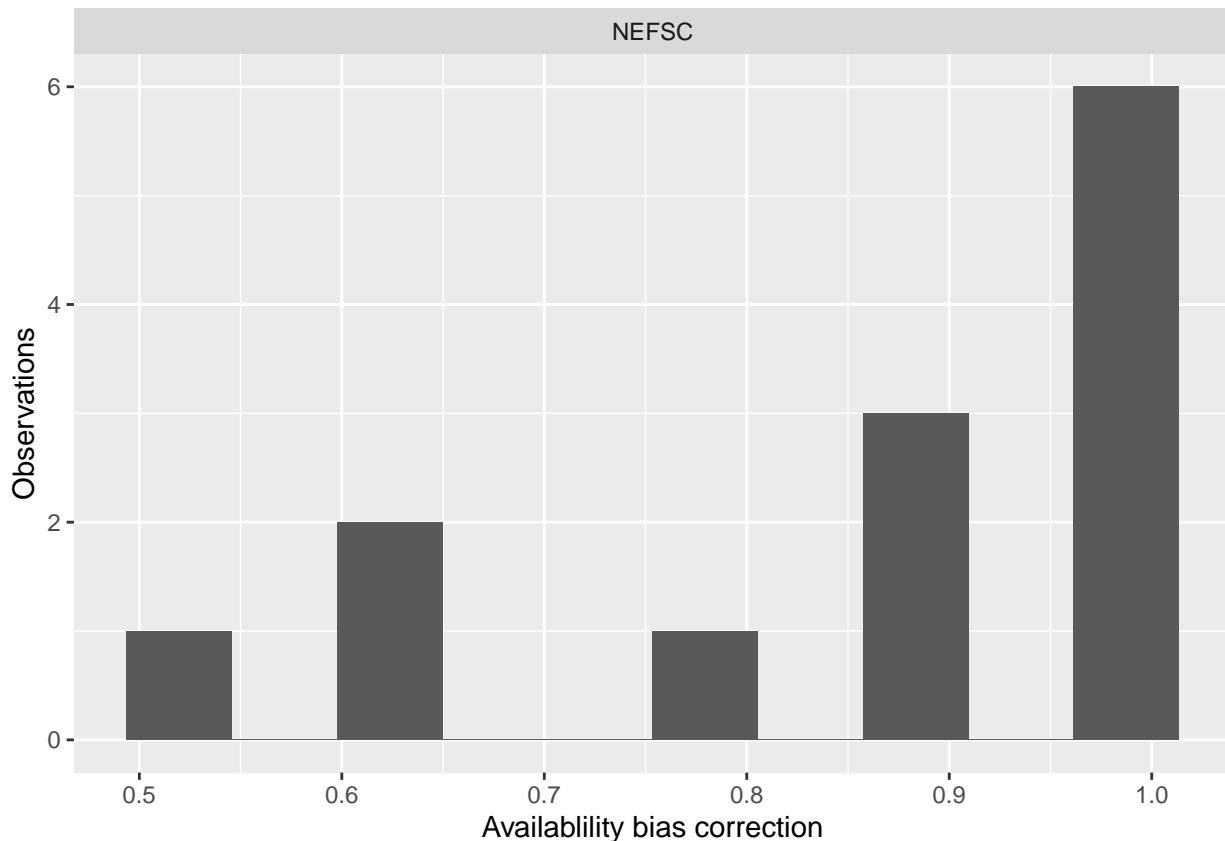


Figure 56: Availability bias corrections for white-beaked dolphin for aerial surveys, by institution.

### 3.2 Shipboard Surveys

Most of the shipboard surveys in our analysis used high-power (25x150), pedestal-mounted binoculars. Similar to aerial surveys, the only institution that reported a sighting of Atlantic white-sided dolphins during high-power binocular surveys

was NOAA NEFSC (Table 1). Palka et al. (2021) developed perception bias corrections using two team, MRDS methodology (Burt et al. 2014) for high-power binocular surveys conducted in 2010-2017 by NEFSC during the AMAPPS program. We applied this correction to the single sighting that occurred.

Palka (2006) also developed a correction  $g_{0P} = 0.27$  for an NEFSC shipboard survey (AJ 99-02) in which the primary team observers searched by naked eye, but it was only for Atlantic white-sided dolphins, as the survey did not sight any white-beaked dolphins. However, this estimate was similar to that of Pike et al. (2019), who estimated  $g_{0P} = 0.31$  for a guild comprised of white-beaked dolphins and Atlantic white-sided dolphins. We applied Palka’s correction to the white-beaked dolphins sighted by the MCR Song of the Whale surveys, which also searched by naked eye but did not have a program-specific estimate. We caution that the platform height for the MCR surveys was lower than the NEFSC survey, and the target survey speed was slower (6 knots for MCR vs. 10 knots for NEFSC).

Given that the dive interval of Atlantic white-sided dolphin (Table 23) was short relative to the amount of time a given patch of water remained in view to shipboard observers, we assumed that no availability bias correction was needed ( $g_{0A} = 1$ ), following Palka et al. (2021).

Table 24: Perception and availability bias corrections for white-beaked dolphin applied to shipboard surveys.

Surveys	Searching Method	Group Size	$g_{0P}$	$g_{0P}$ Source	$g_{0A}$	$g_{0A}$ Source
NEFSC	Binoculars	$\leq 20$	0.52	Palka et al. (2021): NEFSC	1	Assumed
MCR	Naked eye	Any	0.27	Palka et al. (2006)	1	Assumed

## 4 Geographic Strata

With so few sightings, it was not possible to fit a traditional density surface model that related density observed on survey segments to environmental covariates. Nor was it possible to make proper design-based abundance estimates using traditional distance sampling (Buckland et al. 2001), because the aggregate surveys provided very heterogeneous coverage that did not together constitute a proper systematic survey design.

To provide interested parties with at least rough estimates of density in ecologically relevant geographic strata, we first split the study area into five strata (Figure 1) at major habitat boundaries. We placed our first split at the continental shelf break, defined as the 100 meter isobath, separating the study area in into shelf and offshore regions. (We manually cut across the Northeast Channel of the Gulf of Maine, so that the Gulf was considered part of the shelf.) We then split the shelf region at Cape Hatteras, a location where the Gulf Stream separates from the continental shelf, which has previously been used to delineate community structure in marine mammals (Schick et al. 2011). We also split the shelf region at the Nantucket Shoals, which separate the Gulf of Maine from the New York Bight. We split off the bays and sounds of New York, Rhode Island, and southern Massachusetts, generally at the 10 m isobath, on the basis that these inshore areas are rarely visited by cetaceans of any species. Finally, we split the offshore region at the north wall of the Gulf Stream, starting at Cape Hatteras and extending along the north wall of the Gulf Stream, as defined with a long-term climatology of total kinetic energy, to the edge of the study area.

We then derived density estimates for each stratum by fitting a model with no covariates, under the assumption that density would be distributed uniformly within the stratum. This assumption, if true, would mean we would obtain similar density estimates for a given stratum under any sampling design, and therefore it would not matter if there was some heterogeneity in sampling within the stratum. However, we strongly caution that this assumption did not hold for the other, more-common species we successfully modeled with traditional density surface modeling, as evidenced by the non-uniform patterns in density predicted by those species’ models. That said, when those results are viewed at a very coarse, ecoregional scale, the boundaries used here often correlate with boundaries or strong gradients in density in those models. Thus, for the much rarer species, such as white-beaked dolphin documented here, we offer this simplified approach as a rough-and-ready substitute for a full density surface model.

In this section, we present maps of each stratum that contained sightings, with tallies of effort and sightings that occurred.

#### 4.1 Shelf North of Nantucket Shoals

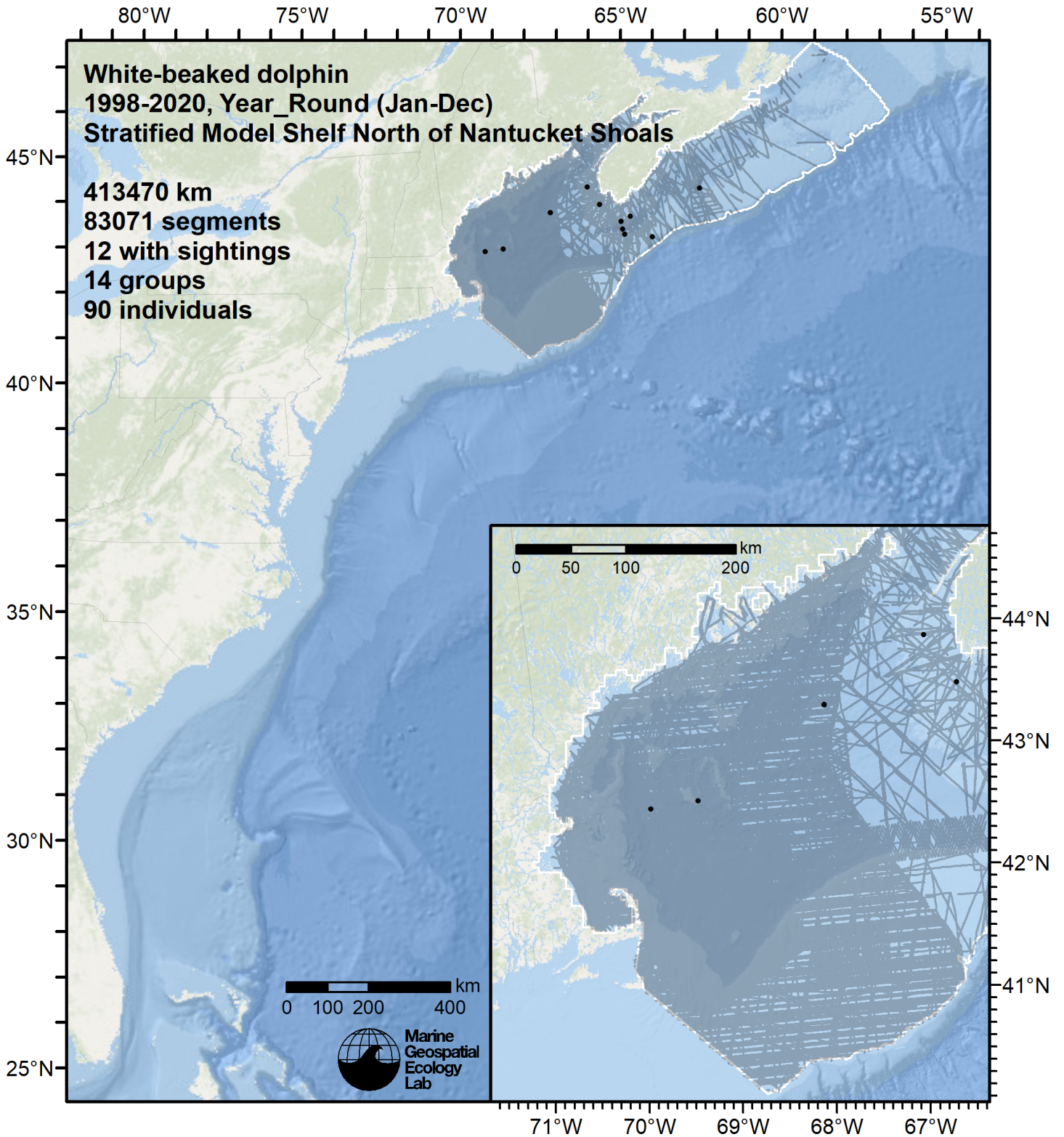


Figure 57: Survey segments and sightings used to estimate white-beaked dolphin density for the "Shelf North of Nantucket Shoals" region. Black points indicate segments with observations.



## 5 Predictions

### 5.1 Summarized Predictions

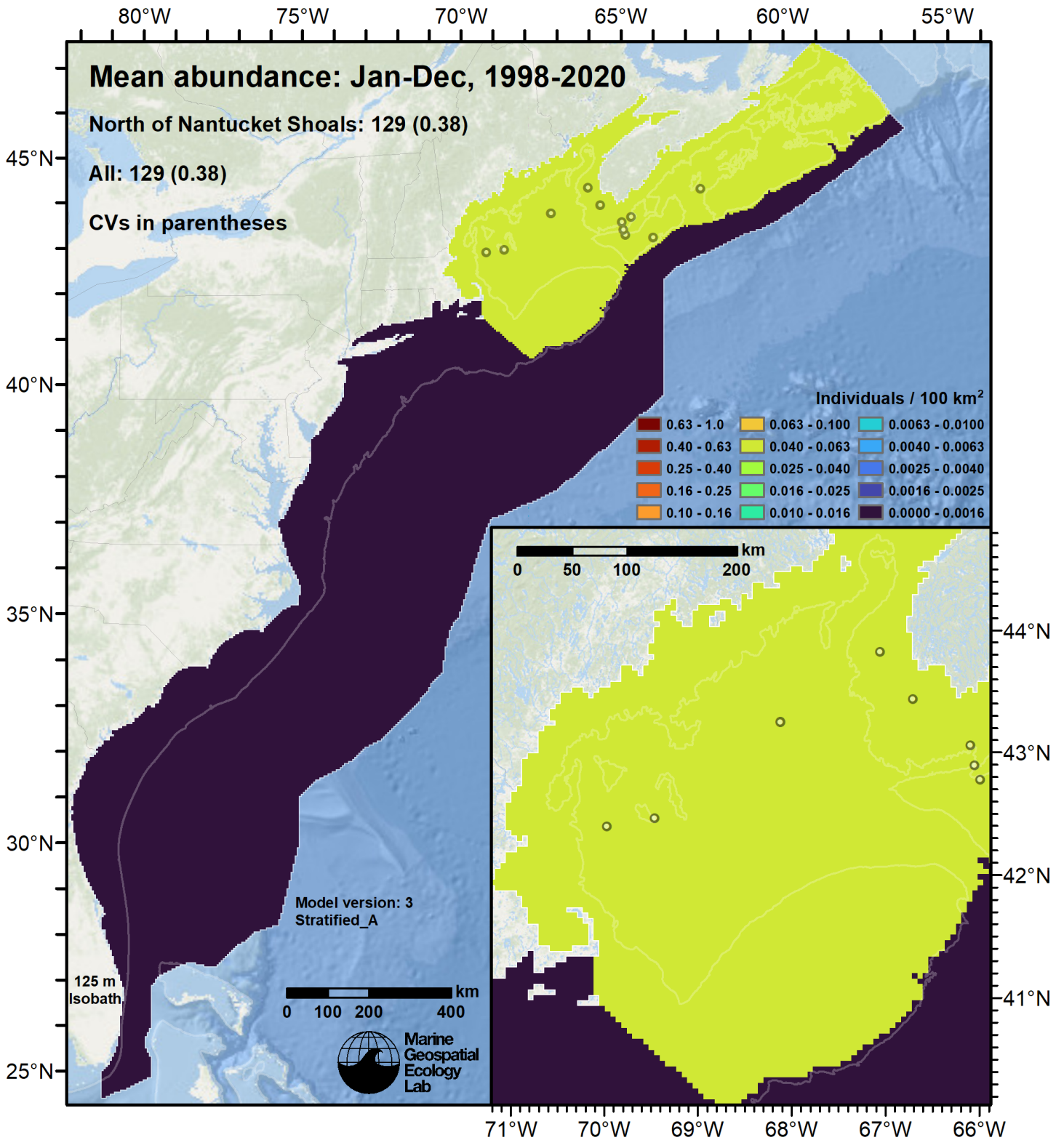


Figure 58: White-beaked dolphin density estimated for the indicated period. Open circles indicate segments with observations. The abundance estimate and its coefficient of variation (CV) are given in the subtitle.

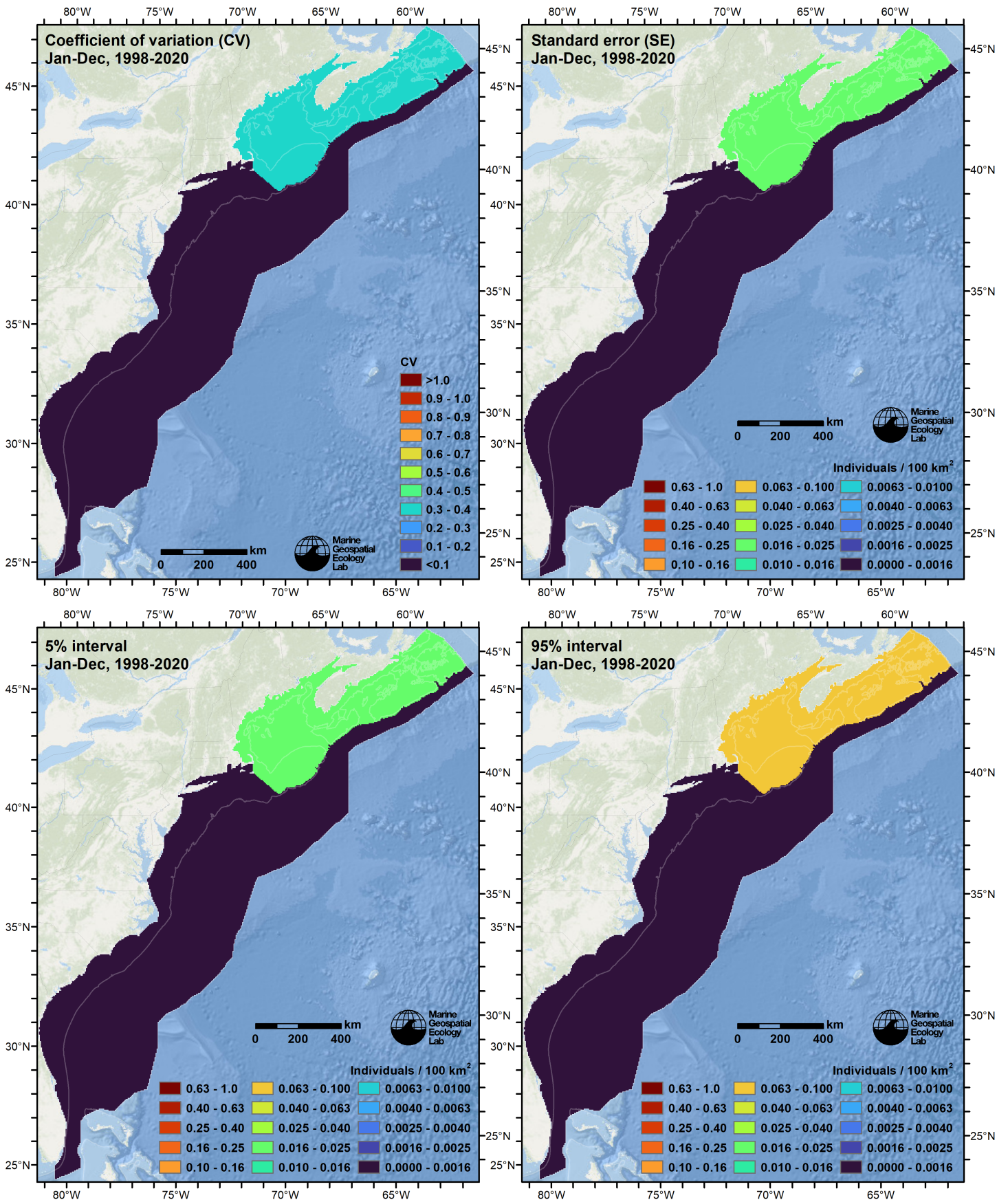


Figure 59: Uncertainty statistics for the white-beaked dolphin estimated density surface (Figure 58).

Table 25: White-beaked dolphin abundance and density estimated for each stratum.

Region	Abundance	CV	95% Interval	Area (km <sup>2</sup> )	Density (indiv. / 100 km <sup>2</sup> )
Offshore Gulf Stream and South	0	0.000	0 - 0	499,300	0.0000
Offshore North of Gulf Stream	0	0.000	0 - 0	253,575	0.0000
Shelf Cape Hatt. to Nant. Shoals	0	0.000	0 - 0	104,425	0.0000
Shelf North of Nantucket Shoals	129	0.377	63 - 265	302,025	0.0429
Shelf South of Cape Hatteras	0	0.000	0 - 0	105,500	0.0000
Sounds of NY, RI, and MA	0	0.000	0 - 0	8,600	0.0000
Total	129	0.377	63 - 265	1,273,425	0.0102



## 5.2 Abundance Comparisons

### 5.2.1 NOAA Stock Assessment Report

Table 26: Comparison of regional abundance estimates from the 2019 NOAA Stock Assessment Report (SAR) (Hayes et al. (2020)) to estimates from this density model extracted from roughly comparable zones (Figure 60 below). The SAR estimates were based on a single year of surveying, while the model estimates were taken from the multi-year mean density surface we provide to model users (Section 5.1).

2019 Stock Assessment Report			Density Model		
Month/Year	Area	$N_{est}$	Period	Zone	Abundance
			Jan-Dec 1998-2020	NEFSC <sup>a</sup>	46
Aug-Sep 2016	Bay of Fundy/Scotian Shelf <sup>b</sup>	5,478	Jan-Dec 1998-2020	Canada	82
Aug-Sep 2016	Newfoundland/Labrador <sup>c</sup>	530,538			
Aug-Sep 2016	Total	536,016	Jan-Dec 1998-2020	Total	128

<sup>a</sup> The SAR did not provide an estimate for this area, likely because no sightings were reported during the 2016 NEFSC AMAPPS aerial survey of this region (Palka (2020)).

<sup>b</sup> Estimate originally from Lawson and Gosselin (2018). However, we believe there are two problems with the SAR's treatment of Lawson and Gosselin's estimate. We discuss this further in Section 6.

<sup>c</sup> Estimate originally from Lawson and Gosselin (2018). This region was beyond our study area. We list it here because it is remarkably larger than Lawson and Gosselin's estimate of 2,636 from their previous survey from 2007 (listed in Table 13 of their report). We discuss this further in Section 6.

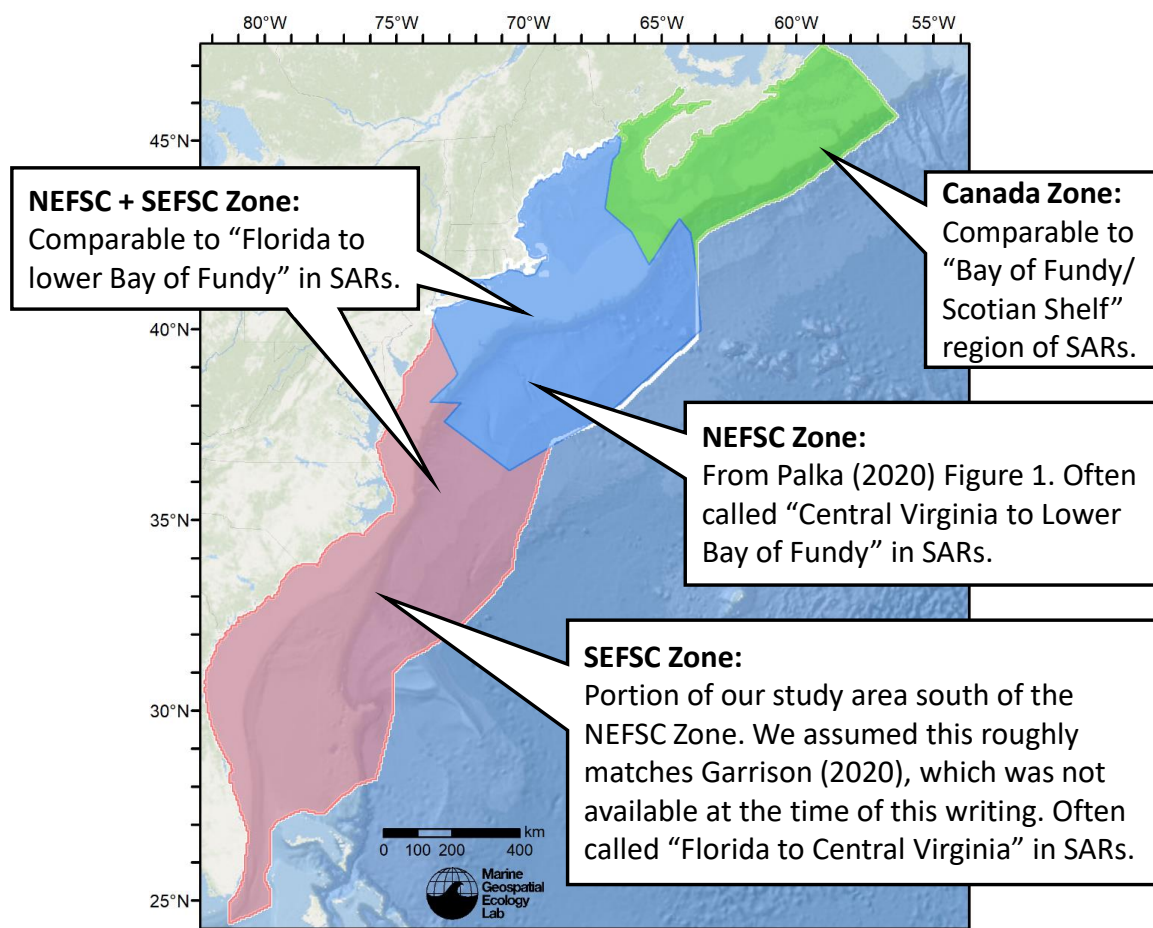


Figure 60: Zones for which we extracted abundance estimates from the density model for comparison to estimates from the NOAA Stock Assessment Report.



## 5.2.2 Previous Density Model

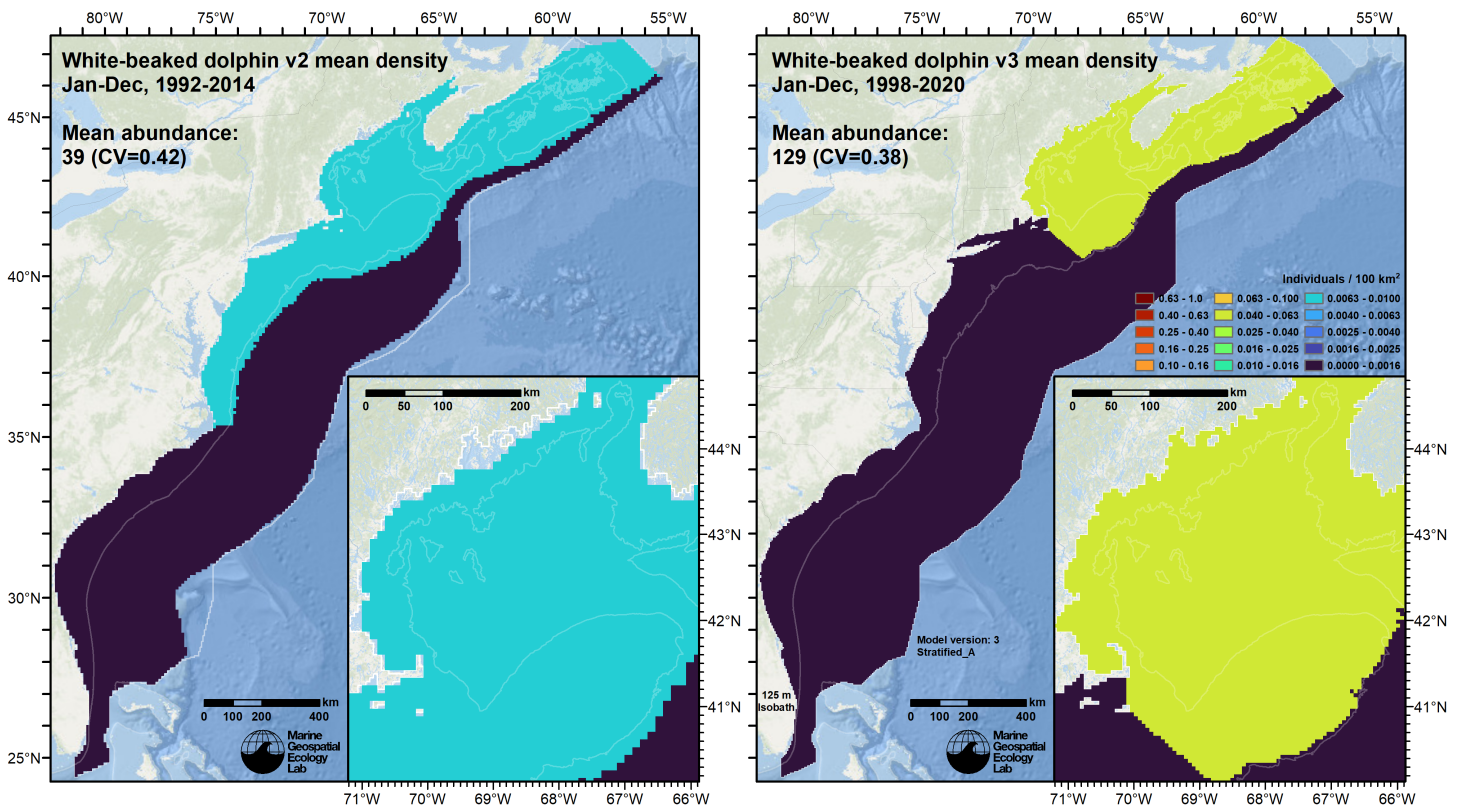


Figure 61: Comparison of the mean density predictions from the previous model (left) released by Roberts et al. (2016) to those from this model (right).

## 6 Discussion

In the western North Atlantic, white-beaked dolphins are a cool-water species that occurs from southern New England to southern Greenland and the Davis Strait (Hayes et al. 2020). The literature reports that during the 1970s, white-beaked dolphins switched habitats with Atlantic white-sided dolphins, with white-beaked dolphins moving from on-shelf to off-shelf, and Atlantic white-sided dolphins moving from off-shelf to on-shelf, possibly due to changes in the abundance of prey species (Kenney et al. 1996; Hayes et al. 2020).

The surveys utilized in our model were conducted after the habitat switch, from 1998-2020, and reported over 2800 sightings of white-sided dolphins. These were concentrated in the Gulf of Maine and southern New England, with comparatively few reported on the continental slope, consistent with the literature reports of their post-switch habitat. The surveys reported only 14 sightings of white-beaked dolphins, which all occurred on the continental shelf (Figure 1). This finding of low abundance on the shelf agrees with the reported habitat switch, but the lack of white-beaked dolphin sightings off-shelf may not. However, survey effort beyond the shelf was very sparse northeast of Georges Bank, where more white-beaked dolphins might be expected. Additional opportunistic sightings of white-beaked dolphins, not utilizable in our model, can be seen in this region in the [OBIS-SEAMAP archive](#) (Halpin et al. 2009).

With insufficient sightings to model density from environmental predictors, we estimated density in five geographic strata with a simplified approach (Section 4). All of the sightings occurred in the shelf stratum north of Nantucket Shoals, yielding a total abundance of 129.

The 2019 NOAA Stock Assessment Report (SAR) was the most recent that included white-beaked dolphin (Hayes et al. 2020). That report listed the abundance of the “Bay of Fundy/Scotian Shelf” area as 5,478, based on an estimate made by Fisheries and Oceans Canada (DFO) from aerial surveys in 2016, reported by Lawson and Gosselin (2018). There were two problems with the SAR’s treatment of Lawson and Gosselin’s estimate. First, the SAR incorrectly omitted the Gulf of St. Lawrence from the stock area. Table 12 of Lawson and Gosselin (2018), from which the abundance of 5,478 was extracted, clearly included the Gulf in the estimate. Second, the SAR should note that Table 10 of Lawson and Gosselin (2018) showed that none of the sightings of white-beaked dolphin were in the Bay of Fundy (BOF) or Scotian Shelf (SS) strata of Lawson

and Gosselin (2018), but all were in the various strata inside and at the mouth of the Gulf. (Figure 4A of Lawson and Gosselin (2018) showed one sighting in the Scotian Shelf region, at the shelf break south of Halifax, but this was not tallied in their Table 10. We presume it was truncated during detection modeling.) In effect, the abundance of white-beaked dolphins for the Bay of Fundy and Scotian Shelf was zero according to DFO's estimate, not 5,478. Therefore, we believe our very small estimate of 82 for this region (Table 26), derived over multiple years of surveys, is consistent with DFO's result.

DFO's Newfoundland/Labrador region was beyond the extent of our study area, but we note that their abundance estimate of 530,538 for that region (Lawson and Gosselin 2018, Table 8), derived from their 2016 survey, was approximately 200 times larger than their prior estimate of 2,636 (Lawson and Gosselin 2018, Table 13) derived from their 2007 survey. This remarkable difference cannot wholly be explained by population growth, and suggests either the movement of a very large number of dolphins (e.g. from off shelf to on shelf) or that the 2007 survey was substantially less likely to detect white-beaked dolphins. We urge that all of these possibilities be investigated, if white-beaked dolphins are a species of concern. In any case, assuming there are no problems with DFO's 2016 estimate, it appears that the white-beaked dolphin may be extremely abundant just north and east of our study area.

In our prior model, we defined a geographic stratum spanning the shelf from Cape Hatteras to the northeastern limit of the study area (Figure 61). We set the southern limit at Cape Hatteras based on the southernmost opportunistic sighting listed in OBIS-SEAMAP occurring there in 1979. Our approach for the 2022 modeling cycle was to split the study area into five geographic strata based on major habitat boundaries (see Section 4), and then estimate abundance within each. Because we only had sightings in the northernmost shelf stratum, the new model estimated zero abundance in all other strata, and the density in the northernmost shelf stratum is substantially higher than in the prior model. As of this writing, OBIS-SEAMAP does not contain any sightings south of Nantucket Shoals after the 1980s. We believe our new strata better reflect the present-day distribution of the white-beaked dolphin.

## References

- Barco SG, Burt L, DePerte A, Digiovanni R Jr. (2015) Marine Mammal and Sea Turtle Sightings in the Vicinity of the Maryland Wind Energy Area July 2013-June 2015, VAQF Scientific Report #2015-06. Virginia Aquarium & Marine Science Center Foundation, Virginia Beach, VA
- Buckland ST, Anderson DR, Burnham KP, Laake JL, Borchers DL, Thomas L (2001) Introduction to Distance Sampling: Estimating Abundance of Biological Populations. Oxford University Press, Oxford, UK
- Burt ML, Borchers DL, Jenkins KJ, Marques TA (2014) Using mark-recapture distance sampling methods on line transect surveys. *Methods in Ecology and Evolution* 5:1180–1191. doi: [10.1111/2041-210X.12294](https://doi.org/10.1111/2041-210X.12294)
- Cole T, Gerrior P, Merrick RL (2007) [Methodologies of the NOAA National Marine Fisheries Service Aerial Survey Program for Right Whales \(\*Eubalaena glacialis\*\) in the Northeast U.S., 1998-2006](#). U.S. Department of Commerce, Woods Hole, MA
- Cotter MP (2019) Aerial Surveys for Protected Marine Species in the Norfolk Canyon Region: 2018–2019 Final Report. HDR, Inc., Virginia Beach, VA
- Foley HJ, Paxton CGM, McAlarney RJ, Pabst DA, Read AJ (2019) Occurrence, Distribution, and Density of Protected Species in the Jacksonville, Florida, Atlantic Fleet Training and Testing (AFTT) Study Area. Duke University Marine Lab, Beaufort, NC
- Garrison LP, Martinez A, Maze-Foley K (2010) [Habitat and abundance of cetaceans in Atlantic Ocean continental slope waters off the eastern USA](#). *Journal of Cetacean Research and Management* 11:267–277.
- Geo-Marine, Inc. (2010) [New Jersey Department of Environmental Protection Baseline Studies Final Report Volume III: Marine Mammal and Sea Turtle Studies](#). Geo-Marine, Inc., Plano, TX
- Halpin P, Read A, Fujioka E, Best B, Donnelly B, Hazen L, Kot C, Urian K, LaBrecque E, Dimatteo A, Cleary J, Good C, Crowder L, Hyrenbach KD (2009) OBIS-SEAMAP: The World Data Center for Marine Mammal, Sea Bird, and Sea Turtle Distributions. *Oceanography* 22:104–115. doi: [10.5670/oceanog.2009.42](https://doi.org/10.5670/oceanog.2009.42)
- Hayes SA, Josephson E, Maze-Foley K, Rosel PE, Byrd B, Chavez-Rosales S, Cole TV, Garrison LP, Hatch J, Henry A, Horstman SC, Litz J, Lyssikatos MC, Mullin KD, Orphanides C, Pace RM, Palka DL, Powell J, Wenzel FW (2020) [US Atlantic and Gulf of Mexico Marine Mammal Stock Assessments - 2019](#). NOAA National Marine Fisheries Service, Northeast Fisheries Science Center, Woods Hole, MA
- Kenney RD, Payne PM, Heinemann DW, Winn HE (1996) Shifts in Northeast shelf cetacean distributions relative to trends in Gulf of Maine/Georges Bank finfish abundance. In: *The Northeast Shelf Ecosystem: Assessment, Sustainability, and Management*. Blackwell Science, Cambridge, MA, pp 169–196

- Laake JL, Calambokidis J, Osmek SD, Rugh DJ (1997) Probability of Detecting Harbor Porpoise From Aerial Surveys: Estimating  $g(0)$ . *Journal of Wildlife Management* 61:63–75. doi: [10.2307/3802415](https://doi.org/10.2307/3802415)
- Lawson JW, Gosselin J-F (2018) Estimates of cetacean abundance from the 2016 NAISS aerial surveys of eastern Canadian waters, with a comparison to estimates from the 2007 TNASS. NAMMCO SC/25/AE/09. In: Proceedings of the NAMMCO 25th Scientific Committee (SC). North Atlantic Marine Mammal Commission, Bergen-Tromsø, Norway,
- Mallette SD, Lockhart GG, McAlarney RJ, Cummings EW, McLellan WA, Pabst DA, Barco SG (2014) Documenting Whale Migration off Virginia’s Coast for Use in Marine Spatial Planning: Aerial and Vessel Surveys in the Proximity of the Virginia Wind Energy Area (VA WEA), VAQF Scientific Report 2014-08. Virginia Aquarium & Marine Science Center Foundation, Virginia Beach, VA
- Mallette SD, Lockhart GG, McAlarney RJ, Cummings EW, McLellan WA, Pabst DA, Barco SG (2015) Documenting Whale Migration off Virginia’s Coast for Use in Marine Spatial Planning: Aerial Surveys in the Proximity of the Virginia Wind Energy Area (VA WEA) Survey/Reporting Period: May 2014 - December 2014, VAQF Scientific Report 2015-02. Virginia Aquarium & Marine Science Center Foundation, Virginia Beach, VA
- Mallette SD, McAlarney RJ, Lockhart GG, Cummings EW, Pabst DA, McLellan WA, Barco SG (2017) [Aerial Survey Baseline Monitoring in the Continental Shelf Region of the VACAPES OPAREA: 2016 Annual Progress Report](#). Virginia Aquarium & Marine Science Center Foundation, Virginia Beach, VA
- Marsh H, Sinclair DF (1989) Correcting for Visibility Bias in Strip Transect Aerial Surveys of Aquatic Fauna. *The Journal of Wildlife Management* 53:1017. doi: [10.2307/3809604](https://doi.org/10.2307/3809604)
- McAlarney R, Cummings E, McLellan W, Pabst A (2018) Aerial Surveys for Protected Marine Species in the Norfolk Canyon Region: 2017 Annual Progress Report. University of North Carolina Wilmington, Wilmington, NC
- McLellan WA, McAlarney RJ, Cummings EW, Read AJ, Paxton CGM, Bell JT, Pabst DA (2018) Distribution and abundance of beaked whales (Family Ziphiidae) Off Cape Hatteras, North Carolina, U.S.A. *Marine Mammal Science*. doi: [10.1111/mms.12500](https://doi.org/10.1111/mms.12500)
- Mullin KD, Fulling GL (2003) [Abundance of cetaceans in the southern U.S. North Atlantic Ocean during summer 1998](#). *Fishery Bulletin* 101:603–613.
- Palka D (2020) [Cetacean Abundance in the US Northwestern Atlantic Ocean Summer 2016](#). *Northeast Fish Sci Cent Ref Doc. 20-05*. NOAA National Marine Fisheries Service, Northeast Fisheries Science Center, Woods Hole, MA
- Palka D, Aichinger Dias L, Broughton E, Chavez-Rosales S, Cholewiak D, Davis G, DeAngelis A, Garrison L, Haas H, Hatch J, Hyde K, Jech M, Josephson E, Mueller-Brennan L, Orphanides C, Pegg N, Sasso C, Sigourney D, Soldevilla M, Walsh H (2021) [Atlantic Marine Assessment Program for Protected Species: FY15 – FY19 \(OCS Study BOEM 2021-051\)](#). U.S. Department of the Interior, Bureau of Ocean Energy Management, Washington, DC
- Palka DL (2006) [Summer abundance estimates of cetaceans in US North Atlantic navy operating areas \(NEFSC Reference Document 06-03\)](#). U.S. Department of Commerce, Northeast Fisheries Science Center, Woods Hole, MA
- Palka DL, Chavez-Rosales S, Josephson E, Cholewiak D, Haas HL, Garrison L, Jones M, Sigourney D, Waring G, Jech M, Broughton E, Soldevilla M, Davis G, DeAngelis A, Sasso CR, Winton MV, Smolowitz RJ, Fay G, LaBrecque E, Leiness JB, Dettloff K, Warden M, Murray K, Orphanides C (2017) [Atlantic Marine Assessment Program for Protected Species: 2010-2014 \(OCS Study BOEM 2017-071\)](#). U.S. Department of the Interior, Bureau of Ocean Energy Management, Washington, DC
- Pike D, Gunnlaugsson T, Mikkelsen B, Halldórsson SD, Víkingsson G (2019) Estimates of the abundance of cetaceans in the central North Atlantic based on the NASS Icelandic and Faroese shipboard surveys conducted in 2015. *NAMMCOSP*. doi: [10.7557/3.4941](https://doi.org/10.7557/3.4941)
- Read AJ, Barco S, Bell J, Borchers DL, Burt ML, Cummings EW, Dunn J, Fougères EM, Hazen L, Hodge LEW, Laura A-M, McAlarney RJ, Peter N, Pabst DA, Paxton CGM, Schneider SZ, Urian KW, Waples DM, McLellan WA (2014) [Occurrence, distribution and abundance of cetaceans in Onslow Bay, North Carolina, USA](#). *Journal of Cetacean Research and Management* 14:23–35.
- Roberts JJ, Best BD, Mannocci L, Fujioka E, Halpin PN, Palka DL, Garrison LP, Mullin KD, Cole TVN, Khan CB, McLellan WA, Pabst DA, Lockhart GG (2016) Habitat-based cetacean density models for the U.S. Atlantic and Gulf of Mexico. *Scientific Reports* 6:22615. doi: [10.1038/srep22615](https://doi.org/10.1038/srep22615)
- Roberts JJ, Yack TM, Halpin PN (2023) Marine mammal density models for the U.S. Navy Atlantic Fleet Training and Testing (AFTT) study area for the Phase IV Navy Marine Species Density Database (NMSDD), Document Version 1.3. Duke University Marine Geospatial Ecology Lab, Durham, NC

- Robertson FC, Koski WR, Brandon JR, Thomas TA, Trites AW (2015) [Correction factors account for the availability of bowhead whales exposed to seismic operations in the Beaufort Sea](#). *Journal of Cetacean Research and Management* 15:35–44.
- Ryan C, Boisseau O, Cucknell A, Romagosa M, Moscrop A, McLanaghan R (2013) [Final report for trans-Atlantic research passages between the UK and USA via the Azores and Iceland, conducted from R/V Song of the Whale 26 March to 28 September 2012](#). Marine Conservation Research International, Essex, UK
- Schick R, Halpin P, Read A, Urban D, Best B, Good C, Roberts J, LaBrecque E, Dunn C, Garrison L, Hyrenbach K, McLellan W, Pabst D, Palka D, Stevick P (2011) Community structure in pelagic marine mammals at large spatial scales. *Marine Ecology Progress Series* 434:165–181. doi: [10.3354/meps09183](#)
- Torres LG, McLellan WA, Meagher E, Pabst DA (2005) [Seasonal distribution and relative abundance of bottlenose dolphins, \*Tursiops truncatus\*, along the US mid-Atlantic coast](#). *Journal of Cetacean Research and Management* 7:153.
- Whitt AD, Powell JA, Richardson AG, Bosyk JR (2015) [Abundance and distribution of marine mammals in nearshore waters off New Jersey, USA](#). *Journal of Cetacean Research and Management* 15:45–59.